

TARG1 protects against DNA ADP-ribosylation stress

Callum Tromans-Coia

Lincoln College

University of Oxford

A thesis submitted for the degree of

Doctor of Philosophy

Michaelmas 2020

Declaration

I declare that this thesis has been composed solely by myself and that it has not been submitted, in whole or in part, in any previous application for a degree. Except where states otherwise by reference or acknowledgement, the work presented is entirely my own.

Callum Tromans-Coia

Lincoln College

Acknowledgements

What can I write here that I will be happy to read years from now? Do I go for something abstract? Or do I make simple acknowledgements? I'll go for the latter.

I would like to start by thanking my mum and dad. They are both fantastic and their support of whatever I do has been incredible. Both of them have also taught me the importance of relaxation, making sure I always take time for myself, which I think has been incredibly important. Onwards and upwards.

I would also like to thank the rest of my family and their curiosity about what I'm up to and their support for whatever it may be. I love the family gatherings we have, in whatever form they take, and cannot wait for the next one.

I would also like to thank Lucy for cheer and support through difficult times. While it has not been easy, I do believe that it has been worth it. The doctorate tests you in ways you can't comprehend before you begin and it impacts everyone differently. I hope that this experience has built strength in both of us.

I would also like to thank Ivan Ahel for creating a friendly lab environment and giving me the creative freedom to explore different ideas that that piqued my curiosity. Namely, programming. I have always struggled to work out what I want to do in life, but learning programming has gotten me the closest to finding out what I like. Still, I don't have any grand plans of where I'll end up, but maybe that's just how it is.

Abstract

ADP-ribosylation is a modification that can target a variety of macromolecules and can regulate an array of important cellular processes. ADP-ribosylation is catalysed by ADP-ribosyltransferases that use NAD^+ as a cosubstrate to transfer ADP-ribose onto target molecules. The resulting modification can be recognised by ADP-ribose binding domains and can also be removed by enzymes collectively known as ADP-ribosylhydrolases. Recently, a toxin termed DarT from bacteria was shown to modify thymidine bases on single-stranded DNA. The antitoxin of DarT is DarG, which shows striking structural homology to the human ADP-ribosylhydrolase TARG1. Here, we show that TARG1 can directly reverse thymidine-linked ADP-ribosylation like DarG. We also use DarT as a genotoxin to induce DNA ADP-ribosylation stress in human cells. We sought to examine how human cells respond to DNA ADP-ribosylation stress and to determine if TARG1 is involved in the response of this form of DNA damage. We find that wild-type cells expressing DarT show no sensitivity to DNA ADP-ribosylation. However, in the absence of TARG1, cells show elevated levels of DNA damage and cytotoxicity. This sensitivity to DNA ADP-ribosylation is rescued with TARG1 wild-type overexpression but not for a catalytically inactive form of TARG1. The damage inflicted by DarT-mediated DNA ADP-ribosylation occurs within replicating cells and co-localises with sites of DNA synthesis. Furthermore, we demonstrate the first detection of reversible ADP-ribosylated genomic DNA *in vivo* from bacterial and human cells. We also examine sensitivity of TARG1-deficient cells to an inhibitor of PARG, another ADP-ribosylhydrolase. PARG inhibitor treated TARG1-deficient cells show signs of replication stress and elevated levels of ADP-ribosylation that is dependent on PARP1-2 activity. We consider if TARG1 and PARG have a shared substrate, perhaps in the form of a nucleic acid. Collectively, our results elucidate the impact of DNA ADP-ribosylation stress in human cells and provides the molecular toolkit for future studies of this largely unknown facet of ADP-ribosylation.

Contents

List of Figures **6**

Abbreviations **9**

1 Introduction **11**

1.1 DNA Damage Response 11

1.2 DNA damage types 12

1.3 DNA damage kinases 20

1.4 DNA damage repair pathways 24

1.5 ADP-ribosylation 33

1.6 Aim and rationale of this thesis 42

2 Results **43**

2.1 TARG1 reverses DNA ADP-ribosylation catalysed by DarT 43

2.2 TARG1-deficient human cells are sensitive to DarT 49

2.3 TARG1-deficient human cells are sensitive to PARG inhibition 85

3 Discussion **94**

3.1 TARG1 protects against DNA ADP-ribosylation 94

3.2 PARG inhibitor sensitivity in TARG1-deficient cells 99

4 Materials and Methods **108**

References **117**

Supplementary Figures **147**

List of Figures

1.1 Representative examples of different types of DNA damage 20

1.2 Representative examples of nucleic acid ADP-ribosylation 40

2.1 Comparison between *Taq*DarG and other macrodomains 44

2.2 TARG1 removes thymidine-linked ADP-ribosylation from DNA 45

2.3 TARG1 confers resistance to DarT toxicity in bacteria 46

2.4 DarG, TARG1, MacroD1 and MacroD2 can remove thymidine-linked ADP-ribosylation from DNA 47

2.5 Only DarG and TARG1 but not MacroD1, MacroD2, ARH3 or PARG rescue DarT toxicity in bacteria 48

2.6 TARG1 KO U-2 OS but not WT cells are sensitive to DarT expression . . 50

2.7 DarT expression induces DNA damage in TARG1 KO cells 52

2.8 TARG1 expression rescues DarT toxicity 54

2.9 DarT induces the DDR in TARG1 KO cells 56

2.10 Chromatin-bound GFP-DarT co-localises with sites of ssDNA and DNA synthesis 57

2.11 Workflow for QIBC analysis 58

2.12 DarT does not completely block DNA replication 59

2.13 Pattern of ssDNA sites induced by DarT expression and other replication poisoning drugs 61

2.14 DarT expression limits, but does not prevent, EdU incorporation when compared to HU, CPT or MMS in TARG1 KO cells 62

2.15 DarT induces DNA damage in PCNA-positive cells 64

2.16 DarT induced DNA damage occurs within S-phase 65

2.17 Protein ADP-ribosylation is not detectable in DarT-treated cells 67

2.18 DarT expressing TARG1 KO cells accumulate ADP-ribosylation in S-phase 69

2.19 Replication stress induced by Chk1 inhibition does not sensitise WT cells to DarT . . . 71
2.20 PARP1 can form PAR chains on DarT modified ssDNA . . . 73
2.21 Formation of PAR-DNA by PARP1 is proportional to the concentration of the thymidine-linked ADP-ribosylated DNA substrate . . . 74
2.22 TARG1 demodifies PAR-DNA formed by DarT and PARP1 . . . 76
2.23 ADP-ribosylation in DarT-treated TARG1 KO cells is in the mono-ADP-ribose form . . . 78
2.24 DarT modified oligonucleotide probed by a panel of ADP-ribose binding reagents by dot blot . . . 80
2.25 Detection of ADP-ribosylated genomic DNA in bacteria . . . 82
2.26 Detection of ADP-ribosylated genomic DNA in human cells . . . 83
2.27 *In vitro* demodification of ADP-ribosylated genomic DNA . . . 84
2.28 TARG1 KO cells treated with PARGi accumulate excessive ADP-ribosylation and replication stress . . . 86
2.29 TARG1 KO cells treated with PARGi accumulate cell cycle markers . . . 87
2.30 Overexpression of TARG1 WT, but not TARG1 K84A, partially rescues TARG1 KO sensitivity to PARGi . . . 89
2.31 PARP inhibition rescues PARGi sensitivity in TARG1 KO cells . . . 91
2.32 Free PAR is detectable by dot blot . . . 93

S1 Quantification of WT or TARG1 KO cells treated with DarT . . . 147
S2 Estimation of the maximum number of DarT modification sites . . . 148
S3 DarT induces γH2AX and RPA2 pS4/8 in S-phase cells . . . 149
S4 Immunofluorescence bleed-through and secondary antibody cross-reactivity test . . . 150
S5 Alternative QIBC cell cycle staging using cyclin A reveals γH2AX is found in S-phase cells . . . 151
S6 Quantification of GFP-DarT expression across cell lines . . . 152

S7 Bacterial gDNA de-ADP-ribosylation assay with DarG, TARG1, MacroD1, PARG, ARH3 153

Abbreviations

6-4PP 6-4 pyrimidine-pyrimidone photoproduct

aEJ Alternative end joining

AGT O^6-alkylguanine-DNA alkyltransferase

AP Apurinic/apyrimidinic site

APE1 Apurinic/apyrimidinic endonuclease 1

ART ADP-ribosyltransferase

BaP Benzo[a]pyrene

BER Base excision repair

BPDE Benzo[a]pyrene diol epoxide

CPD Cyclobutane pyrimidine dimer

DDR DNA damage response

DSB Double-strand break

EXO1 Exonuclease 1

FEN1 Flap endonuclease 1

HPF1 Histone PARylation factor 1

HR Homologous recombination

MARylation Mono-ADP-ribosylation

MMR Mismatch Repair

NER Nucleotide Excision Repair

NHEJ Non-homologous end joining

NNK Nicotine-derived nitrosamine ketone

PARylation Poly-ADP-ribosylation

RER Ribonucleotide excision repair

ROS Reactive oxygen species

SSA Single-strand annealing

SSB Single-strand break

TDP1 Tyrosyl-DNA phosphodiesterase 1

TOP1 Topoisomerase I

XRCC1 X-ray repair cross-complementing protein 1

Chapter 1

Introduction

1.1 DNA Damage Response

The DNA Damage Response (DDR) is a diverse and complex signalling network with the sole focus of maintaining genomic integrity [1]. A failure to preserve the genetic information that is encoded by DNA is often implicated in cancer and age-related diseases. Throughout the normal lifespan of a cell, DNA is repeatedly damaged by internal and external factors and it has been estimated that a cell could accumulate up to 10^5 lesions in a single day [2, 3]. Therefore, it is imperative that damaged DNA is repaired to ensure an intact genome is passed down to future generations.

Damaged DNA can present itself in a variety of forms such as base mismatches, base adducts and breaks in one or both DNA strands. In order to repair this damage, the DDR, in essence, involves two steps: the recognition of damaged DNA and the repair of damaged DNA [4]. In concert with these events, cells may alter other metabolic events to ensure fidelity of repair. These modified pathways may include relaxing chromatin structure to enable access of DNA repair factors to sites of damage or by arresting the cell cycle until the damage is repaired. Cells with an extensive DNA damage burden may choose to exit the cell cycle entirely by becoming senescent, or by undergoing programmed cell death, also known as apoptosis, to prevent propagation of deleterious DNA [5].

Similar to other signalling cascades, the DDR is reliant upon protein modification to initiate and disseminate the response [6]. Within vertebrate cells the DDR is controlled by three related master kinases, known as ATM, ATR, and DNA-PK. These kinases are

activated and recruited to sites of DNA damage by other protein complexes known as sensor proteins and each respective kinase relies on its own sensor protein complex. Once activated, these kinases phosphorylate a plethora of partially overlapping substrates in order harmonise DNA repair with DNA metabolism [4, 6]. Here, we will describe types of DNA damage and its potential sources; how the damage is recognised; and ultimately how DNA damage is repaired.

1.2 DNA damage types

Base loss

The intrinsic chemical nature of DNA makes it prone to certain types of spontaneous damage. The N-glycosidic base-sugar bonds within DNA are susceptible to hydrolysis, leading to release of free bases and a base-free sugar residue being left behind, also known as an apurinic/apyrimidinic (AP) site [7]. Purine bases are particularly sensitive to this form of hydrolysis, with pyrimidine bases being considerably less susceptible [8, 9]. The spontaneous loss of purine bases is known as depurination and is predicted to occur up to 10,000 times per day, per human cell [8]. Interestingly, assuming this estimation is correct, it is possible that in the lifespan of a human nerve cell that up to 10^8 purines could be lost through spontaneous depurination, which is approximately 3% of all purine residues in the human genome [7]. These predicted base losses were based upon *in vitro* data recorded at physiological pH [10]. However, *in vivo* this rate of base hydrolysis and formation of AP sites could be much higher in the presence of DNA damaging agents and action by DNA glycosylases that hydrolyse the N-glycosidic bond during DNA repair.

Base deamination

In addition to base-sugar hydrolysis, DNA bases are also prone to spontaneous hydrolytic deamination [7]. Cytosine bases are the most sensitive to deamination, leading to their conversion into uracil [11]. The methylated form of cytosine, 5-methylcytosine, is deami-

nated at a rate of up to four times that of cytosine, leading to the formation of thymine [12]. However, due to 5-methylcytosine only accounting for up to 3% of cytosine bases, the majority of deamination events in the genome occur on cytosine bases that have not been methylated. The deaminated form of cytosine (uracil) is very attractive to the DNA repair protein uracil glycosylase, which quickly leads to the excision of the damaged base forming a AP site [10]. However, deaminated 5-methylcytosine (thymine) does not lead to activation of the same DNA repair machinery. This conversion instead prompts correction by the mismatch repair machinery. The deamination of other bases can also occur, albeit to a lesser extent. For example, adenine can be deaminated to form hypoxanthine and guanine is converted to xanthine [13]. While capable of being a spontaneous, these deamination reactions can also be enzymatic and has been implicated in immunoglobulin diversification where the C→U transition can be beneficially mutagenic [14, 15].

Base oxidation

DNA bases can also undergo oxidation [7]. This damage can occur as a result of increased reactive oxygen species (ROS) within the cell, known as oxidative stress. These ROS can arise from endogenous sources, such as oxidative phosphorylation, and exogenously from ionising radiation [16]. The electrophilic and highly reactive hydroxyl radical ($^{\bullet}$OH) leads to oxidation of guanine to form 8-oxoguanine. This damaged base then switches its preferred binding partner from cytosine to adenine [17]. As a result, during replication the strand complementary to the template containing 8-oxoguanine can erroneously incorporate adenine instead of cytosine. This creates a 8-oxoG:A base pairing and if 8-oxoguanine is later removed, the gap will be filled with T [18, 19]. This G→T point mutation is called a transversion and has been suggested to be involved in carcinogenesis [20]. Within human cells, 8-oxoguanine is able to be removed by the DNA glycosylase OGG1 but only from 8-oxoG:C pair, leaving behind an AP site [21]. In the case of a 8-oxoG:A pair, the DNA glycosylase MYH removes the adenine to restore 8-oxoG:C pairing which is subsequently targeted by OGG1 [22].

Base alkylation

DNA bases are also susceptible to alkylation, a process in which an alkyl group is added to the base and may distort its function [7]. DNA alkylation can be caused by alkylating agents, a broad group of reactive chemicals that can originate from the environment and from the cell [23]. The most studied alkyl base adduct is the methyl group, which can be catalysed by alkylating agents such as methyl methanesulfonate. This can lead to the formation of N^7-methylguanine and N^3-methyladenine [24]. N^7-methylguanine is the most common and is not immediately cytotoxic as traditional base pairing is maintained. However, N^7-methylguanine is at increased risk on spontaneous depurination and subsequent formation of an AP site [25]. Contrastingly, N^3-methyladenine is considerably more cytotoxic, leading to the blockage of DNA polymerases and therefore preventing efficient DNA replication [26]. Translesion polymerases have been shown to be recruited to sites of N^3-methyladenine to facilitate replication across these lesions [27]. Similar to other forms of base adducts, specific DNA glycosylases, such as alkyladenine DNA glycosylase, are able to remove the lesion, resulting in an AP site [28].

However, not all DNA methylation is deleterious [29]. Enzymatic methylation of cytosines to form the aforementioned 5-methylcytosine is an essential pathway involved in regulating gene expression. In this context, removal of 5-methylcytosine has been suggested to rely on intermediate steps that utilise deamination to convert 5-methylcytosine to thymine and subsequent glycosylase activity to repair the T:G mismatch. This process reverses the modification as there exists no mechanism for cleaving the bond between the cytosine and the methyl group, revealing that canonical DNA damage repair machinery can be involved in active DNA demethylation [29].

Alkyl groups other than methyl groups can be added onto DNA bases. For example, tobacco smoke contains a litany of compounds that can cause genomic insults, such as

nitrosamines [30]. The tobacco specific nitrosamine NNK can be activated by the P450 enzymes and can subsequently alkylate O^6 of guanine to form either O^6-methylguanine or O^6-[4-oxo-4-(3-pyridyl)butyl]-guanine (O^6-POB-guanine) [31–33]. Of the sites on guanines that can be alkylated, the aforementioned N^7 linked is most common, then N^3, followed by O^6 [23]. Interestingly, the O^6 alkylated guanine can be repaired by sacrificial proteins called O^6-alkylguanine-DNA alkyltransferases (AGTs), introduced later.

Base adducts

It is also important to note that large hydrocarbons can be also be covalently attached to DNA bases and form large base adducts [7]. The source of these genomic insults can arise from chemotherapeutic agents and carcinogens from the environment. Benzo[a]pyrene (BaP) from tobacco smoke undergoes activation by P450 to form Benzo[a]pyrene diol epoxide (BPDE) which subsequently reacts mainly with the N^2 position of guanine to form BPDE-guanine [30, 34]. BPDE-guanine blocks DNA replication and if bypassed by translesion polymerases can lead to G→T transversions [35, 36]. BPDE adducts also preferentially form on guanines adjacent to 5-methylcytosines. This leads to areas of methylated CG dinucleotides becoming mutational hotspots when exposed to BaP. The most striking example of this in the tumour suppressor *p53* gene, where BPDE binds to some of the most frequently mutated guanine nucleotides in smoking induced lung cancer [37–39].

DNA crosslinks

Covalent linkages between bases can also form within DNA [40, 41]. Crosslinks between bases on the same strand are known as intrastrand crosslinks. These can arise due to the actions of the hydroxyl radical ($^\bullet$OH) that attacks the C5=C6 double bond of the cytosine, thymine and 5-methylcytosine. Alternatively, $^\bullet$OH can abstract a hydrogen from the 5-methyl group of thymine or 5-methylcytosine [42]. Both reactions yield pyrimidine base-centred secondary radicals which subsequently attack their adjacent purine bases to form intrastrand crosslinks [43–46]. UV radiation can also generate crosslinks between

neighbouring pyrimidines through a photocycloaddition reaction to form a cyclobutane pyrimidine dimer (CPD), the most abundant form being the thymine-dimer [47]. Adjacent pyrimidines can also form 6-4 pyrimidine-pyrimidone photoproduct (6-4PP) lesions after exposure to UV light. All of these aforementioned intrastrand crosslinks between bases can cause distortion of the DNA double helix [48]. Such distortions have been shown to block DNA replication and have been suggested to recruit translesion polymerases and therefore promote mutagenesis if not repaired [49–51].

Covalent linkages that form between bases on opposite strands pose a considerably more deleterious threat to the cell [40, 41]. These linkages prevent the normal separating of DNA strands and therefore impedes both replication and transcription. Chemotherapeutic drugs, such as cisplatin, are some of the best characterised in the formation of interstrand crosslinks but there has been suggestion that interstrand crosslinks can also form following UV radiation *in vitro* [52]. Moreover, nature contains potential sources of crosslinking agents, such as natural psoralens, and even AP sites have been suggested to form interstrand crosslinks [41, 53]. However, the structural complexity of DNA in living systems and the stereoisomeric nature of individual bases makes the formation of both intra- and interstrand crosslinks potentially more diverse than has been previously understood. As such, crosslinking agents may form covalent linkages in both an intra- and interstrand manner. Regardless, because interstrand crosslinks involve both strands of DNA, the potential loss of genetic information is higher than if the damage were only on a single strand. This is due to the repair machinery being unable to rely upon copying from an intact template strand in the case of interstrand crosslinks. As a result, interstrand crosslinks have been associated with point mutations, large deletions and translocations [41]. Due to this threat, the restoration of interstrand crosslinks relies on a careful and complex harmonisation of multiple repair pathways to ensure genomic integrity is maintained.

Crosslinks between DNA and protein can also occur. Protein-DNA crosslinks can

be induced by some chemotherapeutics in addition to exogenous and endogenous agents [54]. These substantial DNA lesions are highly toxic as they can block DNA unwinding, transcription and replication [55–57]. For example, DNA-protein crosslinks can form as a result of a chemotherapeutic, such as camptothecin, blocking the resolution of a reaction intermediate in normal enzymatic activity, leading to the enzyme becoming trapped on DNA [54]. In this scenario, camptothecin and its derivatives poison topoisomerase I and prevents DNA religation, thereby trapping topoisomerase I on DNA [58, 59]. Some endogenous and exogenous agents can also cause non-specific crosslinking of proteins that are in close proximity to DNA [54, 60]. Furthermore, proteins that are bound tightly to the DNA can also be perceived by the cell as a DNA-protein crosslink, such as PARP1 that is inhibited by olaparib [54, 61]. The aforementioned cisplatin can induce crosslinks between DNA and proteins that are associated with chromatin [62]. Endogenous sources of DNA-protein crosslinks can also arise from AP sites within the nucleosome, which can crosslink to histones [63].

Ribonucleotide misincorporation

Ribonucleotides are the precursor to RNA and are present in the cell at almost double the concentration of deoxyribonucleotides, the precursors to DNA [64, 65]. However, despite DNA polymerases possessing mechanisms to discriminate between these nucleotide precursors, this exclusion is imperfect and the sheer abundance of ribonucleotides results in their misincorporation into DNA [66]. It is predicted that an average of one ribonucleotide is misincorporated into DNA every 1,000 bases *in vitro* [67]. A failure to resolve misincorporation has been shown to result in over 1,000,000 ribonucleotides in DNA in mouse embryonic fibroblast cells [68]. This frequency of ribonucleotide misincoproration in DNA establishes this lesion as the most common form of endogenous damage. If not removed, ribonucleotides can accumulate over time and impair the processivity of DNA polymerases, lead to additional DNA damage and disrupt epigenetic marks [68–70]. However, it is also important to note that the incorporation of ribonucleotides into DNA is can be a normal aspect of DNA metabolism. During lagging-strand DNA replication,

RNA primase synthesises ∼10 nucleotide long RNA primers in order to initiate Okazaki fragment synthesis, which are subsequently removed during Okazaki fragment maturation [71].

Single-strand breaks

The sugar-phosphate backbone of DNA can also be damaged [72]. Discontinuities in a single strand of DNA are called single-strand breaks (SSBs) and can arise from endogenous sources such as ROS. $^{\bullet}$OH can abstract a hydrogen from deoxyribose and this oxidation ultimately leads to deterioration of deoxyribose to form AP sites or SSBs. [73, 74]. SSBs can also form during the repair of damaged bases or AP sites by enzymatic cleavage of the phosphodiester backbone by AP endonuclease [75]. Breaks in the phosphodiester backbone of DNA can also be a normal part of DNA metabolism. During transcription or replication, topoisomerase I (TOP1) relieves torsional stress by transiently forming a protein-linked SSB with the 3' end of DNA being covalently linked to TOP1 [76]. However, failure of TOP1 to religate the phosphodiester bond can lead to TOP1 becoming stuck on DNA, which is known as a TOP1 cleavage complex. If the transcription or replication machinery collides with a TOP1 cleavage complex it can lead to the formation of either a SSB or a DSB with TOP1 remaining covalently linked to the 3' of DNA in both scenarios [72, 77]. This TOP1 cleavage complex is also an example of an aforementioned protein-DNA crosslink. A failure to repair SSBs has been linked with neurodegeneration and the potential conversion of SSBs into the more clastogenic DSBs, which can lead to genomic instability [72, 78, 79].

Double-strand breaks

Breaks in the sugar-phosphate backbone of both strands of DNA in close proximity to one another is known as a double strand break (DSB) [80]. This form of damage can arise from a plethora of exogenous and endogenous sources such as ionising radiation, genotoxic agents or nucleases. DSBs can also be generated as a result of the DNA replication machinery encountering other lesions in the DNA [81]. DNA lesions such as pyrimidine

dimers or alkylated bases impede the processivity of the DNA polymerase, an event which can lead to the replication fork becoming stalled. Persistently stalled forks can eventually collapse and DSBs can be generated as a result of nuclease activity in an attempt to restart the replication fork [82].

Alternatively, DSBs can be generated from exogenous sources such as ionising radiation in an S-phase independent manner [80]. Ionising radiation creates hydroxyl radicals through the radiolysis of water that then attacks DNA and leads to the deterioration of the deoxyribose of DNA, similar to that described in the aforementioned SSB section. Ionising radiation results in the 3' ends of the DNA break possessing a 3'-phosphate or 3'-phosphoglycolate instead of the 3'-OH end that is typically generated as a result of nuclease activity [83]. Consequently, these break ends require further processing before effective repair can take place.

Regardless of their source, a failure to repair DSBs can lead to catastrophic genetic alterations such as deletions, translocations and inversions [80]. Owing to the highly mutagenic nature of DSBs, this form of damage frequently contributes to the development of cancer. However, cells can also use DSBs to their advantage. The intentional generation of DSBs can be used to induce genetic rearrangements between homologous chromosomes during meiosis or to generate antibody diversity in lymphocytes through V(D)J recombination [84]. Together, these endogenous processes use the mutagenicity of DSBs to generate near infinite diversity in a finite genome.

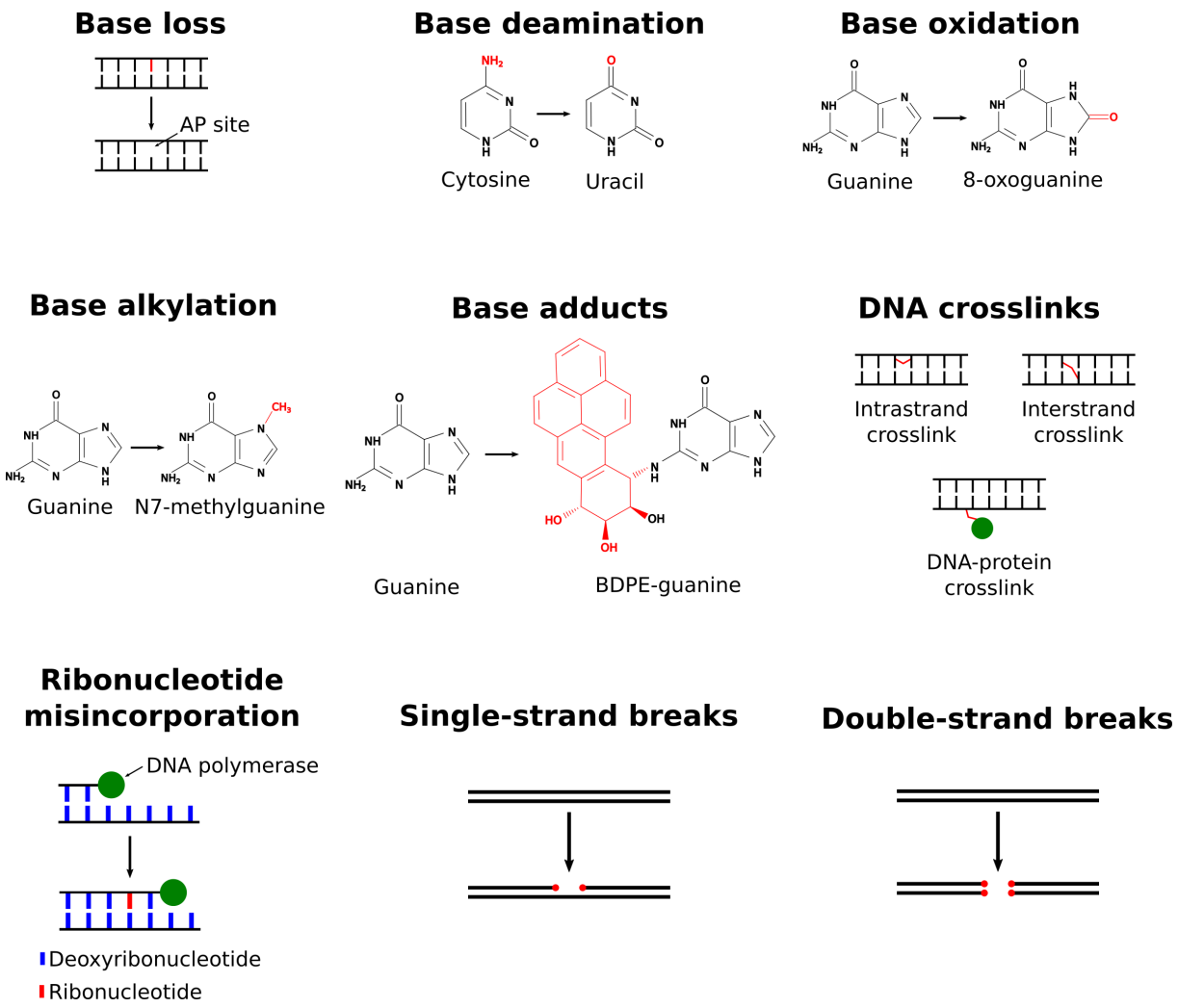


Figure 1.1: Representative examples of different types of DNA damage.

1.3 DNA damage kinases

Akin to other signalling pathways, the DDR relies on sensors, transducers, and effectors to coordinate a variety of responses to damaged DNA [6]. In this signalling pathway, it is the aberrant DNA that is the signal which can be recognised by sensor protein complexes. Transducers then interact with these sensor proteins to activate and amplify the DDR signalling. These activated transducers are typically kinases which phosphorylate and activate downstream effector proteins to modulate a vast array of cellular processes such as DNA repair, DNA replication, transcription, cell cycle arrest, and apoptosis. Within

vertebrate cells, the master regulatory kinases ATM, ATR and DNA-PK are responsible for the orchestration of these cellular processes in response to DNA damage [6].

ATM

ATM is involved in the cellular response to DSBs [6]. The recruitment of ATM to DSBs involves its direct interaction with NBS1, a member of the MRE11-RAD50-NBS1 (MRN) complex. In addition to interacting with the MRN complex, it has also been shown *in vitro* that MRN induces ATM kinase activity [85]. Once active, an initial event in the ATM signalling cascade is the phosphorylation of the histone variant H2AX at serine 139, a modification also known as γH2AX [86]. This modification can be observed in the chromatin up to 500 kb away from the original DSB site, creating an expansive platform of γH2AX for the recruitment of subsequent DDR proteins and chromatin remodelers [87]. ATM can also phosphorylate CHK2, a kinase, which leads to a 'second-wave' of ATM signalling and expands the reach of ATM. This second-wave involves the phosphorylation of the phosphatase CDC25A, which targets it for degradation [6]. This is an event that subsequently prevents CDC25A from removing the inhibitory phosphate and activating CDK2. When CDK2 fails to be activated, it is no longer able to interact with cyclins E or A and is therefore unable to promote DNA replication [88, 89].

The tumour suppressor p53 is also phosphorylated by ATM at S15. This phosphorylation event has been suggested to block binding of p53 by MDM2, a ubiquitin ligase, thereby stabilising p53 [90, 91]. However, such phosphorylation of p53 by ATM has also been suggested to not be involved in its stabilisation [92]. Regardless, what seems to be clear is that a plethora of substrates are phosphorylated by ATM, such as MDM2, in order to stabilise p53, rather than solely S15 phosphorylation [93]. Once activated, p53 can induce the transcriptional activation of target genes involved in cell cycle arrest or apoptosis [94, 95]. A failure to stabilise p53 prevents its genome protective activity that can lead to genomic instability and cellular immortalisation. It is therefore unsurprising that p53 is the most frequently mutated tumour suppressor in human cancer [96].

ATR

ATR is involved in the response to a wide range of DNA damage types, contrasting ATM and DNA-PK (introduced later) that are primarily activated by DSBs [6]. The recruitment of ATR to sites of DNA damage is dependent upon its direct interaction with ATRIP. This recruitment is additionally dependent on the interaction of ATRIP with RPA, a heterotrimer that binds to ssDNA [6]. This mechanistically reveals why ATR responds to a vast array of DNA damage types as ssDNA can form through multiple processes. For example, ssDNA may be generated through nuclease processing of DNA damage, such as in DSBs, or as a result of the helicase uncoupling from the polymerase during DNA replication, termed replication stress [97–99]. Due to this involvement, its unsurprising that ATR is vital for proliferating cells, unlike ATM and DNA-PK [100]. This is likely due the involvement of ATR in monitoring DNA replication, as even in unperturbed conditions cells experience low levels of replication stress [101].

Once activated at sites of DNA damage, ATR phosphorylates the kinase CHK1 which in turn phosphorylates CDC25A, promotes its degradation, and leads to inhibition of S-phase progression via CDK2 inhibition, similar to the aforementioned ATM-CHK2 pathway [102]. While ATR activity is usually confined to sites of ssDNA, such as that at stalled forks, CHK1 propagates this signal throughout the nucleus. Most notably, the activity of CHK1 prevents the firing of dormant replication origins, mediated by CDK2 [103]. Indeed, a failure to prevent unscheduled replication when a cell is under replicative stress leads to generation of excessive ssDNA. Consequently, this ssDNA is bound and protected by RPA. However, this pool of RPA is finite and RPA is quickly sequestered as more origins fire and helicases expose more ssDNA [99]. Unprotected ssDNA at sites of replication then become prone to fork breakage, generating DSBs. ATR has also been shown to phosphorylate H2AX independently of ATM in response to replication stress [104].

DNA-PK

DNA-PK is involved in the repair of DSBs. The recruitment of DNA-PK catalytic subunit (DNA-PKcs) to sites of DNA damage is dependent upon its interaction with Ku80, which in combination with Ku70, forms the Ku heterodimer [6]. This heterodimer forms a ring structure which encircles dsDNA at DSBs without any sequence specificity [105]. Ku binding to DSBs leads to the rapid recruitment of DNA-PKcs and its kinase activity is induced. This complex of Ku and DNA-PKcs is termed DNA-PK. Activated DNA-PK has been shown to phosphorylate PKB, a kinase that controls metabolism, proliferation, and cell survival [106]. PKB phosphorylation by DNA-PK induces a pro-survival signal to the cell in response to DNA damage [107]. It has also been shown that following ionising radiation that DNA-PK is able to phosphorylate ATM targets, such as H2AX, in ATM-deficient cells [108]. Furthermore, DNA-PK can be phosphorylated by both ATM and ATR under certain genotoxic stresses [109, 110]. Activated DNA-PKcs can also autophosphorylate and phosphorylated DNA-PK leads to the recruitment of break processing enzymes such as Artemis [111, 112]. Artemis endonuclease activity has the ability to remove 3'-phosphoglycolate from DNA ends, a break termini that can occur following ionising radiation [113]. The DSB ends bound by DNA-PK can also form a bridge with other DNA-PK coated DSB ends, forming what is referred to as a synapsis, bringing DNA ends that are to be ligated together in close proximity [114, 115].

Taken together, it is clear that the DNA damage kinases are partially overlapping in their signalling pathways, proffering redundant mechanisms to ensure the repair of damaged DNA. This is more apparent when you consider synthetic lethality between the kinases. For example, ATM and DNA-PK are synthetically lethal for each other, suggesting that one is able to 'pick up the slack' for the other in the repair of DSBs [116]. Furthermore, it has been observed that there exists a synthetic lethality between ATM and ATR [117]. However, a synthetic lethality is not observed between DNA-PK and ATR

[118]. Regardless, knowledge of these synthetically lethal relationships may be exploited and therefore an attractive means for treating cancers deficient in any such kinase.

1.4 DNA damage repair pathways

Direct DNA damage repair

Perhaps the most effective mechanism of DNA damage repair is the direct reversal of damage [119]. This process allows for covalent DNA adducts to be reversed without requiring incision into the DNA phosphodiester backbone, a nucleotide template or DNA synthesis. As a result, this efficient form of DNA repair is considered to be error-free and is often carried out by a single enzyme. The aforementioned O^6-alkylguanine-DNA alkyltransferases (AGTs) are direct DNA repair factors that reverse O^6 alkylation of guanine bases. This repair factor can reverse a range of guanine alkylations, such as O^6-methylguanine, O^6-ethylguanine and bulky adducts like O^6-benzylguanine [120]. Interestingly, AGT is a sacrificial protein since the alkyl group is irreversibly transferred from guanine bases to AGT. This alkylated form of AGT is then ubiquitylated and targeted for degradation [119, 121]. Base methylation can also be reversed by dioxygenases. The dioxygenase AlkB removes base methylation through a process known as oxidative demethylation from a range of substrates, such as N^3-methylcytosine and N^1-methyladenine [122, 123]. DNA damage induced by UV radiation can also be repaired directly. The aforementioned cyclobutane pyrimidine dimers (CPDs) and 6-4 pyrimidine-pyrimidones (6-4PP) can be repaired by lesion specific photolyases, which utilise visible light and the cofactor $FADH^-$ to reverse UV-light induced DNA damage [119, 124]. However, human cells do not possess a photolyase homolog to repair CPD or 6-4PP lesions and instead rely upon the less efficient nucleotide excision repair pathway, introduced later. As effective as direct DNA repair enzymes are, their specificity means that they are unable to accommodate repair of all DNA lesions. Therefore, cells use more complex pathways composed of multiple enzymes in order to repair a wider range of DNA damage types.

Base excision repair

The base excision repair (BER) pathway is able to repair a variety of DNA base damage, such as the aforementioned deamination, depurination, alkylation, and oxidation [125]. The BER pathway begins with the recognition and removal of the damaged base by damage specific DNA glycosylases that cleave the N-glycosidic base-sugar bond [126]. This leads to release of the damaged base and formation of an AP site. Next, the DNA backbone at the AP site is cleaved by APE1 which forms a nick with 3'-OH and 5'-deoxyribose phosphate terminals. Certain bifunctional glycosylases, such as those which recognise oxidised bases, are also able to cleave the DNA backbone [127]. Following cleavage of the DNA backbone, the BER pathway can continue via short- or long-patch repair. In short-patch repair, a single nucleotide is inserted by DNA polymerase β [128]. Once inserted, the nick can be ligated by DNA ligase I or DNA ligase III in complex with the scaffold protein XRCC1. In long-patch repair the DNA polymerase continues to synthesise DNA beyond the first damaged base, displacing the upstream strand and forming a DNA flap structure. The endonuclease FEN1 cleaves this flap and the remaining nick in DNA is repaired by DNA ligase I [129]. In long-patch repair, between 2-13 nucleotides are removed and replaced from the site of base damage.

Nucleotide excision repair

Nucleotide excision repair (NER) is involved in the repair of a diverse set of bulky lesions that distort the DNA double helix [130]. DNA damage that is a target for NER includes UV-induced adducts such as CPD and hydrocarbon adducts such as BPDE, which is derived from tobacco smoke [131]. The mechanism by which NER functions involves the excision of an oligonucleotide containing the aberrant base, contrasting that of BER which removes the damaged base directly. The NER pathway can be divided into two subpathways: global genomic NER (GG-NER) and transcription coupled NER (TC-NER) [132]. These two subpathways differ in the method of damage recognition, but the sequence of repair events following detection is similar.

In GG-NER, helix distortions are recognised by XPC throughout the entire genome. However, some lesions only create a mild distortion of the DNA duplex, such as CPDs, which require the action of the DDB2-DDB1 heterodimer to form a kink in the DNA that can subsequently be recognised by XPC [133–136]. Following XPC recognition of damaged DNA, TFIIH is recruited [137]. TC-NER allows for the prompt repair of lesions found on the actively transcribed strand of DNA. The first step in TC-NER is initiated by the stalling of RNA polymerase at a lesion. The arrested transcription machinery then triggers the recruitment of CSB, CSA, UVSSA and subsequently TFIIH [138, 139].

Both GG-NER and TC-NER following lesion recognition converge upon TFIIH binding, which melts the DNA to form a bubble surrounding the lesion [132]. Next, XPA and RPA are then recruited to form the pre-incision complex. The oligonucleotide containing the damaged DNA is then excised at the 5' by ERCC1-XPF and at the 3' by XPG. The resulting gap is filled by either DNA polymerase $\delta/\epsilon/\kappa$ in complex with PCNA-RFC-RPA [140]. The final ligation step is performed by DNA ligase I in replicating cells or by DNA ligase III-XRCC1 in quiescent cells [131].

Mismatch repair

A mismatch is when the binding partner of a base is incorrect [141]. Mismatches can occur as a result of nucleotide misincorportation during DNA replication, by chemical modification of the base or from recombination between slightly different sequences. The process involved in the repair of these mismatched bases is termed mismatch repair (MMR). However, a number of the steps in the MMR process still remain hypothetical [141]. Regardless, the current experimental observations of the MMR pathway satisfies the prominent molecular switch/sliding clamp model [142]. In eukaryotes, this model posits that the mismatch is recognised by MSH proteins (MSH2-6 or MSH2-3 heterodimers) which bind and form closed clamp-like structures that translocate along the DNA, away from the lesion. Then, these sliding clamps recruit the MLH-PMS heterodimer which

nicks the newly synthesised DNA strand containing the error. The nascent DNA strand is then degraded by EXO1, though it is believed that EXO1-independent mechanisms also exist [143]. The resulting gap is then filled by DNA polymerase δ in unison with PCNA, RFC, and RPA. The newly synthesised strand is then ligated by DNA ligase I [144, 145].

Crosslink repair

Intra- and interstrand crosslinks can be repaired by a variety of pathways [40, 41]. Intrastrand crosslinks, such as the aforementioned CPDs, are able to be repaired by the NER pathway. However, interstrand crosslinks (ICLs), such as those generated by cisplatin, require a more complex sequence of events for repair [41]. ICLs in G0/1 can also be repaired, in part, by the NER machinery. In this scenario, ERCC1-XPF excises one of the crosslinked strands which is then 'flipped out'. Translesion polymerase then synthesises DNA past the lesion and the ICL is subsequently excised entirely and the resulting gap is filled by polymerases and sealed by DNA ligases. However, translesion polymerase cannot bypass all ICLs, which can lead to what is known as a futile cycle of excision and ligation of the ICL [146]. During S-phase the replication fork can collide with ICLs that leads to the recruitment of the Fanconi anaemia (FA) proteins. The FA pathway then 'unhooks' the ICL by making dual incisions either side of the lesion, thereby uncoupling the sister chromatids, forming a DSB on one chromatid and an flipped out ICL on the other[147, 148]. The strand containing the ICL is bypassed by translesion polymerase and then the DSB is repaired by HR. Alternatively, the DNA glycosylase NEIL3 can cleave the N-glycosidic bond of one of the two crosslinked bases thereby 'unhooking' sister chromatids at the expense of generating an AP site but circumventing the formation of a DSB [149]. This AP site can then bypassed by translesion polymerases and the AP site repaired by base excision repair machinery.

DNA-protein crosslinks can arise between any nuclear protein and DNA. Thus, the DNA-protein crosslink repair pathway is general in its recognition of these lesions [54]. In order to accommodate repair of a diverse range of DNA-protein crosslinks, repair

subpathways can target one of three characteristics of DNA-protein crosslinks. These include: the DNA, which can be cleaved by nucleases; the protein, which can be degraded by proteases; or the crosslink itself, which can be hydrolysed in order to release the trapped protein. These subpathways are not mutually exclusive and can work in unison to resolve DNA-protein crosslinks [54]. Each DNA-protein crosslink repair subpathway utilises different proteins to restore the original DNA sequence and to remove the crosslinked protein.

Subpathway choice can depend upon the nature of the DNA-protein crosslink. Protein adducts found at DSBs stimulates activation of the nucleolytic subpathway which utilises the MRN complex [150–152]. The MRN complex begins by performing an endonucleolytic incision into one strand downstream, away from the DSB with protein crosslink. Then, MRN resects the nick in the 3'-5' direction before making another incision into the complementary strand [153]. This event releases the end fragment of DNA with the protein crosslink [151, 152]. The resulting cleansed DSB can then repaired by non-homologous end joining and homologous recombination, introduced later. Some DNA-protein crosslinks can be repaired by direct hydrolysis of the crosslink. For example, TOP1 cleavage complexes possess a bond between the 3' end of a SSB and a tryosine residue in the active site of TOP1 [154]. Tyrosyl-DNA phosphodiesterase 1 (TDP1) can efficiently cleave this crosslink between TOP1 and DNA [154]. However, TDP1 requires partial proteasomal degradation of TOP1 in order to grant access to the crosslink [155, 156]. Following hydrolysis of the crosslink by TDP1, the remaining SSB is repaired by the SSB repair machinery, introduced later [157]. DNA-protein crosslinks can also be repaired by proteases. This process is triggered by stalling of DNA synthesis or DNA unwinding [158]. Stalling of either the helicase or polymerase triggers the recruitment of the DNA-protein crosslink protease spartan (SPRTN) [159–163]. The crosslinked protein is then almost entirely degraded by SPRTN, leaving behind only a small peptide linked to DNA. Translesion polymerase can then be recruited to bypass this remaining peptide [158]. It has also been hypothesised that the NER pathway could conceivably remove the crosslinked peptide following proteolysis [54].

Ribonucleotide excision repair

Ribonucleotides that are misincorporated into DNA can be repaired by the ribonucleotide excision repair (RER) pathway [164]. Following misincorporation, the ribonucleotide can be recognised by the enzyme RNase H2, which cuts the 5'-phosphodiester backbone of DNA at the ribonucleotide site [165]. Following incision into the DNA backbone, DNA polymerase δ or ϵ synthesise new DNA at the damage site and displace the original strand [164]. This process forms a flap structure that can then be cleaved by the endonuclease FEN1 or degraded by the exonuclease Exo1 [164]. The final step in RER involves sealing of the nick by DNA ligase I [164].

Single-strand break repair

Single-strand breaks (SSBs) are discontinuities in one of the strands of DNA [72]. SSBs can form indirectly during BER by incision of the DNA at AP sites by APE1 or by bifunctional glycosylases. Typically, these indirect breaks are a step in the normal BER pathway. Direct SSBs can form as a result of the aforementioned ROS and abortive topoisomerase I activity. Direct SSBs are recognised by PARP1 or PARP2, which upon DNA binding are activated and auto-modify to form poly-ADP-ribose chains [166, 167]. PARP1 activation promotes the recruitment of XRCC1, a scaffold protein and core component of the SSB repair machinery. XRCC1 then supports DNA repair by recruiting enzymes to process SSB break termini into conventional 3'-OH and 5'-phosphate moieties prior to ligation. This termini processing can also occur in the BER pathway [72, 168]. Specifically, break termini containing 3'-phosphates and 3′-phosphoglycolate can form following oxidative damage with the former being repaired by PNKP and the latter by APE1 [169, 170]. SSBs arising from abortive TOP1 activity have the 3'-TOP1 complex hydrolysed by TDP1 [171]. The final ligation step in SSB repair can also fail, leading to the formation of 5'-AMP, a termini that is processed by aprataxin [172]. Following end processing to 3'-OH and 5'-phosphate, any intervening gap in the DNA can be filled by various DNA polymerases, such as polymerase β [173]. The XRCC1-dependent recruitment of DNA ligase III can

then seal the remaining nick in the DNA, which also possesses redundancy with DNA ligase I but recruitment of DNA ligase I requires interaction with PCNA rather than XRCC1 [174–176]

Double-strand break repair

Double-strand breaks (DSBs) can be repaired by a variety of pathways depending on the cellular context, such as cell cycle phase [80, 177]. The predominant pathways involved in DSB repair are non-homologous end joining (NHEJ) and homologous recombination (HR). However in conditions where these pathways components are unavailable, alternative pathways are utilised to ensure the repair of potentially clastogenic DSBs.

The NHEJ subpathway called classical NHEJ (cNHEJ) facilitates the joining of two DNA ends with limited homology and does not require an intact repair template [80]. This repair pathway is triggered by the recognition of blunt end DSBs by Ku70 and Ku80, which subsequently recruits DNA-PKcs. Following the formation of a synapse between DNA ends, additional NHEJ factors are recruited and the DSB is ligated by DNA ligase IV and XRCC4 [178]. However, prior to ligation, the synaptic complex can shift between short- and long-range states. End processing enzymes such as PNKP have been suggested to only repair DNA ends in the short-range state [179]. Shifting between these two states also allows for the diverse range of possible DNA ends to be effectively processed and end compatibility checked prior to ligation. Due to the NHEJ pathways involving the ligation of broken DNA ends with minimal homology, it is often regarded as being error prone, as used to its benefit in CRISPR-Cas9 gene editing [180]. However, despite the absence of a repair template, the cNHEJ pathway is believed to be predominantly error-free [181]. Moreover, in cells treated with ionising radiation, its predicted that up to 80% of DSBs outside of S-phase are repaired by DNA-PK dependent cNHEJ [182].

When cNHEJ components are not present, cells may resort to using alternative end joining (aEJ), which is categorised as NHEJ in the absence of cNHEJ factors [183]. The

current model for aEJ proposes that this pathway is initiated following MRN-dependent end resection of DSBs to generate 3'-ssDNA overhangs up to 100 nt in length which are rapidly bound and protected by RPA [184]. DNA polymerase θ can then displace RPA from the 3'-ssDNA in order to facilitate microhomology binding between DNA strands [185]. Next, Polθ activity can then use the opposing overhang as a template to extend the 3' DNA end and therefore stabilise the linkage between the two DNA ends prior to ligation [186]. However, DSBs repaired by aEJ are often associated with deletions at the repair site. This is believed to be caused by the 3'-ssDNA after resection annealing to microhomologies distant from the DSB site, making this a mutagenic form of repair [187].

The single-strand annealing (SSA) pathway for repairing DSBs is similar to aEJ in that they both require end resection to reveal sequence homology [188]. However, SSA requires additional sequence homology prior to annealing, therefore requiring extensive end resection. This resection can be performed by the nucleases EXO1 or DNA2 [189]. The resulting 3'-ssDNA overhangs are then coated by RAD52 which mediates the annealing of ssDNA tails. However, because SSA relies on the annealing of homologous repeat sequences, the binding between ssDNA strands is imperfect, leading to deletions between repeats at sites of damage [188]. Tails of the 3'-ssDNA that do not anneal are then be cleaved by the NER component XRCC1-XPF, which emphasises the often overlapping nature of DNA damage repair [190].

Homologous recombination (HR) is the other major pathway involved in the repair of DSBs [7]. While NHEJ can occur throughout the cell cycle, HR is only available to the cell when there is an intact sister chromatid to act as a repair template [177]. HR is initiated following the resection of a DSB by the MRN complex to expose ssDNA which is then rapidly bound and protected from degradation and secondary structure formation by RPA [191]. BRCA2, in complex with BRCA1 and PALB2, then loads RAD51 onto RPA-coated ssDNA which forms a nucleoprotein filament. The RAD51 nucleoprotein filament initiates the homology search by invading the template DNA duplex [191]. This

then leads to the formation of a three strand repair intermediate involving the invading strand, its bound complementary strand, and the displaced, unbound strand of the invaded duplex, collectively known as the displacement loop (D-loop) [191, 192]. The 3' end of the invading strand can then be elongated by DNA polymerase δ using the invaded duplex as a template to restore the original sequence [193]. For HR to complete, the nascent strand can dissociate and anneal to the other end of the DSB, followed by ligation. Alternatively, the second end of the DSB can also be captured and extended by DNA polymerase, leading to the formation of an interlaced DNA intermediate, flanked by two Holliday junctions (HJ) [191]. HR in this scenario is concluded by HJ dissolution by helicases or resolution by nucleases, which, depending on cleavage orientation, can lead to genetic crossover as seen in meiotic gene conversion [194, 195].

It is clear that DSBs can be repaired by a variety of pathways but which pathway is selected is context dependent. The two predominant DSB repair pathways, cNHEJ and HR, are restricted to particular stages of the cell cycle [177]. For breaks in G1 and G2, cNHEJ is the pathway of choice. However, in mid S-phase, when DNA replication is highest, DSBs are repaired primarily by HR [196]. This is likely due to HR being essential in the repair of one-ended DSBs which arise when the replication fork encounters a SSB [197]. Furthermore, under conditions of replication stress, the fork can become stalled or even reversed and can utilise HR to faithfully restart replication [198]. However, the kinetics of HR are slower than cNHEJ, which, in addition to a lack of DNA replication, may explain why cNHEJ is predominant in G2 phase, despite the presence of a sister chromatid [199]. The more mutagenic repair pathways SSA and aEJ are considered to be opportunistic, repairing DSBs that have failed to be repaired by the preferred cNHEJ and HR pathways.

1.5 ADP-ribosylation

ADP-ribosyltransferases

ADP-ribosylation is catalysed by enzymes which are collectively known as ADP-ribosyltransferases (ARTs) [200, 201]. Some ARTs transfer only a single ADP-ribose unit onto the target molecule, which is known as mono-ADP-ribosylation (MARylation). Other ARTs following the transfer of the initial ADP-ribose unit can attach subsequent ADP-ribose units through a glycosidic ribose-ribose bond to form chains of up to 200 ADP-ribose units in length in a process that is known as poly-ADP-ribosylation (PARylation) [202]. Some ARTs are also able to catalyse branching within PAR chains that can occur every 20-50 ADP-ribose units [202]. The molecular targets for ADP-ribosylation so far include protein, DNA, RNA, and small molecule antimicrobials [203–206]. For protein-based modification, target residues for ADP-ribosylation can change depending on the ART and the context in which it was activated. Modified protein residues include glutamate, aspartate, lysine and serine, among others [207–209]. The modification of nucleic acids has also been shown to occur on different sites, such as on DNA bases or on phosphates at DNA and RNA ends. The ADP-ribosylation of DNA will be discussed in more detail later.

The ART superfamily is tremendously diverged at the sequence level [210]. However, all ARTs possess a strongly conserved fold that is their catalytic domain and source of transferase activity [200, 201]. Conserved residues found within this core fold have allowed for ARTs to be categorised into distinct families [211]. Of these reported families, the best characterised are: Diphtheria toxin-like ADP-ribosyltransferases (ARTDs), also known as poly-ADP-polymerases (PARPs), and cholera toxin-like ADP-ribosyltransferases (ARTCs) [210]. There are 17 identified PARPs in mammalian cells but contrary to what the name may suggest, only a subset of them catalyse the formation of PARylation [200]. PARPs 1-2 and PARPs 5a and 5b (aka Tankyrase 1 and Tankyrase 2) can form poly-ADP-ribose (PAR) chains, whereas PARPs 3, 4, 6, 10, 14, 15 and 16 only catalyse MARylation. PARPs

9 and 13 posses no ART activity at all, which is deemed to be a consequence of no NAD^+ binding site [212].

Of all the PARPs, PARP1 has been the most intensely studied [213, 214]. PARP1 has been shown to bind both SSBs and DSBs through its N-terminal zinc finger domains and acts as an early sensor for DNA damage [215, 216]. PARP2, a close homologue of PARP1, is also involved in the initial response to DNA damage [166]. It has recently emerged that serine becomes the major residue to be ADP-ribosylated following DNA damage. This shift of preferred ADP-ribosylation target is dependent upon the interaction of PARP1 or PARP2 with the protein cofactor HPF1 [217–220]. After PARP1 binds to DNA damage, PARP1 undergoes a conformational change that leads to the release of an auto-inhibitory domain from its active site [221, 222]. Once activated, PARP1 then forms PAR chains on itself and target substrates, such as histones, which can act as a scaffold to recruit DDR proteins involved in pathways such as SSB and DSB repair. For example, upon SSB binding, PARP1 forms PAR chains that facilitates the recruitment of the SSB repair scaffold protein XRCC1 [223, 224]. The recruitment of XRCC1 can also be facilitated by PAR chains generated by PARP2 [167]. Following the recognition of DSBs, PARP1 has been suggested to participate in various modes of DSB repair [166]. For example, PARP1 is involved in promoting DNA end resection during HR through the PAR-dependent recruitment of MRE11. This PAR-dependent recruitment of MRE11 has also been implicated in the end resection step of the aEJ pathway [225]. Alternatively, the activity of PARP1 at DSBs can promote the PAR-dependent recruitment of CHD2, which in turn can recruit the NHEJ factors XRCC4 and DNA ligase IV [166, 226]. Furthermore, the action of PAR and CHD2 at sites of DNA damage relaxes the chromatin structure, which is believed to grant DNA repair proteins access to the DNA, thereby facilitating effective DNA damage repair [226].

Pathogenic bacteria during infection can also utilise ART exotoxins to disrupt host metabolism. Diphtheria toxin from *Corynebacterium diphtheriae* once inside human cells

MARylates eukaryotic elongation factor 2 (eEF2) [227]. Following MARylation, eEF2 fails to associate with other components of the translation machinery, thereby blocking protein synthesis in the host. The pathogenic mechanism of *Vibrio cholera* also relies on protein MARylation [228, 229]. Once the toxin has infiltrated the host cell, cholera toxin MARylates the alpha subunit of heterotrimeric G-proteins that subsequently leads to constitutive activation of the host adenylate cyclase. In turn, this causes an increase in cyclic AMP concentration and leads to secretion of Cl^- and water from epithelial cells infiltrated by the pathogenic bacteria. This ultimately results in the dehydration and electrolyte loss that is associated with cholera pathogenesis [228, 229].

ADP-ribosylhydrolases

Enabling the dynamic nature of ADP-ribosylation are the enzymes collectively known as ADP-ribosylhydrolases [200]. ADP-ribosylhydrolases hydrolyse the bond linking ADP-ribose to the target molecule or bonds linking multiple ADP-ribose units together in PAR chains. The ADP-ribosylhydrolase primarily responsible for ADP-ribose catabolism in human cells is the macrodomain containing protein PARG, an enzyme that is able to cleave the ribose-ribose bond within PAR chains [230, 231]. PARG possesses both exo- and endo-glycohydrolase activity leading to the release of ADP-ribose units or PAR chains, respectively, but seems to predominantly function as an exo-glycohydrolase [232, 233]. The presence of PARG is essential to constrain excessive PAR production in response to replication stress. PARG-depleted cells treated with the replication inhibitor hydroxyurea display elevated levels of PAR that impacts the binding of RPA to ssDNA and eventually leads to replication fork collapse [234]. The development of a novel class of small molecule PARG inhibitors (PARGi) has also revealed new sites of endogenous PARP activity in the absence of genotoxic stress [235, 236]. By utilising short incubations with PARGi it was revealed that PARP activity is partially involved in Okazaki fragment maturation during S-phase. In this scenario, it is proposed that PARP-dependent SSB repair is involved in the ligation of some Okazaki fragments [236].

However, PARG is unable to cleave the linkage between target proteins and the substrate-linked ADP-ribose unit [200]. The final ADP-ribose units can instead be removed by ADP-ribosylhydrolases such as MacroD1, MacroD2, and TARG1. MacroD1 and MacroD2 are specifically mono-ADP-ribosylhydrolases that cleave the O-glycosidic ester bond between ADP-ribose and aspartate or glutamate residues [237]. TARG1 also contains a macrodomain but its catalytic mechanism is suggested to be distinct from other macrodomains, such as those in MacroD1 or PARG [238]. The catalytic dyad of TARG1 also shows similarities to the DNA glycosylase OGG1 [239]. TARG1 has been shown *in vitro* to cleave both MAR and PAR from glutamate and aspartate residues. Moreover, patients deficient in functional TARG1 have been shown to develop a neurodegenerative disorder [239]. When overexpressed, TARG1 has been shown to shuttle between nucleoli and the nucleoplasm and TARG1 re-locates to sites of DNA damage in a PAR-dependent manner [239, 240]. Furthermore, TARG1 was suggested to interact with ribosomes and factors involved in ribosome biogenesis, likely during its nucleoli localisation, but a physiological role for these interactions is unknown [240]. Loss of TARG1 has also been linked to elevated levels of transcription but the pathophysiological relevance of this remains to be determined [241].

Other ADP-ribosylhydrolases that can remove ADP-ribose are members of the ADP-ribose hydrolase (ARH) family [242]. Humans encode three ARH proteins: ARH1, ARH2, and ARH3. ARH1 is reported to be an active arginine hydrolase and has been shown to protect mice against cholera toxin [243]. ARH2 is catalytically inactive against ADP-ribosylated substrates [244]. ARH3 has been shown to effectively hydrolyse serine linked ADP-ribose [245]. In addition to cleaving the serine-linked ADP-ribose, ARH3 can also hydrolyse PAR, albeit not as effectively as PARG [246]. Interestingly, the aforementioned MacroD1, MacroD2 and TARG1 are unable to hydrolyse serine linked ADP-ribose, demonstrating the importance of ARH3 in reversing DNA damage dependent ADP-ribosylation.

ADP-ribose readers

Due to the addition of negatively charged and potentially large ADP-ribose chains to target molecules, ADP-ribosylation can act as a protein recruiting scaffold [201]. This recruitment relies on the presence of ADP-ribose 'reader' domains within the protein that can bind ADP-ribose. The classical and best characterised ADP-ribose reader domains are as follows: PAR-binding motifs (PBMs), tryptophan-tryptophan-glutamate (WWE) domains, PAR-binding zinc finger (PBZ) domains, and the aforementioned macrodomains [200, 213]. PBM, WWE and PBZ domains are able to bind PAR whereas the macrodomain can bind both MAR and PAR. These ADP-ribose readers are best studied in the context of DDR protein recruitment to sites of DNA damage. For example, the DNA repair protein APLF is recruited to sites of damage via interaction of its PBZ domains with PAR [247]. Additionally, the E3 ubiquitin ligase RNF146 utilises its WWE domain for its recruitment to sites of PAR [248, 249].

DNA ADP-ribosylation

Traditionally, ADP-ribosylation has been studied as a protein modification. However, growing research demonstrates that the PARP enzymes and other ARTs can ADP-ribosylate DNA [250]. A possible explanation for the delay in the study of DNA ADP-ribosylation, when compared to its protein counterpart, could be down to the similarity of ADP-ribose to nucleic acids or the lability of the linkage between ADP-ribose and DNA, both of which could make the modification difficult to detect. However, as new methods are developed to detect DNA ADP-ribosylation and new DNA modifying ARTs are discovered, a new dimension of ADP-ribosylation regulation may be revealed.

The first report of DNA ADP-ribosylation came from the cabbage butterfly protein pierisin, a member of the ARTC family [251]. It was revealed that pierisin MARylates the N2 position of guanine in dsDNA. The physiological role of pierisin was proposed to be a defence factor against parasites [252]. Alternatively, because pierisin induces

cell death and shows increased expression in larvae stages, it was also suggested to be involved in metamorphosis, inducing apoptosis in order to facilitate the removal of larvae cells during development [253]. This strong induction of apoptosis was also observed when pierisin was introduced into HeLa cells, a human cancer cell line [254, 255]. The response of HeLa cells to pierisin intoxication may suggest that the ADP-ribosylation of DNA catalysed by pierisin is unable to be reversed by ADP-ribosylhydrolases or that the pierisin overwhelms the cell with a burden of damage that is outwith its ability to repair. Following the discovery of pierisin, other closely related ADP-ribosylating toxins were also discovered, such as CARP-1 from the edible clam *Meretrix lamarckii*, which was revealed to similarly MARylate the N2 group of guanines in dsDNA [256]. Furthermore, the proteins Sco5461 from *Streptomyces coelicolor* and Scabin from *Streptomyces scabies* can also modify guanines in dsDNA [257, 258].

It is known that PARP1-3 are involved in DNA repair through auto-modification or ADP-ribosylation of target proteins [213, 214]. However, recent work has revealed that, *in vitro*, PARP1-3 can also modify DNA, with PARP1-2 PARylating and PARP3 MARylating DNA substrates [259–262]. PARP1 has been shown to modify 5'- and 3'-phosphates of ssDNA and dsDNA [259]. PARP1, PARP3 and PARP10 were also shown to ADP-ribosylate 5'-phosphates in recessed DNA [260]. PARP1 and PARP10, but not PARP3, were shown to ADP-ribosylate 3'-phosphates in recessed DNA [260]. Additionally, it has also been suggested that PARP1 may have a preference for ADP-ribosylation of 3'-phosphates over its own auto-modification, suggesting that in the correct DNA context this could be an abundant modification *in vivo* [263]. PARP2-3 seem to preferentially modify the 5'-phosphates in a DNA duplex [260–262]. It was also revealed that the hydrolases TARG1, MacroD2, ARH3 and PARG are effective at reversing the PARP1 or PARP3 catalysed phosphate-linked ADP-ribosylation of DNA [260]. Interestingly, TARG1, MacroD2, and ARH3 have been shown to remove MARylation on protein substrates but PARG shows no such activity [200]. It is curious in the case of DNA ADP-ribosylation that PARG is able to remove the final ADP-ribose unit, perhaps due to less steric hindrance at

sites of DNA ADP-ribosylation when compared to protein ADP-ribosylation or due to similarity between the phosphate-linked ADP-ribose and the ribose-ribose bonds found in PAR chains. Other enzymes that are closely related to PARPs have also been shown to ADP-ribosylate phosphates on DNA ends [264, 265]. Previous work has demonstrated that tRNA 2′-phosphotransferase 1 (TRPT1/Tpt1/KptA) from bacteria and fungi, which is considered by some to be the 18th PARP, can ADP-ribosylate 5'-phosphates of DNA and RNA [210, 264]. Following this, it was shown that the human homolog TRPT1 can also MARylate the 5'-phosphates of ssDNA and RNA [265].

These aforementioned studies attempt to find the preferred DNA structures required for PARP-mediated DNA ADP-ribosylation. However, it's likely that the range of ADP-ribosylated DNA structures is diverse. Nevertheless, it seems that, from *in vitro* work, not all phosphates at DNA ends are ADP-ribosylated [250]. Additional factors that may determine if the phosphate can be modified might involve the proximity of the phosphate to the PARP binding site. Alternatively, phosphate ADP-ribosylation may be additionally facilitated by other protein cofactors *in vivo* that, for example, could physically bring the phosphate within range of the catalytic site of the PARP or may further process the DNA structure, such as through end resection, to enable phosphate ADP-ribosylation.

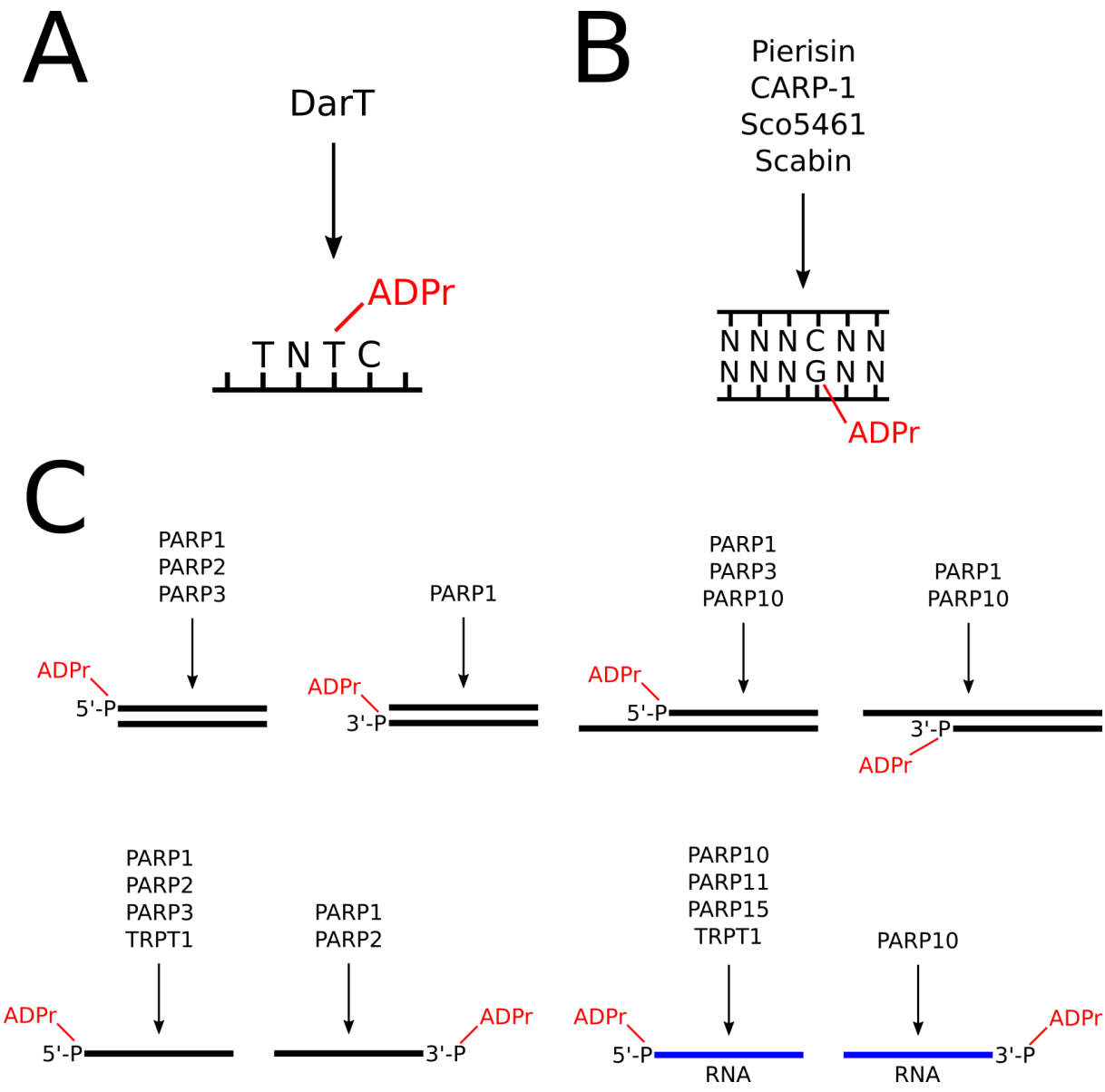


Figure 1.2: Representative examples of nucleic acid ADP-ribosylation. **(A)** ADP-ribosylation of thymidines in a TNTC motif in ssDNA by the *Thermus aquaticus* toxin DarT. **(B)** ADP-ribosylation of guanines in dsDNA by pierisin, CARP-1, Sco5461 or Scabin. **(C)** Examples of phosphate ADP-ribosylation substrates modified by PARP1, PARP2, PARP3, PARP10, PARP11, PARP15, or TRPT1.

Recently, DarT, a novel DNA modifying PARP-like endotoxin from bacteria was described [203]. DarT catalyses the transfer of a single ADP-ribose unit onto thymidine bases of ssDNA in a sequence specific manner with no activity towards dsDNA, protein,

or RNA. The antitoxin of DarT is DarG, a macrodomain containing protein which shows striking structural homology to the human ADP-ribosylhydrolase TARG1. DarG is able to hydrolyse the ADP-ribose-thymidine linkage, thereby reversing the modification. DarT can be found in thermophiles such as *Thermus aquaticus* in addition to pathogens such as *Mycobacterium tuberculosis* and enteropathogenic *Escherichia coli* (EPEC) [203]. However, it is unknown if DarT can be secreted as an exotoxin under pathogenic conditions by invading bacteria [203, 266].

The physiological role of DarT in bacteria is speculative, but due to thymidine-linked ADP-ribosylation blocking DNA replication it is proposed to induce a transient state of dormancy and enabling bacterial persistence in response to challenging environmental pressures or antibiotics, such as during pathogenic conditions. Once these pressures are relieved, the activity of DarG can restore bacterial growth, thereby allowing bacteria to persist. The striking impact DarT can have on bacterial growth made the cloning of DarT difficult [203]. Routine cloning methods resulted in DarT containing mutations that rendered it catalytically inactive due to leaky expression in the transformed bacteria. However, by cloning DarT into a plasmid under the control of a repressed arabinose promoter, DarT expressed was tightly controlled and allowed for successful cloning [203].

Recent work on DarT has suggested that in the absence of DarG, RecF-mediated HR in combination with NER can repair thymidine-linked ADP-ribose lesions catalysed by an attenuated mutant of DarT from EPEC, albeit not as effectively as DarG [266]. In bacteria, RecF-mediated HR is involved in the repair of ssDNA gaps [267]. In this scenario, the thymidine-linked ADP-ribose on ssDNA is transferred to dsDNA by RecF-mediated HR. This results in a DNA duplex distortion that activates the NER pathway, which subsequently repairs the ADP-ribose lesion. This provides interesting insight into how the repair machinery perceives the thymidine-linked ADP-ribose adduct, transforming it from a ssDNA to a dsDNA lesion with one pathway, and repairing this transformed lesion with another, further demonstrating the interconnected nature of DNA damage repair.

1.6 Aim and rationale of this thesis

Growing *in vitro* evidence implicates PARPs and other ARTs in the modification of both protein and nucleic acids. However, due to the possibility that ARTs can modify multiple macromolecule types (protein and DNA, for example) within the cell, it is difficult to delineate and detect nucleic acid ADP-ribosylation specifically as it could be masked by protein-based modification. Here, we use DarT as a genotoxin to induce DNA ADP-ribosylation specifically. To achieve this, we created a system for heterologous expression of DarT in human cells in order to determine the pathways involved in response to this form of DNA damage. We find that the human ADP-ribosylhydrolase TARG1 is remarkably efficient at reversing thymidine-linked ADP-ribosylation and protects against extensive DNA damage.

There is currently no evidence that DarT is secreted into human host cells by bacteria under pathogenic conditions. However, thousands of sequenced bacterial genomes possess DarT-like sequences, including global pathogens, so it is feasible that a DarT orthologue could be used as an effector toxin during bacterial infection. Previously, it has been shown that the ADP-ribosylhydrolase ARH1 protects against the toxic effects of the bacterial ART cholera toxin during infection [243]. Perhaps TARG1 also possesses a similar protective role and defends against DNA ADP-ribosylation by DarT-like toxins.

Regardless, the unique nature of DarT modifying DNA, with no activity towards other macromolecules, allows us to specifically examine the impact DNA ADP-ribosylation can have on the cell, how this damage is perceived and how we can detect it. Together, we hope that the work in this thesis can take us one step closer to being able to delineate the targets of human ART activity and to gain insight into the nucleic acids they modify *in vivo* and under what conditions.

Chapter 2

Results

2.1 TARG1 reverses DNA ADP-ribosylation catalysed by DarT

Jankevicius and Ariza et al. recently described the DNA ADP-ribosylating toxin DarT and its antitoxin DarG [203]. This work also revealed that DarT ADP-ribosylation of DNA is reversible by the macrodomain containing antitoxin DarG. Interestingly, the macrodomain structure of DarG is strikingly similar to that of TARG1, a human ADP-ribosylhydrolase which has been implicated in removal of protein ADP-ribosylation but as yet has no defined physiological role (Figure 2.1) [239].

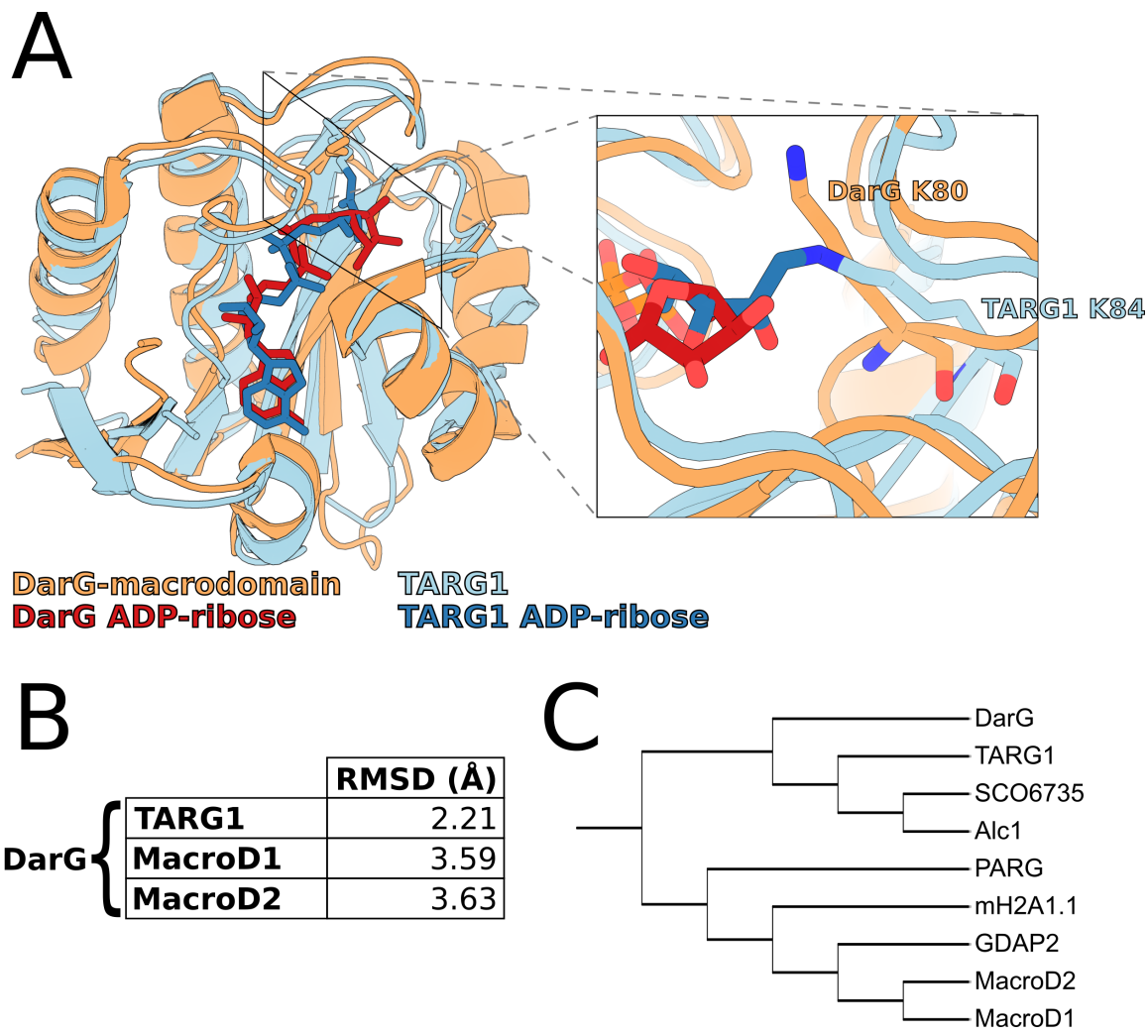


Figure 2.1: Comparison between *Taq*DarG and other macrodomains. **(A)** Superimposition of *Taq*DarG-macrodomain (orange) bound to ADP-ribose (red) and TARG1 (light blue) with a covalent lysyl-ADP-ribose linkage (dark blue). To the right is a detailed view of the DarG catalytic lysine 80 (orange sticks) and TARG1 catalytic lysine 84 (blue sticks) covalently bound to ADP-ribose (dark blue). **(B)** RMSD values for the protein mono-ADP-ribosylhydrolases TARG1, MacroD1 or MacroD2 when compared to the *Taq*DarG-macrodomain. **(C)** Phylogenetic tree of different macrodomain-containing protein sequences.

Due to this striking similarity between catalytic macrodomains, we wanted to investigate if TARG1, like DarG, can also reverse thymidine-linked ADP-ribosylation. To do so, we modified a ssDNA oligonucleotide containing a TNTC motif with recombinant DarT from

Thermus aquaticus (*Taq*). This thymidine-linked ADP-ribosylated oligonucleotide was then purified by gel electrophoresis followed by gel extraction. The purified thymidine-linked ADP-ribosylated oligonucleotide was then incubated with either DarG or TARG1 (Figure 2.2). This revealed that TARG1, like DarG, is able to reverse thymidine-linked DNA ADP-ribosylation. However, this *in vitro* reaction does not assess if TARG1 would be able to efficiently reverse thymidine-linked ADP-ribosylation within a physiological context and combat DarT toxicity, similar to DarG, in bacteria.

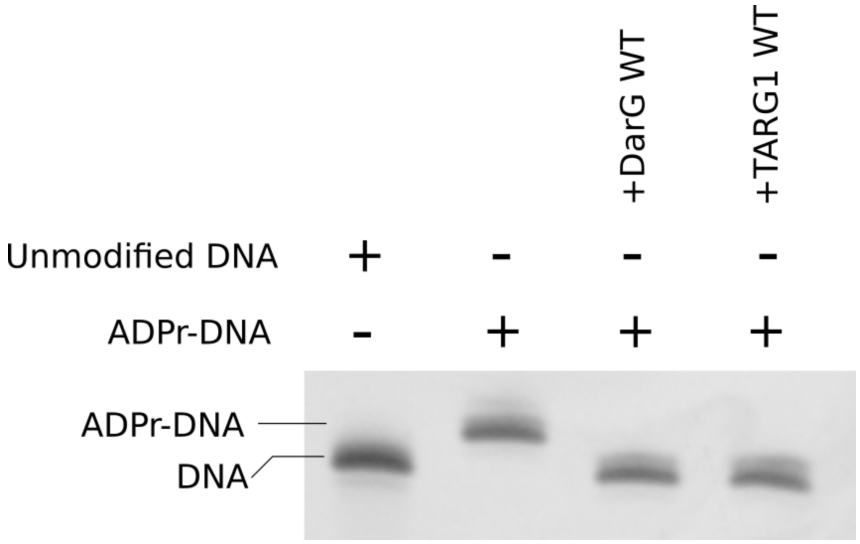


Figure 2.2: TARG1 removes thymidine-linked ADP-ribosylation from DNA. UV detection of a DarT modified DNA oligonucleotide, containing a single TNTC motif, de-ADP-ribosylation reactions with *Taq*DarG-macrodomain or TARG1

To test this, we performed a bacterial rescue assay, akin to that performed by Jankevicius and Ariza et al. [203]. We concomitantly overexpressed *Taq*DarT WT with *Taq*DarG or TARG1, or their equivalent catalytic mutants K80A or K84A, respectively, in BL21 DE3 cells. Both DarG and TARG1 were able to rescue DarT toxicity and enable bacterial growth, whereas the DarG K80A and TARG1 K84A mutations were unable to rescue DarT toxicity (Figure 2.3A, B). This suggests that TARG1 can effectively reverse thymidine-linked ADP-ribosylation and rescue DarT toxicity similar to that of DarG.

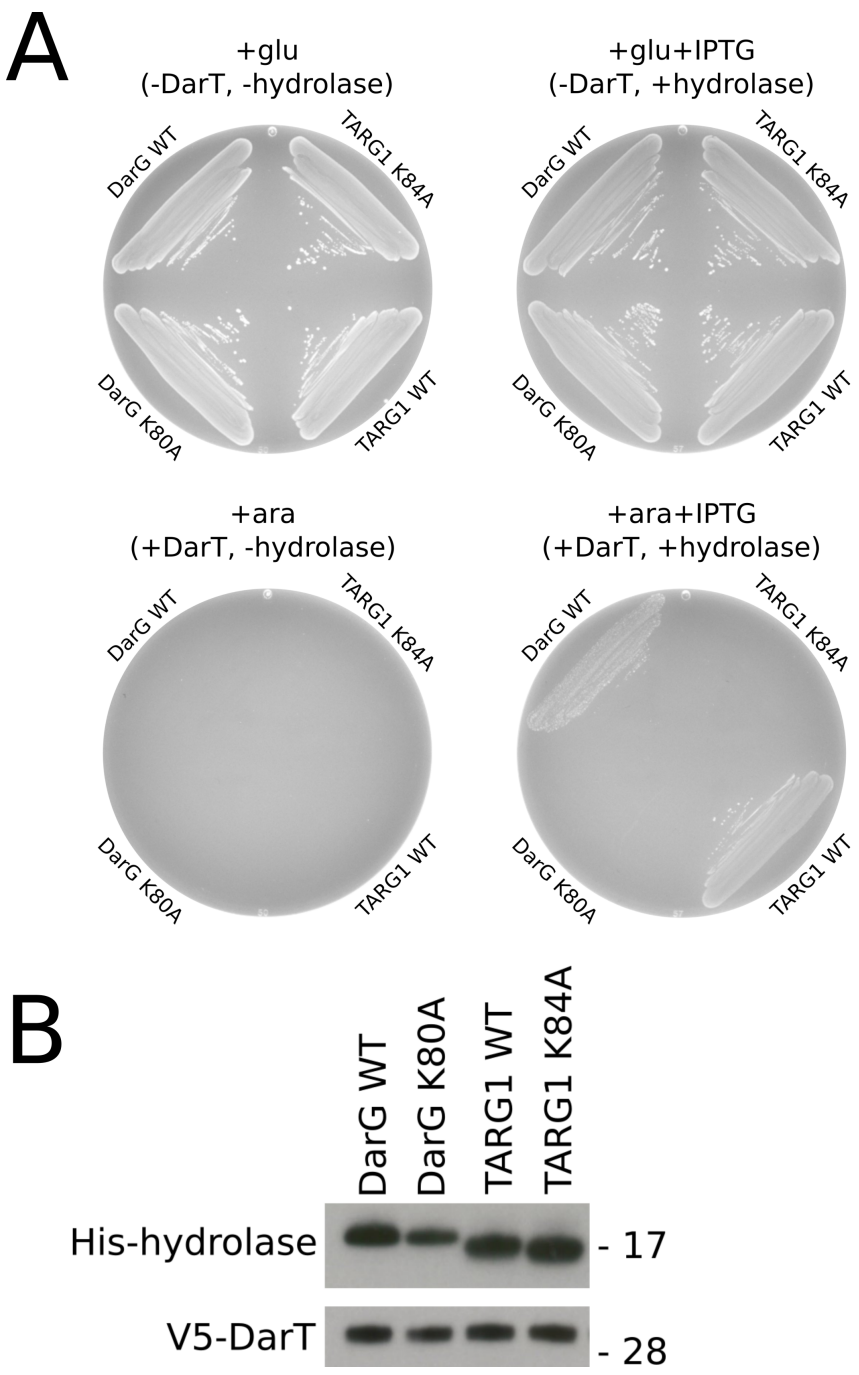


Figure 2.3: TARG1 confers resistance to DarT toxicity in bacteria. **(A)** Bacterial DarT toxicity rescue assay in BL21 DE3 using pBAD DarT and pET encoding DarG-macrodomain WT, DarG-macrodomain K80A, TARG1 WT or TARG1 K84A. pBAD expression is repressed or induced with glucose or arabinose, respectively, and pET expression is controlled with IPTG. **(B)** Cells from **A** were induced with arabinose and IPTG, lysed, and immunoblotted with the indicated antibodies to detect DarT and ADP-ribosylhydrolase expression.

Due to TARG1 being a human ADP-ribosylhydrolase, we next wanted to determine if other human ADP-ribosylhydrolases could also de-ADP-ribosylate thymidine-linked ADP-ribosylation. To test this, we performed an *in vitro* de-ADP-ribosylation assay using a thymidine-linked ADP-ribosylated oligonucleotide incubated with DarG, TARG1, ARH3, PARG, MacroD1 or MacroD2 (Figure 2.4). Interestingly, the macrodomain containing ADP-ribosylhydrolases MacroD1 and MacroD2 were able to partially, or fully de-ADP-ribosylate thymidine-linked ADP-ribosylated DNA, respectively. However, ARH3 and PARG hydrolases were unable to reverse thymidine-linked ADP-ribosylation. To investigate this further we examined if this same panel of ADP-ribosylhydrolases could also rescue DarT toxicity in bacteria. However, despite showing activity against thymidine-linked ADP-ribosylated DNA *in vitro*, MacroD1 and MacroD2 were unable to rescue DarT toxicity and (Figure 2.5A, B). ARH3 and PARG also failed to rescue. This could suggest that the ADP-ribosylhydrolase activity of MacroD1 and MacroD2 is less than that of DarG and TARG1 in a physiological context when removing thymidine-linked ADP-ribosylation and are therefore unable to overcome DarT toxicity.

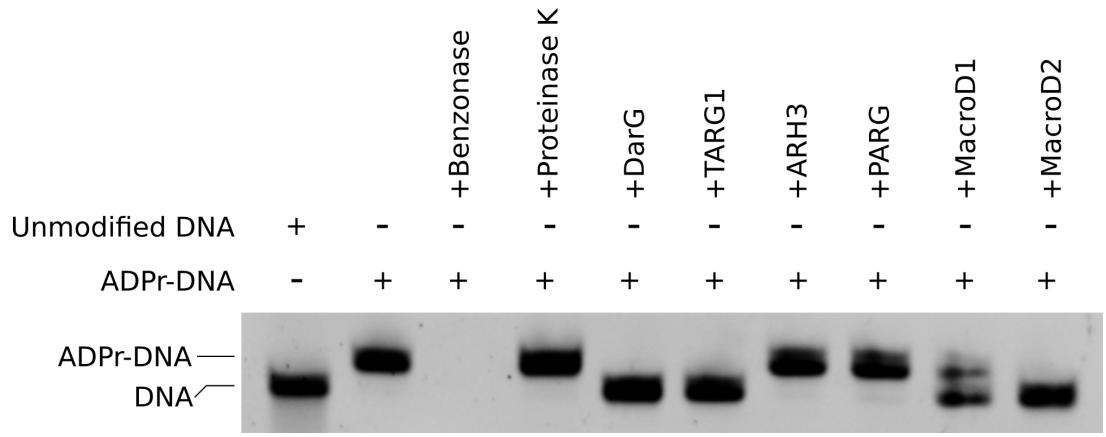


Figure 2.4: DarG, TARG1, MacroD1 and MacroD2 can remove thymidine-linked ADP-ribosylation from DNA. UV detection of DarT modified thymidine-linked ADP-ribosylated DNA oligonucleotide de-ADP-ribosylation reactions with the indicated hydrolases.

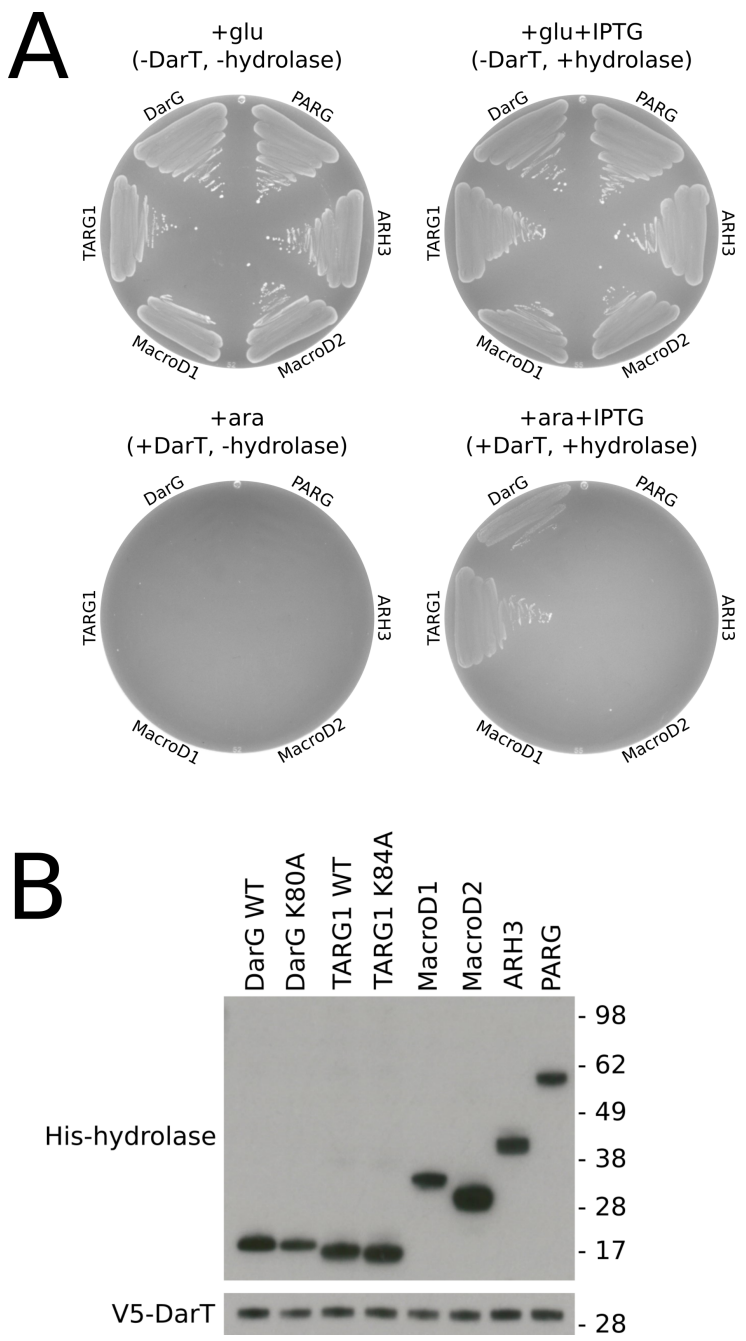


Figure 2.5: Only DarG and TARG1 but not MacroD1, MacroD2, ARH3 or PARG rescue DarT toxicity in bacteria. **(A)** Bacterial DarT toxicity rescue assay in BL21 DE3 using pBAD DarT and pET encoding DarG-macrodomain, TARG1, MacroD1, MacroD2, ARH3 or PARG. pBAD expression is controlled with glucose or arabinose and pET expression is controlled with IPTG. **(B)** Cells from **A** were induced with arabinose and IPTG, lysed, and immunoblotted with the indicated antibodies to detect DarT and ADP-ribosylhydrolase expression.

2.2 TARG1-deficient human cells are sensitive to DarT

Since TARG1 is a human ADP-ribosylhydrolase, we next began to ponder the impact the bacterial toxin DarT could have in human cells. To study this, we generated cell lines with doxycycline inducible expression of *Taq*DarT WT or the catalytic mutant E160A in either wild-type (WT) or TARG1-deficient (TARG1 KO) U-2 OS cells. U-2 OS cells were selected as attempts to make TARG1-deficient cells in other cell types failed. Additionally, U-2 OS cells are beneficial in that they have negligible DNA damage in unchallenged conditions and possess normal cell cycle profiles and replication. Additionally, U-2 OS cells are flat with high adhesion to coverslips for immunofluouresence. Together, these traits of U-2 OS cells make them an ideal model cell line for studying genotoxins. Long-term clonogenic survival revealed that DarT WT expression is cytotoxic in TARG1 KO cells (Figure 2.6A. Quantification: Supplementary Figure S1A). Interestingly, no such sensitivity was observed in WT cells treated with DarT WT. We sought to determine if this cytotoxicity in TARG1 KO cells could be rescued through knock-in of TARG1. To do so, we generated cell lines in a TARG1-deficient background that constitutively expressed untagged TARG1 WT or the catalytic mutant K84A in either the aforementioned DarT WT or E160A cell lines. In response to DarT expression, the TARG1 WT expressing cells rescued DarT cytotoxicity whereas TARG1 K84A expressing cells were unable (Figure 2.6B. Quantification: Supplementary Figure S1B).

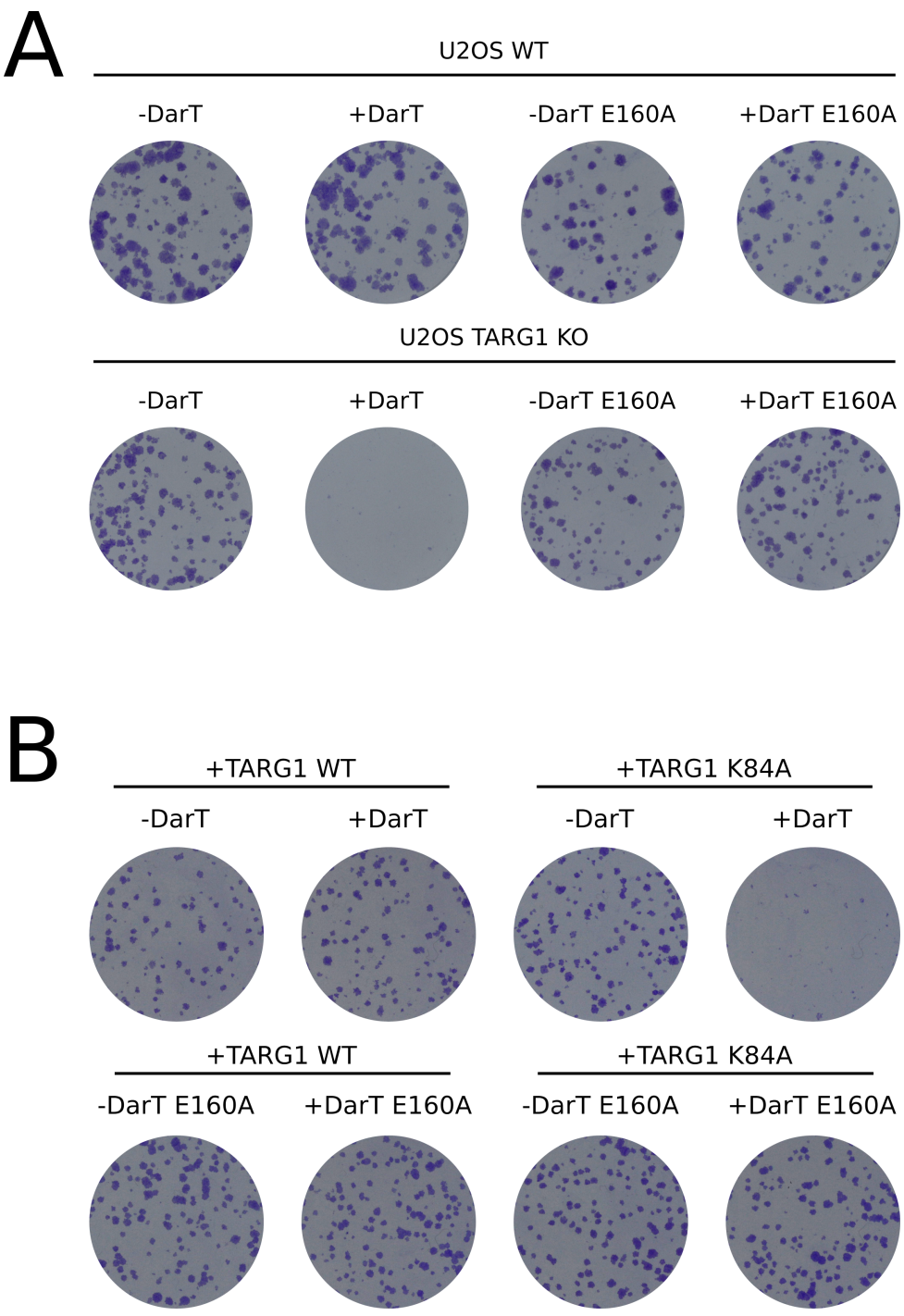


Figure 2.6: TARG1 KO U-2 OS but not WT cells are sensitive to DarT expression. **(A)** Representative images of clonogenic survival in U-2 OS WT or TARG1 KO cells expressing pLIX_403 GFP-DarT WT or GFP-DarT E160A. pLIX_403 expression controlled with doxycycline. **(B)** Representative images of clonogenic survival in U-2 OS TARG1 KO cells expressing DarT WT or E160A in the presence of constitutively expressed pLX304 TARG1 WT or TARG1 K84A.

Previous work has shown that the expression of DarT in bacteria leads to induction of the SOS response, which is the bacterial DNA damage response, as indicated by elevated levels of RecA [203, 266]. Due to DarT-mediated ADP-ribosylation being recognised as a type of DNA damage by bacteria, we wanted to determine if the DNA damage response (DDR) was also induced in human cells. In order to do so, we expressed DarT in WT or TARG1 KO cells over a 0-72h time-course. In TARG1 KO cells, a strong induction of the DNA damage markers KAP1 (pS824), Chk1 (pS317), RPA2 (pS4/8), RPA2 (pT21) and H2AX (pS139, hereafter termed γH2AX) was observed at the 24h time point (Figure 2.7). Remarkably, there was no induction of DNA damage signalling in WT cells, suggesting that the presence of endogenous TARG1 is able to completely protect these cells against DNA ADP-ribosylation by DarT. Interestingly, in DarT-treated TARG1 KO cells, some DNA damage signal markers, such as Chk1 pS317, seem to decrease over time. This could be due to DarT initially triggering replication stress and therefore ATR activation that then shifts towards ATM activation as forks begin to collapse and ATR signalling becomes futile [99]. Alternatively, it could be that this reduction in some DDR markers is a result of cell death being triggered. Future work should aim to examine the status of Chk2 phosphorylation, an ATM target, and other cell death markers for their induction over this time-course. We next wanted to examine if this induction of DNA damage could be rescued by overexpression of TARG1. To do so, we used the rescue cell lines used in figure 2.6B and reveal that constitutive expression of TARG1 is able to rescue DarT induced DNA damage but the K84A mutant is not (Figure 2.8A).

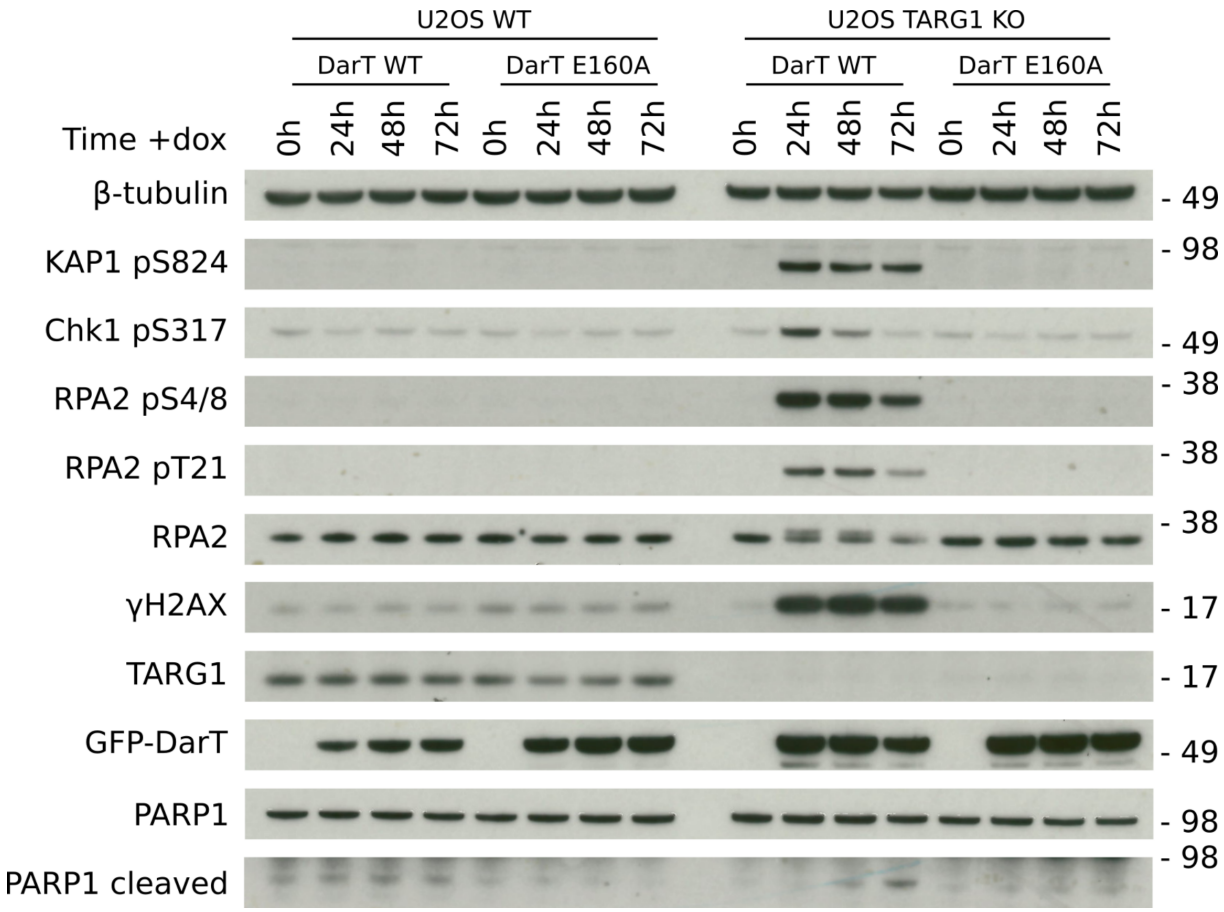


Figure 2.7: DarT expression induces DNA damage in TARG1 KO cells. Time-course induction of DarT in U-2 OS WT or TARG1 KO. Levels of DDR proteins KAP1 pS824, RPA2 pS4/8, RPA2 pT21, γH2AX and apoptosis marker cleaved PARP1 were assessed.

Recently, it was revealed that the combined actions of the RecF-mediated HR and NER pathways in bacteria can rescue the toxicity of DarT [266]. This was shown using DarT from enteropathogenic *Escherichia coli* (EPEC) which contained a G49D mutation that reduced, but did not ablate, DarT activity. The G49 residue in EPEC DarT is not conserved in *Taq*DarT. We therefore questioned if TARG1-independent DNA damage repair pathways could repair low levels of DNA ADP-ribosylation by *Taq*DarT in human cells. We reasoned that titration of doxycycline in TARG1 KO cells could reduce the burden DarT-mediated DNA ADP-ribosylation into a range that other pathways could repair. We show that as DarT expression was reduced, the DNA damage burden was also

lessened (Figure 2.8B). However, there did not exist a point at which DarT expression was detected with no induction of the DDR. This could suggest that other DNA repair pathways are unable to repair DNA ADP-ribosylation in TARG1 KO cells. However, it is instead likely that there exists a level of DarT expression that is tolerable by TARG1 KO cells but is outwith the detection range of a western blot. Future work could use more sensitive methods, such as immunofluorescence, to determine if there exists a level of DarT expression with no detectable damage. Additionally, more direct methods to measure DNA damage, such as pulsed-field gel electrophoresis or comet assay, could be used to detect DSBs directly. Inversely, it would also be of interest to titrate DarT expression in U-2 OS WT cells, or bacteria, to determine if there is a maximum level of DNA ADP-ribosylation that TARG1 can repair in WT cells.

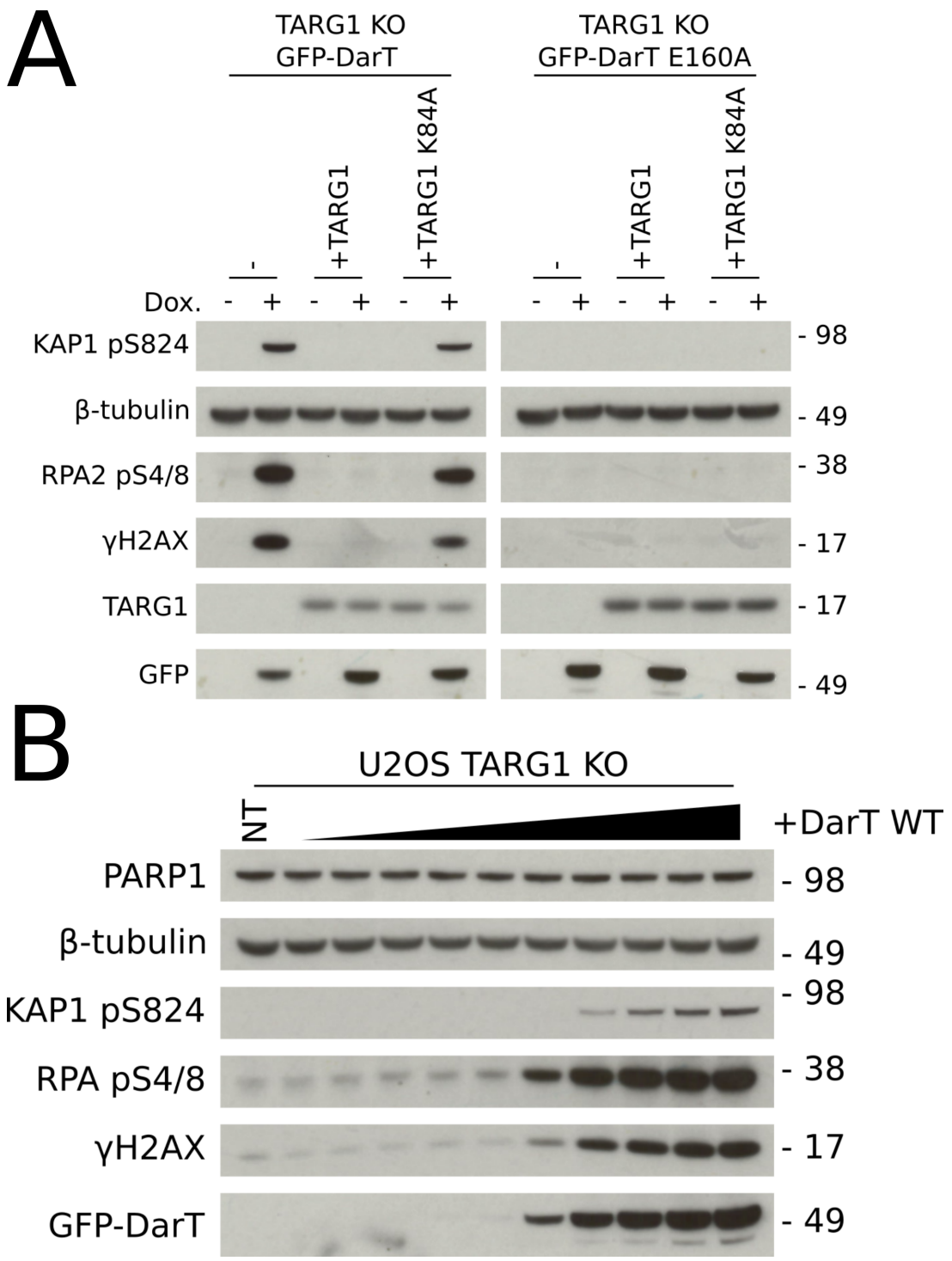


Figure 2.8: TARG1 expression rescues DarT toxicity. **(A)** U-2 OS TARG1 KO cells expressing either DarT WT or E160A (24h) in combination with constitutively expressed pLX304 TARG1 WT or K84A. Levels of DDR proteins KAP1 pS824, RPA2 pS4/9 and γH2AX were measured. **(B)** DarT expression (24h) induced in TARG1 KO cells using a titration of doxycycline.

We next wanted to compare DarT as a DNA ADP-ribosylating genotoxin against a panel of other widely used genotoxins: hydroxyurea (HU), a DNA replication inhibitor; camptothecin (CPT), a topoisomerase I (Top 1) inhibitor; and methyl methanesulfonate (MMS), an alkylating agent that methylates DNA bases. In response to HU, CPT and MMS treatment, the induction of DDR signalling is similar between WT and TARG1 KO cells, demonstrating that the DDR is not compromised between WT and TARG1 KO cells (Figure 2.9). This suggests that the damage inflicted by DarT in TARG1 KO cells is due to the direct removal of the thymidine-linked ADP-ribose lesion by TARG1 and not due to a misregulation of the DDR in TARG1 KO cells. While the magnitude of DarT induced DNA damage is greater than that of other genotoxin treatments, the pattern of damage inflicted by DarT has similarities to that of HU and CPT treatments. Since HU and CPT have been shown to cause DNA damage through the impediment of DNA replication and replication fork collapse, we postulated that DarT in TARG1 KO cells may also impact replication [268]. Indeed, it has previously been shown that DarT limits BrdU incorporation in bacteria [203, 266].

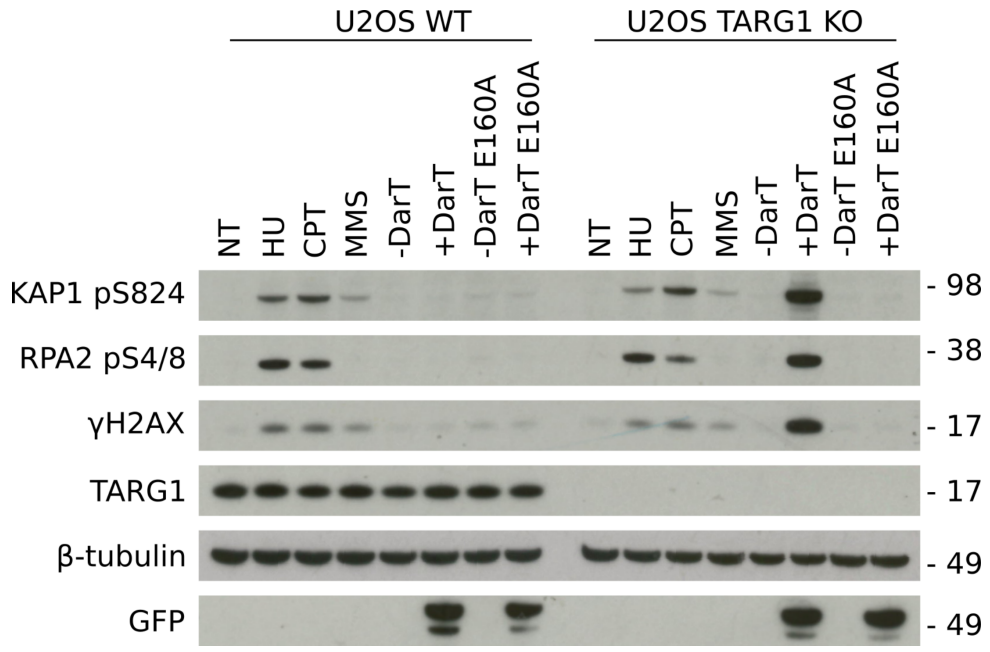


Figure 2.9: DarT induces the DDR in TARG1 KO cells. U-2 OS WT or TARG1 KO cells treated with HU (2 mM, 24h), CPT (1 µM, 1h), MMS (2 mM, 1h), DarT WT (24h), DarT E160A (24h). Levels of DDR proteins KAP1 pS824, RPA2 pS4/8, γH2AX were analysed in response to the aforementioned genotoxins.

To examine this in human cells, we evaluated the incorporation of the nucleotide analog EdU in order to measure DNA synthesis. We found that short incubations with EdU demonstrated that DarT severely impedes DNA synthesis in TARG1 KO cells, but low levels of EdU incorporation are still detectable (Figure 2.10). Interestingly, immunofluorescence also revealed that GFP-tagged DarT forms distinct, chromatin-bound foci that co-localise with sites of EdU incorporation in a subset of cells. Moreover, these foci also co-localise with chromatin-bound RPA2, a marker for ssDNA. Together, this suggests that DarT binds to ssDNA exposed at sites of DNA replication.

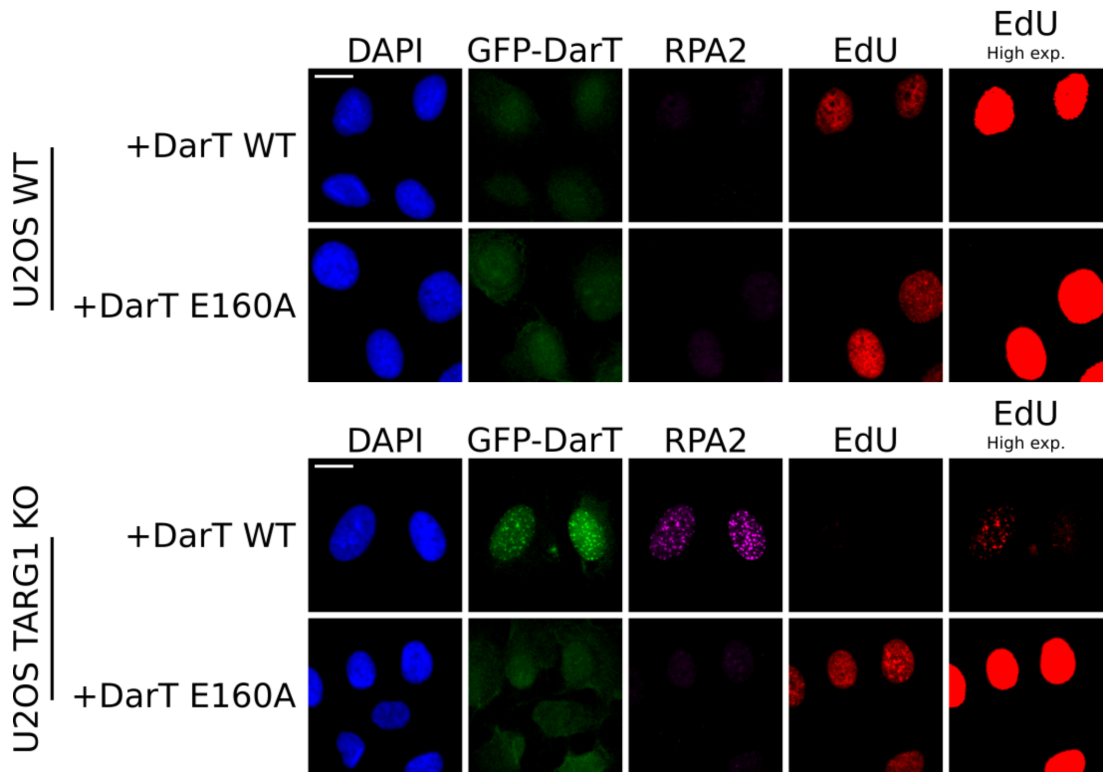


Figure 2.10: Chromatin-bound GFP-DarT co-localises with sites of ssDNA and DNA synthesis. Representative images of U-2 OS WT or TARG1 KO cells expressing DarT WT or E160A (24h). Cells were incubated with EdU (10 µM, 30 minutes) prior to pre-extraction and fixation. Cells were immunostained as indicated. Scale bar 20 µm.

To examine this further, we next developed an image analysis pipeline using automated microscopy, CellProfiler and R to perform quantitative image based cytometry (QIBC) in order to assess the incorporation of EdU over a large (>1000) population of cells at low and high DarT expression levels (Figure 2.11). QIBC revealed that for short incubations with EdU (30 minutes), low levels of DarT expression resulted in only a mild reduction of DNA synthesis when compared to uninduced DarT cells (Figure 2.12A). Higher levels of DarT expression lead to an almost complete ablation of DNA synthesis, enabling only low levels of EdU in early S-phase to be incorporated. Longer (24h) incubations with EdU suggest that DNA synthesis is able to take place in both low and high DarT expression conditions, though the incorporation of EdU remains less than in uninduced DarT cells (Figure 2.12A, B). Assuming that TNTC is the only DNA sequence ADP-ribosylated by

DarT, this motif has an occurrence of only 1.8% in human autosomal DNA (Supplementary Figure S2). This suggests that there will exist regions of DNA in which replication can proceed unperturbed by DarT, which could explain the high incorporation of EdU after a 24h incubation in high DarT expression cells. However, since DarT expression was also induced for 24h, there may be a lag in the induction of DarT expression and could enable DNA replication to continue in the absence of replication impediments by DarT. This may lead to the false-positive that DNA synthesis still progresses, albeit slowly, when DarT is expressed. Future work should aim to determine the lag-time until DarT expression is detectable and then subsequently incubate with EdU in order to better determine the rate of DNA synthesis over longer durations. These data also suggest that there may be TARG1-independent DNA repair pathways that enable low levels of thymidine-linked ADP-ribosylation to be tolerated and permit low levels of DNA replication, such as HR and NER, as seen in bacteria expressing an attenuated form of DarT [266]. Collectively, the short incubations of EdU reveal that low levels of DNA synthesis are able to take place in DarT expressing cells and that these sites of active DNA synthesis co-localise with DarT and ssDNA foci.

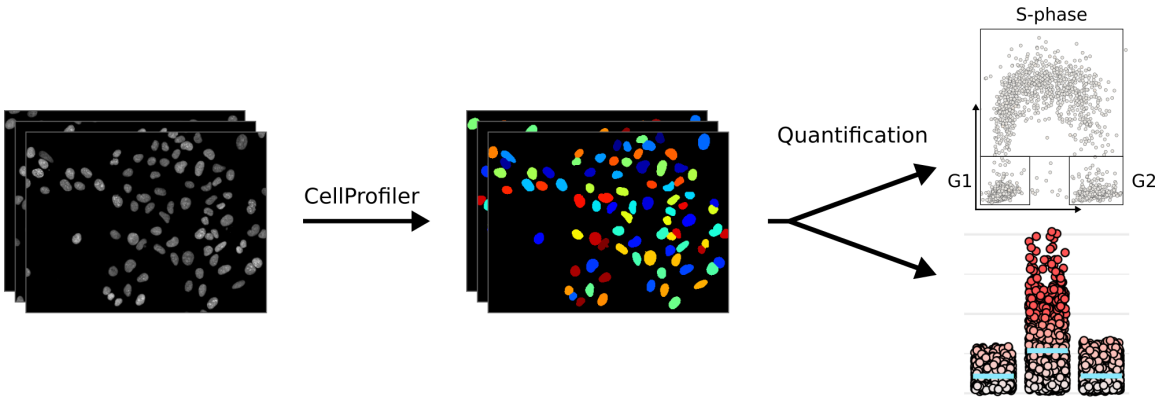


Figure 2.11: Workflow for QIBC analysis.

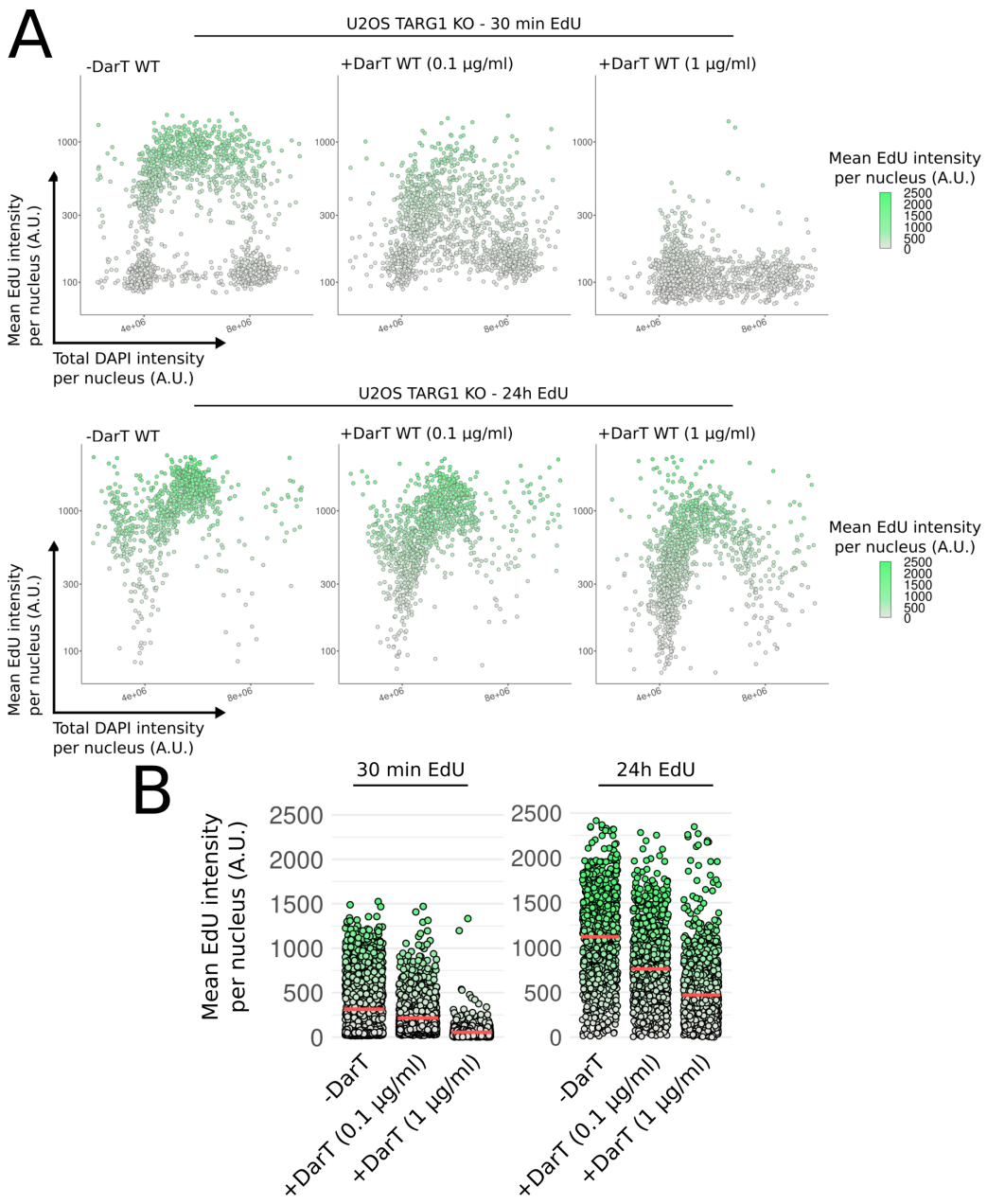


Figure 2.12: DarT does not completely block DNA replication. **(A)** Quantitative image-based cytometry (QIBC) analysis of TARG1 KO cells. DarT expression was induced with the indicated concentrations of doxycycline for 24h. Cells were incubated with 10 µM EdU for either 30 minutes (top) or 24h (bottom) prior to fixation. Total DAPI intensity and mean EdU intensity were determined for >1,000 individual cells per condition and visualised in a 3-variable scatter plot. Points are coloured based on mean EdU intensity for that given nucleus. **(B)** Individual EdU intensities per nucleus from **A** visualised as a bar plot. Red bars represent the population mean EdU intensity for each condition.

Next, we wanted to compare both the incorporation of EdU and sites of ssDNA in DarT-treated cells, or those treated with the genotoxins HU, CPT or MMS. Immunofluorescence revealed that the pattern of chromatin-bound RPA2 in DarT-treated cells has similarities to that of HU and CPT-treated cells, forming distinct foci, albeit to a lesser extent (Figure 2.13). In order to quantify EdU incorporation we utilised QIBC to measure EdU pixel intensities for all genotoxin treatments. This demonstrated that HU ablated, CPT partially reduced, and MMS greatly reduced EdU incorporation. For DarT-treated TARG1 KO cells, EdU incorporation was reduced but not completely lost whereas WT cells showed no impact on DNA synthesis following DarT treatment (Figure 2.14A). We next wanted to quantify the progression of genotoxin-treated cells through the cell cycle using, QIBC to compare single cell intensities for DNA content, mean EdU intensity and chromatin-bound RPA2. This revealed that the chromatin-bound RPA2 signal we observe in DarT-treated TARG1 KO cells is found predominantly within the S-phase population of cells (Figure 2.14B). However, accurate determination of cell cycle stage using EdU is unreliable as EdU incorporation is impacted by the genotoxin. Despite this, these results suggest that the accumulation of ssDNA in DarT-treated TARG1 KO cells is found in cells that are actively replicating DNA but a more reliable method of quantifying cell cycle stage is required. Future work could use a native BrdU assay to measure ssDNA within cells, however it is unknown if thymidine-linked ADP-ribosylation can block BrdU antibody binding or, for that matter, RPA binding.

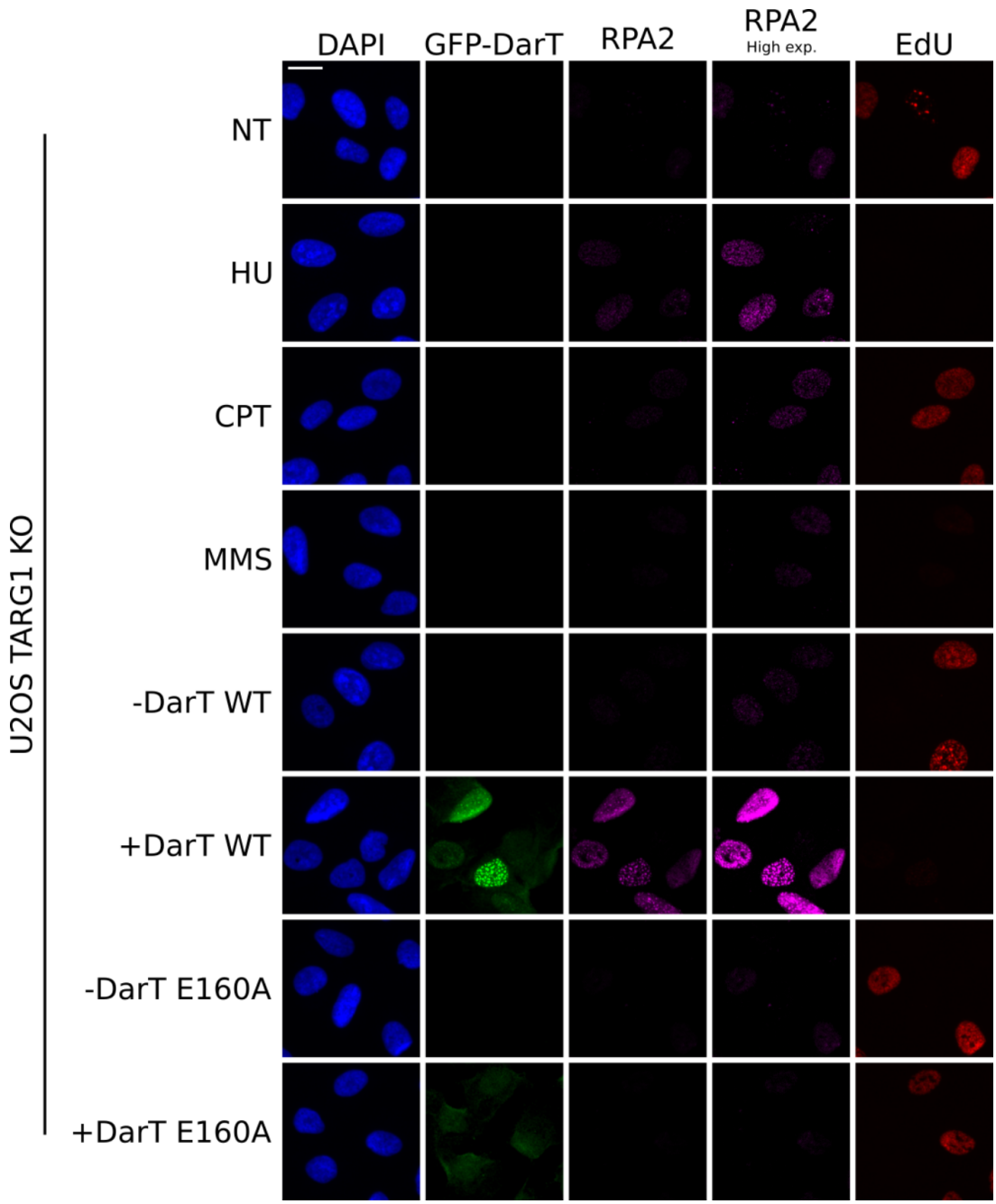


Figure 2.13: Pattern of ssDNA sites induced by DarT expression and other replication poisoning drugs U-2 OS TARG1 KO cells were treated with HU (2 mM, 24h), CPT (1 µM, 1h), MMS (2 mM, 1h), DarT WT (24h), DarT E160A (24h). Cells were incubated with EdU (10 µM, 30 minutes) prior to pre-extraction and fixation. Cells were immunostained as indicated. Scale bar 20 µm.

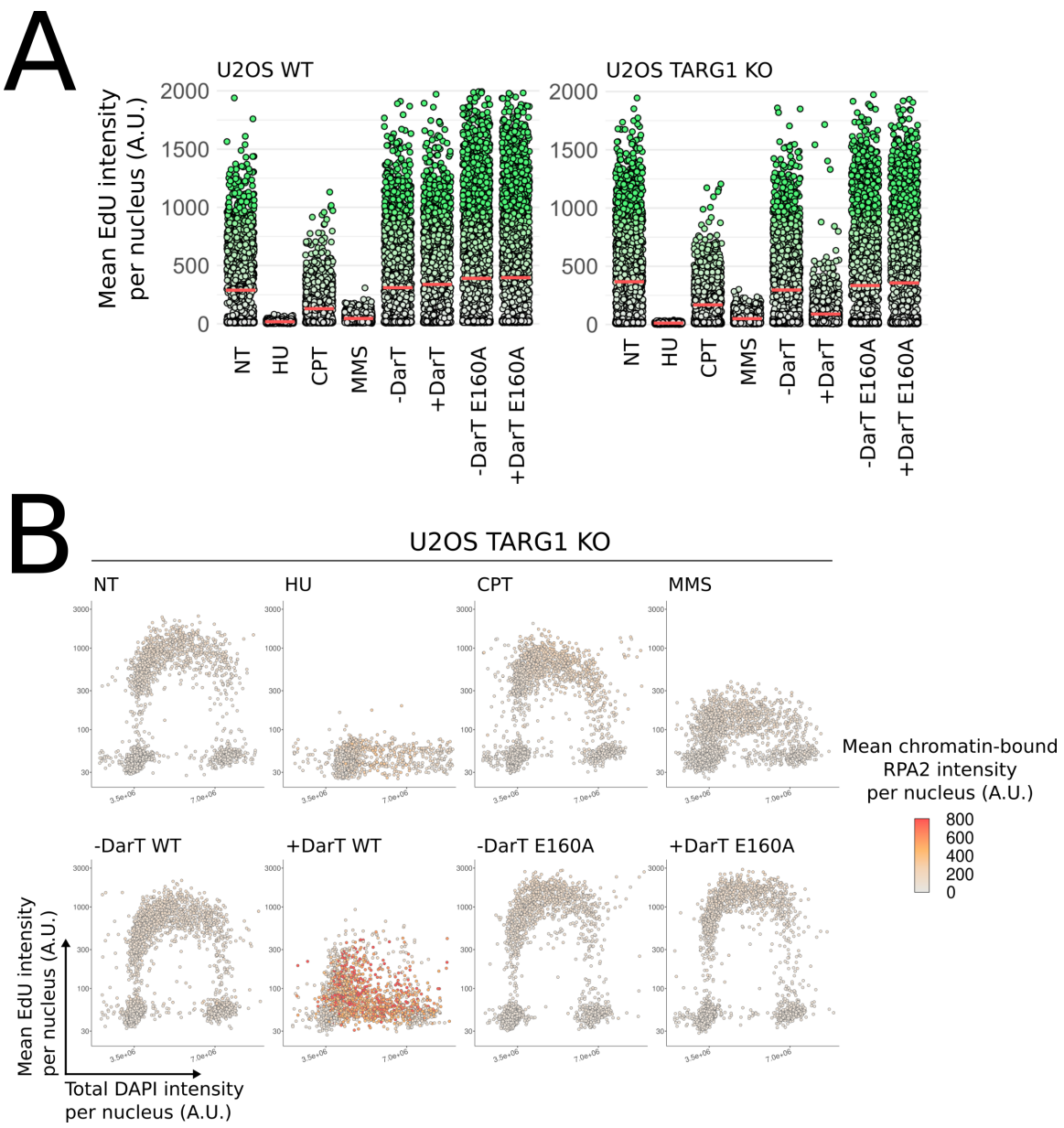


Figure 2.14: DarT expression limits, but does not prevent, EdU incorporation when compared to HU, CPT or MMS in TARG1 KO cells. **(A)** U-2 OS WT or TARG1 KO cells were treated with the indicated genotoxins (as in Figure 2.9) and incubated with EdU (10 µM, 30 minutes) prior to pre-extraction and fixation. Mean intensities of EdU per nucleus were determined by QIBC. The red line represents the population mean for EdU intensity. **(B)** QIBC analysis of TARG1 KO cells treated as in **A**. Total DAPI and mean EdU intensities were visualised in a 3-variable scatter plot. Individual points were coloured based on the mean intensity of chromatin-bound RPA2 per nucleus.

To better validate if DarT also inflicts damage in replicating cells, we next utilised chromatin-bound PCNA instead of EdU as a DNA synthesis independent marker for replicating cells and examined the induction of the DNA damage markers γH2AX and RPA2 pS4/8 in response to genotoxin treatments. Immunofluorescence revealed that γH2AX and RPA2 pS4/8 is found in PCNA-positive cells in response to DarT treatment in TARG1 KO cells (Figure 2.15A, B). A subset of DarT-treated TARG1 KO cells also show the formation of distinct, co-localising foci for DarT, γH2AX or RPA2 pS4/8 and PCNA (Figure 2.15A, B). Together, this further suggests that it is at sites of DNA replication during S-phase where DNA damage is inflicted by DarT. Moreover, we also observe that a subset of cells show a pan-nuclear signal for γH2AX, suggesting extensive DNA breakage within these cells. We next used QIBC to further quantify these images and reveal that over a large population (>1000 cells) the observed γH2AX and RPA2 pS4/8 signal occurs within PCNA positive cells (Figure 2.16A, B. Full QIBC: Supplementary Figure S3A, B). Additionally, formation of γH2AX was also found in S-phase cells using cyclin A as an alternative to PCNA staining for cell cycle staging (Supplementary Figure S5). Similar QIBC patterns were observed in multiple, independent repeats. Collectively, these results suggest that DarT results in damage in S-phase cells.

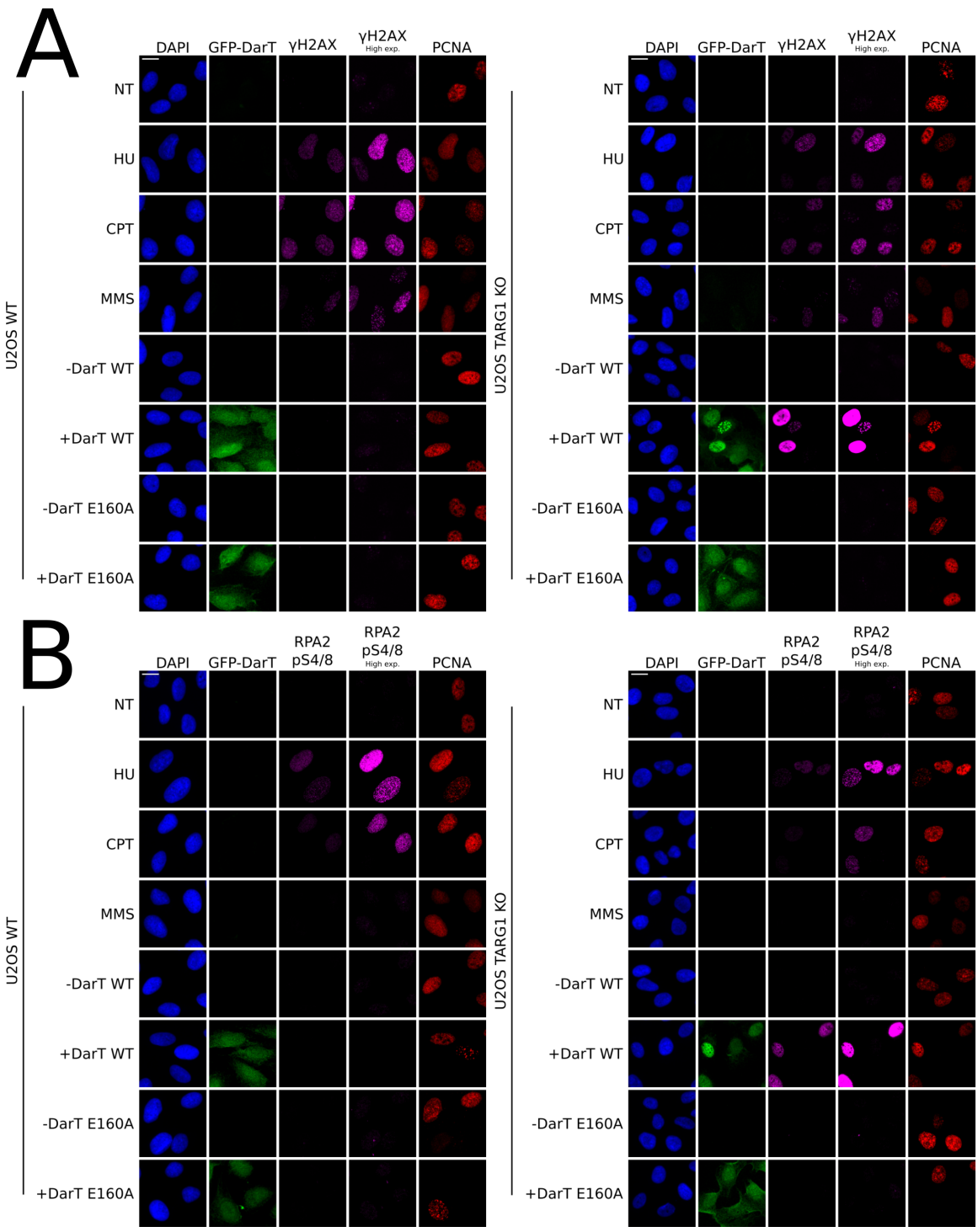


Figure 2.15: DarT induces DNA damage in PCNA-positive cells. **(A)** Representative images of U-2 OS WT or TARG1 KO were treated as in Figure 2.9 and immunostained as indicated. **(B)** Representative images of U-2 OS WT or TARG1 KO were treated as in **A** and immunostained as indicated. Scale bar 20 µm.

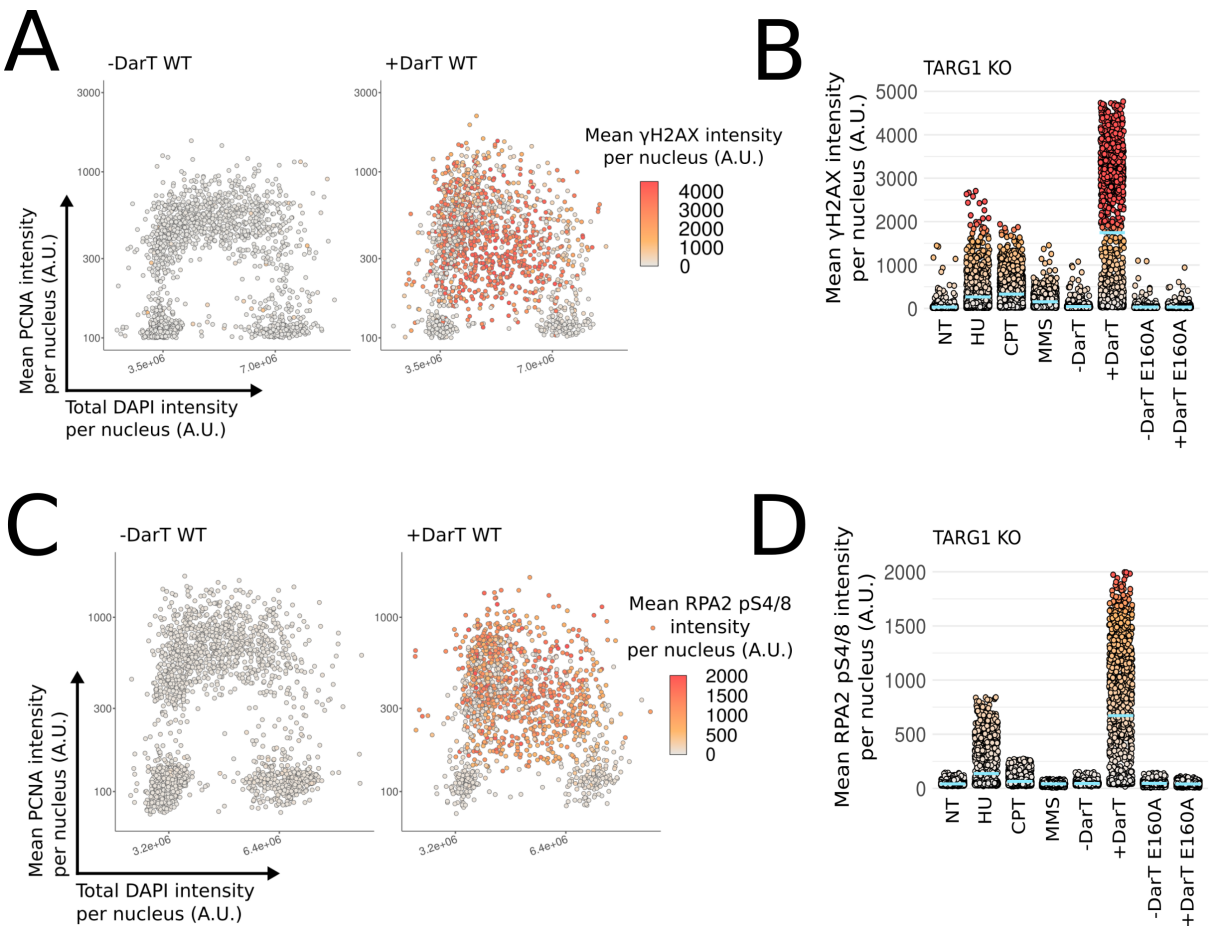


Figure 2.16: DarT induced DNA damage occurs within S-phase. **(A)** QIBC analysis of asynchronous U-2 OS TARG1 KO cells expressing DarT WT for 24h. Cells were pre-extracted, fixed and immunostained as in Figure 2.15A. QIBC was used to record total DAPI intensity, mean PCNA and mean γH2AX intensities per nucleus for >1,000 cells. Total DAPI and mean PCNA intensities for individual cells were used to generate the scatter plot and mean γH2AX intensity was used to colour points. **(B)** Mean intensities of γH2AX as determined by QIBC for the indicated genotoxins in TARG1 KO cells. Blue bar represents the population mean γH2AX intensity for a given condition. **(C)** U-2 OS TARG1 KO were treated and analysed as in **A** followed by immunostaining as in Figure 2.15B. **(D)** U-2 OS TARG1 KO cells analysed as in **C** for the mean intensity of RPA2 pS4/8 in response to the indicated genotoxin treatments. Blue bar represents the population mean RPA2 pS4/8 intensity for a given condition. intensity for a given condition.

Since DarT is an ART, we next examined the levels of ADP-ribosylation in response to DarT and other genotoxins. Remarkably, despite leading to a robust activation of the DDR in TARG1 KO cells, no protein ADP-ribosylation was detected in DarT-treated cells when analysed by western blot (Figure 2.17). This contrasts the strong PARP1 auto-modification observed in MMS-treated cells, which is activated in order to repair single-strand breaks following excision of the methylated base [23]. This suggests protein ADP-ribosylation is not triggered in response to the DNA damage structures found in DarT-treated cells. Therefore, we next examined the levels of ADP-ribosylation, with the same antibody, using immunofluorescence.

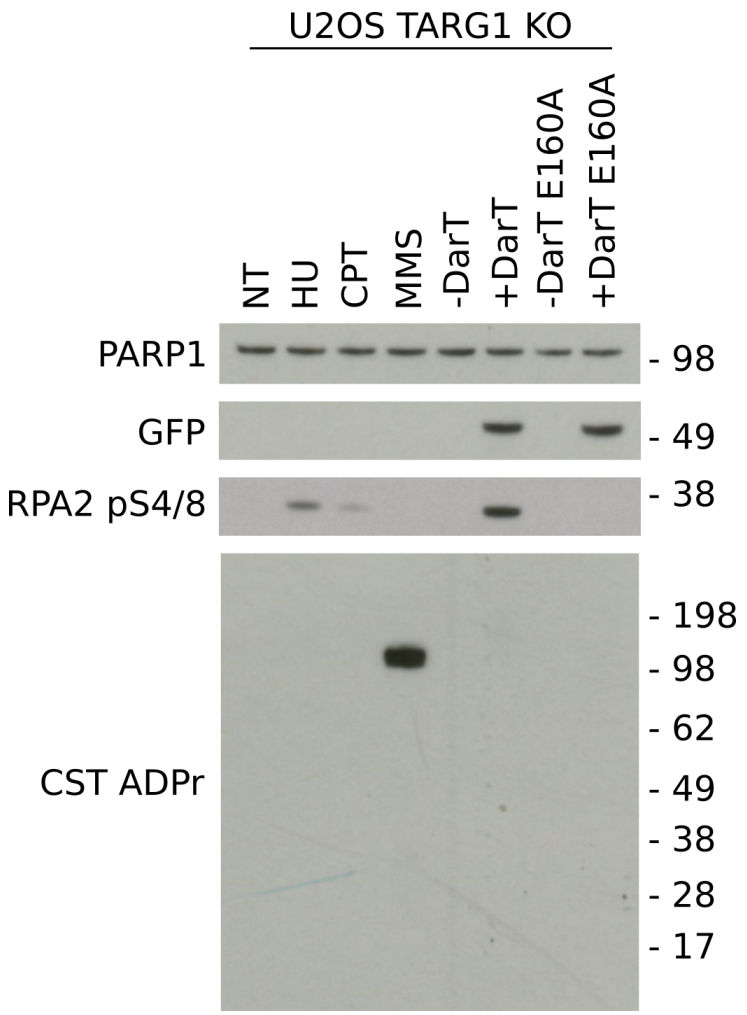


Figure 2.17: Protein ADP-ribosylation is not detectable in DarT-treated cells. U-2 OS TARG1 KO cells treated with HU (2 mM, 24h), CPT (1 µM, 1h), MMS (2 mM, 1h), DarT (24h) or DarT E160A (24h). Levels of PARP1 and RPA2 pS4/8 were assessed in addition to ADP-ribosylation levels using the CST poly/mono ADP-ribose antibody in response to the aforementioned genotoxins.

With the finding that the DNA damage in DarT-treated TARG1 KO cells occurs in S-phase, we hypothesised that it was only the ssDNA exposed during DNA replication that was ADP-ribosylated by DarT, which in turn limits DNA replication and induces activation of the DDR. To address this, we used immunofluorescence to examine ADP-ribosylation in cells treated with the aforementioned genotoxins. This revealed that, like γH2AX and RPA2 pS4/8, ADP-ribosylation is found within PCNA-positive cells in DarT-treated TARG1 KO cells (Figure 2.18A). Cells presenting GFP-DarT foci also co-localise with

ADP-ribosylation foci at sites of DNA replication. We next investigated these images further by using QIBC. Interestingly, QIBC revealed that the population mean for ADP-ribosylation intensity in DarT-treated cells across a large population was comparable to that of MMS treated TARG1 KO cells (Figure 2.18B). Moreover, QIBC analysis revealed that all of the ADP-ribosylation formed in DarT-treated cells occurs in PCNA-positive cells, whereas in MMS treated cells ADP-ribosylation forms indiscriminately of cell cycle stage (Figure 2.18C). It is important to also note that the pattern of ADP-ribosylation observed in response to DarT and MMS is markedly different. DarT induces large ADP-ribosylation foci at sites of replication whereas the foci MMS induces are small and found in most cells. This ADP-ribosylation pattern inflicted by MMS reflects the activation of PARP-dependent SSB repair following the action of BER glycosylases and APE1 cleavage of the DNA backbone at AP sites [72, 167, 269]. Taken together, these results suggest that ssDNA exposed during DNA replication in S-phase is targeted for ADP-ribosylation by DarT, which subsequently leads to activation of the DDR and replication slowing. Furthermore, this data also suggests that the ADP-ribosylation signal we observe is found on DNA, as indicated by the lack of detectable protein ADP-ribosylation by western blot.

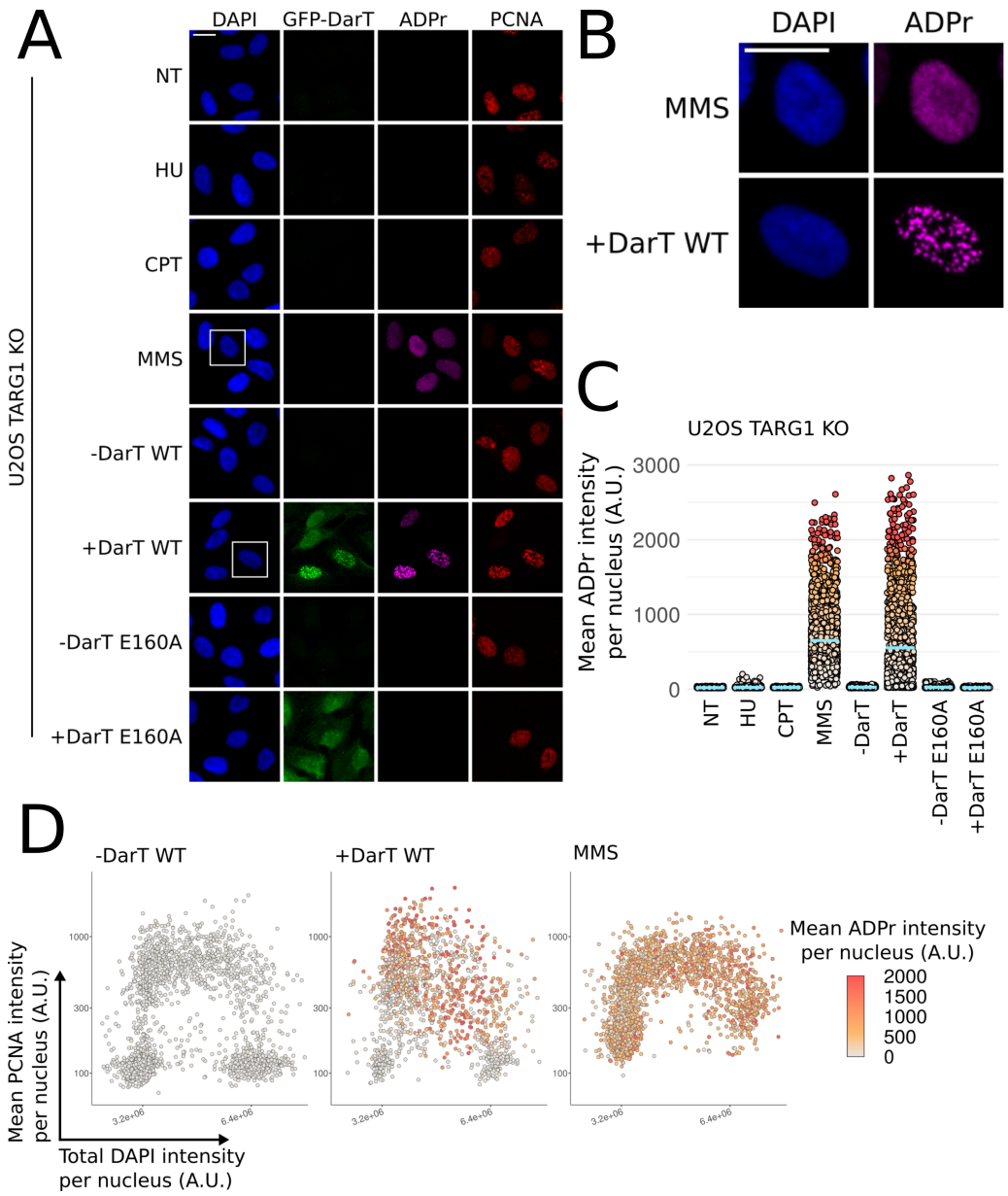


Figure 2.18: DarT expressing TARG1 KO cells accumulate ADP-ribosylation in S-phase. **(A)** U-2 OS TARG1 KO cells were treated with the indicated genotoxins, pre-extracted and fixed. Cells were then immunostained for the indicated antibodies. Scale bar 20 µm. **(B)** Magnified view of the region enclosed by the white square in **A** for DarT and MMS treated cells. Scale bar 20 µm. **(C)** Cells from **A** were analysed by QIBC. The blue line represents the population mean ADP-ribosylation intensity. **(D)** DarT and MMS treated TARG1 KO cells from **A** were analysed by QIBC and total DAPI and mean EdU intensities were plotted onto a scatter diagram. Individual points were coloured corresponding to mean ADP-ribosylation intensity per nucleus.

We next wanted to investigate if WT cells can be sensitised to DNA ADP-ribosylation by DarT. We reasoned that based on the behaviour of DarT targeting ssDNA during S-phase, inhibition of Chk1, which protects against excessive ssDNA generation through the suppression of dormant origins, would increase the available ssDNA substrate for DarT to modify. However, we find that Chk1 inhibition does not lead to an increased sensitivity to DarT above Chk1 inhibitor induced DNA damage in WT cells (Figure 2.19). We did observe that PARP1 auto-modification is induced in Chk1 inhibitor treated cells. This is likely due to an increase in stalled replication forks due to excessive origin firing, which PARP1 binds and synthesises ADP-ribosylation in order to stabilise these stalled forks [99, 270–273]. This PARP1 auto-modification correlates with the concentration of Chk1 inhibitor used.

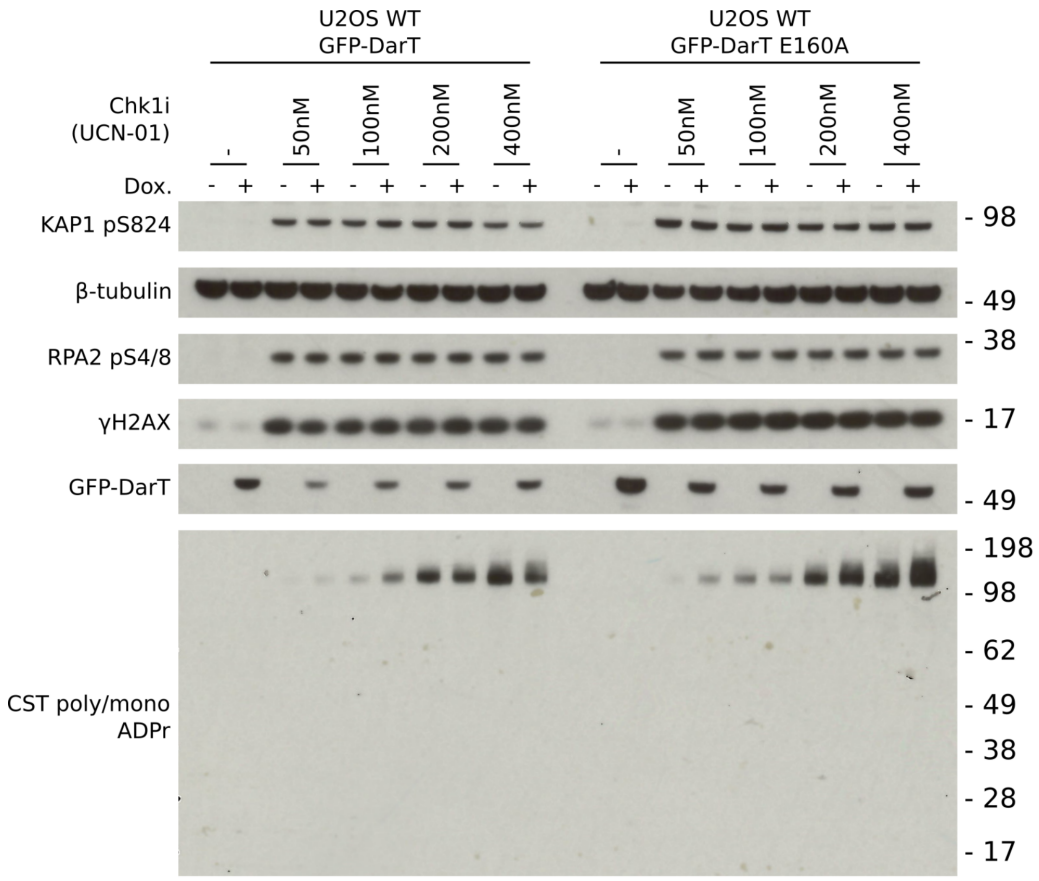


Figure 2.19: Replication stress induced by Chk1 inhibition does not sensitise WT cells to DarT. U-2 OS WT cells expressing either DarT WT or E160A were treated with the indicated concentrations of Chk1i for 24h and immunoblotted for the indicated proteins and ADP-ribosylation using the CST poly/mono ADP-ribose antibody.

PARP1 extends thymidine-linked ADP-ribosylation

A subset of the known PARPs in human cells possess only mono-ADP-ribosylation activity. Additionally, it has previously been shown that PARP3 can mono-ADP-ribosylate phosphates on DNA, which in turn can be extended by other PARPs to form phosphate-linked poly-ADP-ribosylated DNA *in vitro* [262]. We hypothesised that thymidine-linked mono-ADP-ribosylation could similarly be extended to form thymidine-linked poly-ADP-ribosylation. To address this question, we incubated a thymidine-linked mono-ADP-ribosylated DNA oligonucleotide (MAR-DNA) with PARP1. We find that PARP1 can indeed extended mono-ADP-ribosylation to form thymidine-linked poly-ADP-ribosylated DNA (PAR-DNA) (Figure 2.20A). This form of DNA-linked ADP-ribosylation is resistant to proteinase K and is lost following benzonase treatment, suggesting that the modification is indeed DNA-linked and not contamination of free PAR chains formed by active PARP1 (Figure 2.20B). Together, this suggests that the DNA ADP-ribosylation catalysed by DarT in human cells could also be in the poly-ADP-ribose form following elongation by PARP1 or other transferases.

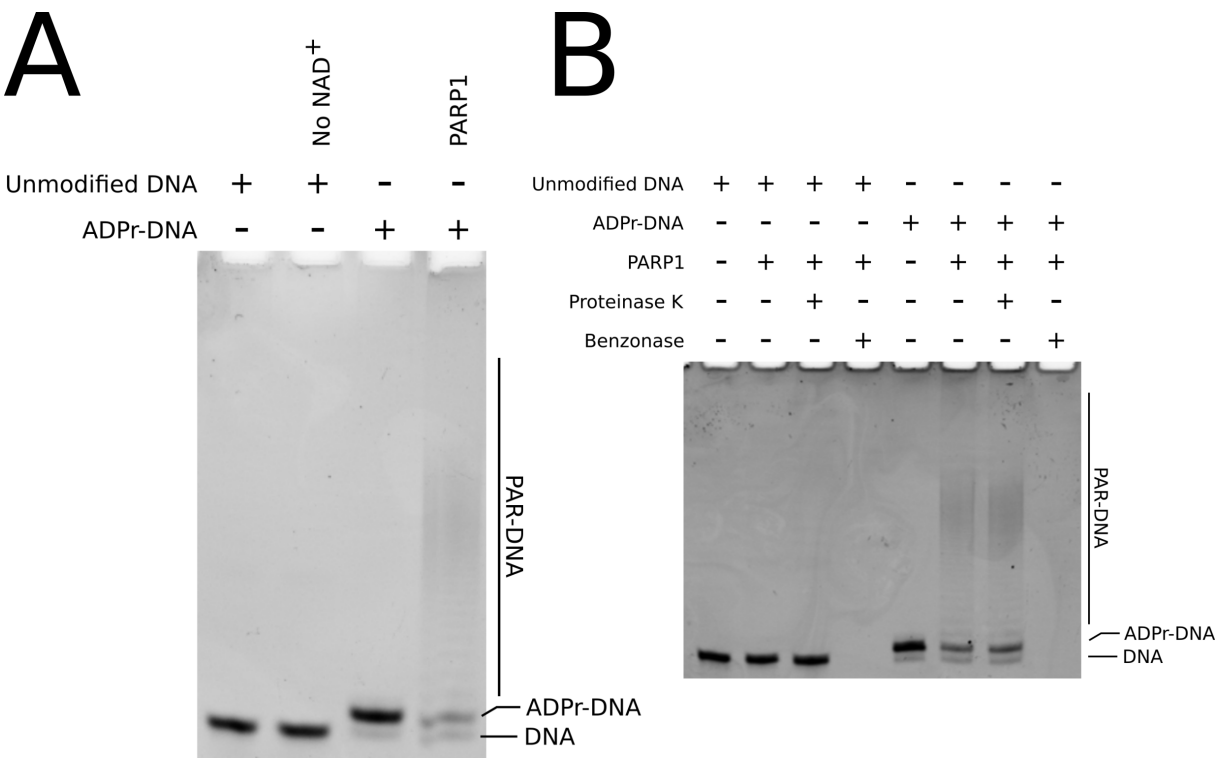


Figure 2.20: PARP1 can form PAR chains on DarT modified ssDNA. **(A)** UV detection of thymidine-linked ADP-ribosylated oligonucleotide incubated with PARP1 (0.2 µM, 30 minutes). Laddering in lane 4 represents PAR chains of different lengths forming on the DNA oligonucleotide. **(B)** UV detection of thymidine-linked ADP-ribosylated oligonucleotide incubated with PARP1 (0.2 µM, 30 minutes) where indicated. Following PARP1 incubation, reactions were then incubated with proteinase K (50 ng/µL, 30 minutes) or benzonase (125U, 30 minutes) as indicated.

We next explored the optimal conditions for PARP1 extension of thymidine-linked mono-ADP-ribosylation. We find that neither an excess of NAD^+ or PARP1 improve the yield of PAR-DNA (Figure 2.21A, B). However, titration of the MAR-DNA oligonucleotide leads to a proportional change in the generation of PAR-DNA (Figure 2.21C). Taken together, this suggests that only a proportion of MAR-DNA can be poly-ADP-ribosylated *in vitro*. This could be a result of the steric hindrance of an accumulating PAR-DNA preventing PARP1 from extending additional sites.

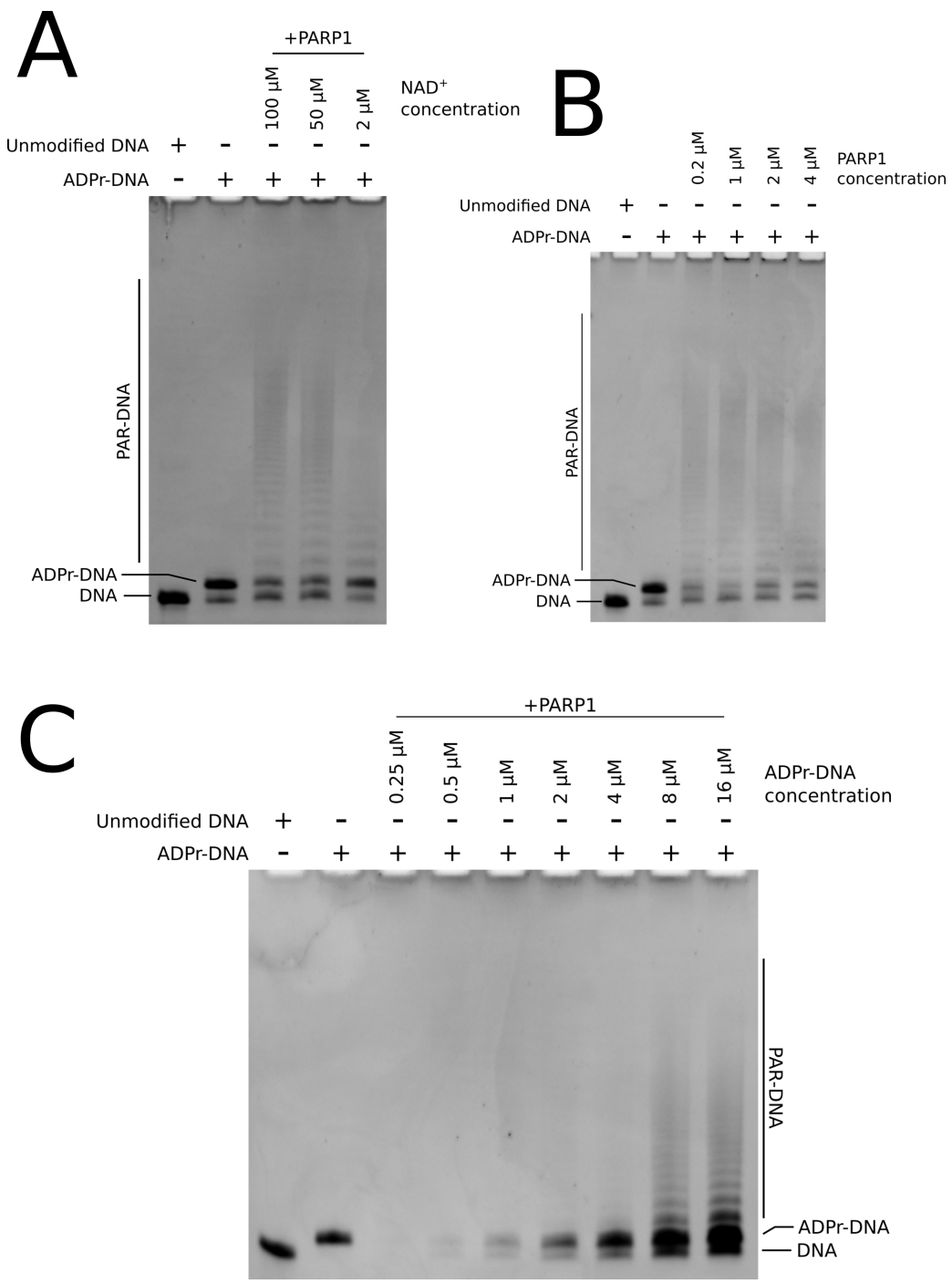


Figure 2.21: Formation of PAR-DNA by PARP1 is a proportion of the thymidine-linked ADP-ribosylated DNA substrate. **(A)** UV detection of PARP1 modification of thymidine-linked ADP-ribosylated DNA with the indicated concentrations of NAD^+. **(B)** UV detection of PARP1 modification of thymidine-linked ADP-ribosylated DNA with the indicated concentrations of PARP1. **(C)** UV detection of the indicated concentrations of thymidine-linked ADP-ribosylated DNA with PARP1.

This *in vitro* data suggests that thymidine-linked PAR-DNA could form in human cells following the activity of PARP1 on DarT ADP-ribosylated DNA. We therefore investigated the action of human hydrolases against PAR-DNA. We find that TARG1 is able to effectively reverse thymidine-linked poly-ADP-ribosylation completely (Figure 2.22A). Whether TARG1 removes full chains or iteratively removes individual ADP-ribose units from DNA has not been determined, but previous work has suggested that TARG1 can release PAR chains from ADP-ribosylated protein [239]. The limitation of this assay is using ethidium bromide for DNA detection, which does not stain ADP-ribose chains. Future work could utilise silver staining or radioactively labelled ADP-ribose to resolve if the released ADP-ribose is in the mono or poly form. We also find that PARG effectively removes the poly form of the modification but cannot remove the thymidine-linked ADP-ribose, as we showed previously (Figure 2.22B). We also find that ARH3 can hydrolyse some PAR-DNA and has no activity against the thymidine-linked ADP-ribose, also as we showed previously (Figure 2.22C). We find that ARH3 seems to have a preference for longer PAR chains in this modification context, as shown by reduction in the slower running long PAR-DNA oligonucleotides and accumulation of shorter ADP-ribose-DNA oligonucleotides in the 1-3mer range. The inability of PARG and ARH3 to remove thymidine-linked mono-ADP-ribose contrasts their ability to remove mono-ADP-ribosylation from phosphates at DNA ends [260].

We next wanted to examine the activity of PARP1 in combination with the cofactor HPF1 in the elongation of thymidine-linked ADP-ribosylation. We observed that PARP1 in combination with equimolar HPF1 reduces the formation of PAR-DNA (Figure 2.22D). This suggests that HPF1 constrains ADP-ribose elongation activity of PARP1, as has previously been shown for HPF1 directing PARP1 to modify serine *in trans* instead of PARP1 auto-modification *in cis* [217, 218, 220]. Collectively, this demonstrates that PAR-DNA can be partially degraded by PARG and ARH3 but that it is only TARG1 that is able to completely reverse thymidine-linked ADP-ribosylation. This suggests that in DarT-treated cells, PARG and ARH3 are likely to trim PAR chains into their mono form

but it is TARG1 that is required to fully reverse this modification.

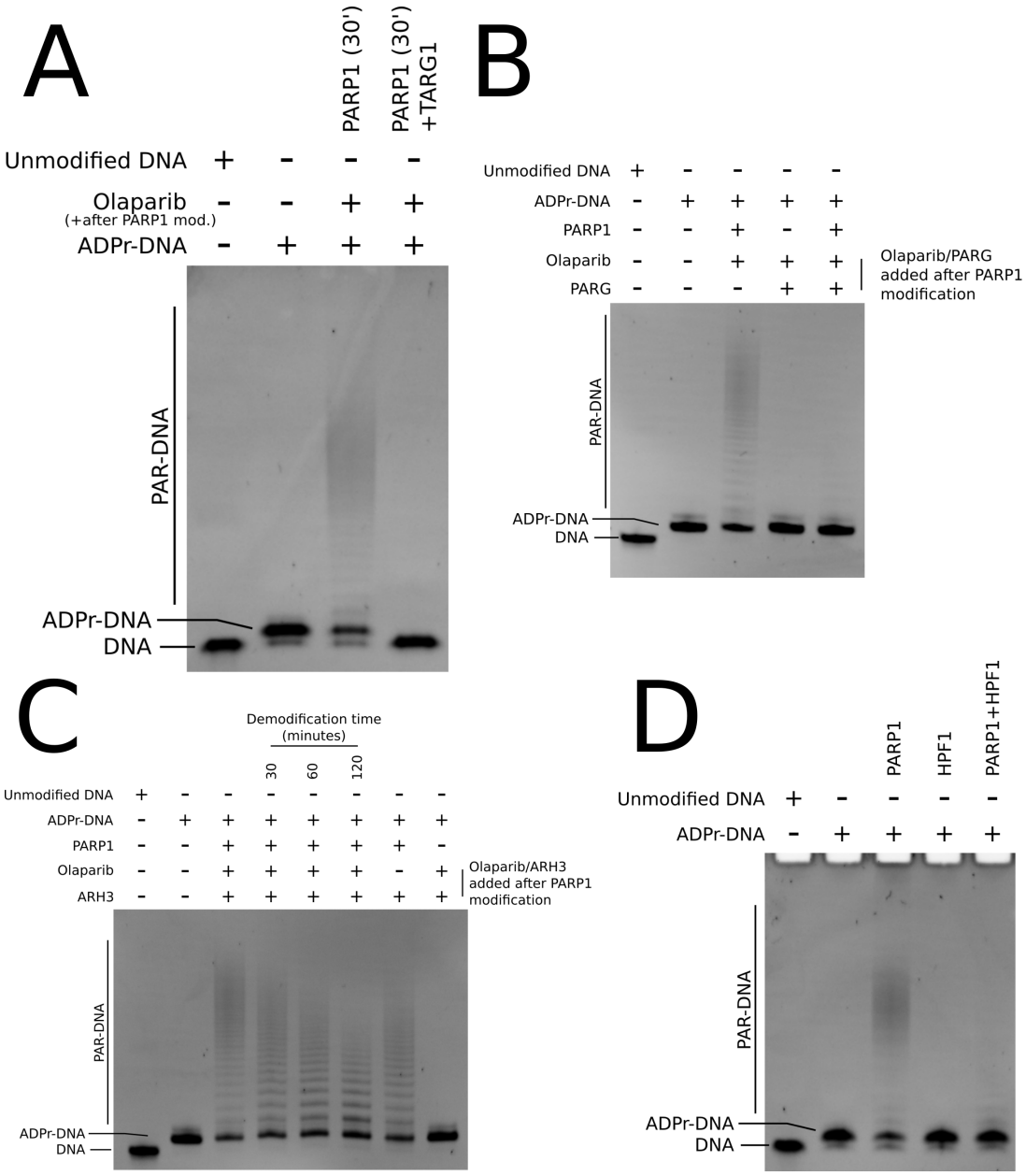


Figure 2.22: TARG1 demodifies PAR-DNA formed by DarT and PARP1. **(A)** UV detection of DNA incubated with TARG1 following PARP1 modification of thymidine-linked ADP-ribosylated DNA. **(B)** UV detection of PAR-DNA incubated with PARG (1 µM, 30 minutes) in combination with olaparib. **(C)** UV detection of PAR-DNA incubated with ARH3 (1 µM) for the indicated durations in combination with olaparib. **(D)** UV detection of PAR-DNA formation in the presence of either PARP1 alone or PARP1 in combination with HPF1 (0.2 µM for both, 30 minutes).

Detection of *in vivo* DNA ADP-ribosylation

Our data have indicated that thymidine-linked poly-ADP-ribosylation can be formed *in vitro* through the combined action of DarT and PARP1. We also find that DarT leads to ADP-ribosylation in S-phase cells. We therefore hypothesised that some of the ADP-ribosylation signal we observed in S-phase cells could be in the poly rather than mono form. To study this, we aimed to use PARP inhibitors in DarT-treated cells and examine the levels of ADP-ribosylation detected. We reasoned that by inhibiting PARP activity we would observe only the activity of DarT and therefore mono-ADP-ribosylation.

Before examining this *in vivo*, we first determined if DarT activity was inhibited by a range of PARP inhibitors and confirmed that none inhibited DarT transferase activity (Figure 2.23A). We next examined TARG1 KO cells treated with either DarT or MMS in combination with olaparib or veliparib. We show that the damage induced by DarT is not impacted by PARP inhibition (Figure 2.23B). Of note, olaparib results in untreated and MMS cells showing an increase in RPA2 pS4/8. This is likely a result of PARP becoming trapped on DNA by olaparib, colliding with replication forks and resulting in replication stress, an outcome that is exacerbated in MMS treated cells due to more DNA binding by PARP1 [166].

We next examined if the immunofluorescence pattern of ADP-ribosylation changed in TARG1 KO cells treated with either DarT or MMS. We confirm that both olaparib and veliparib ablate MMS-induced PARP ADP-ribosylation activity but olaparib and veliparib have no impact on DarT ADP-ribosylation (Figure 2.23C). Collectively, this suggests that the ADP-ribosylation signal we observe in DarT-treated cells is in the mono-ADP-ribose form, perhaps due to the activity of PARG and ARH3 trimming long chains of ADP-ribose into the mono form. The mono-ADP-ribosylation of thymidine bases then persists in TARG1 KO cells.

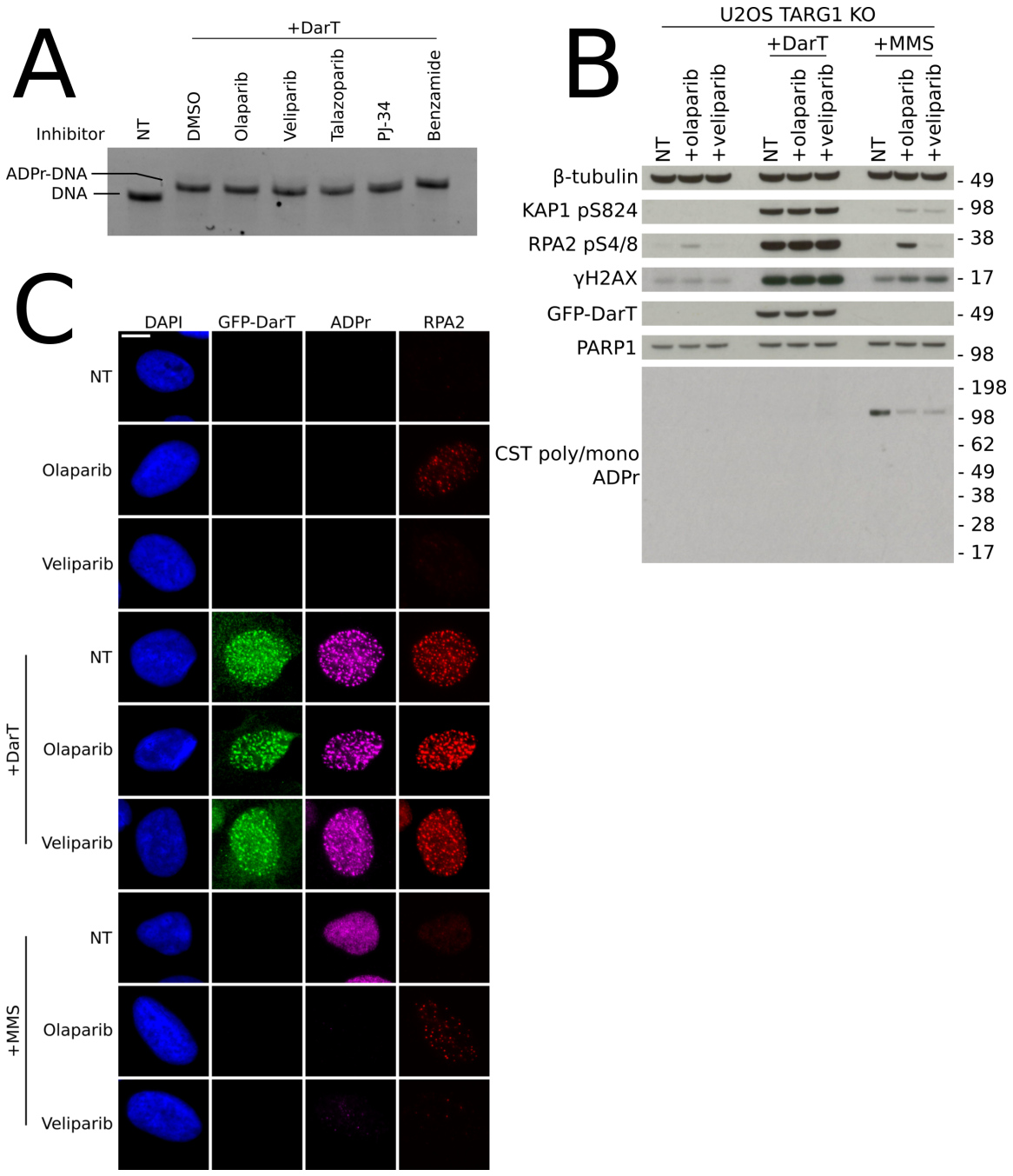


Figure 2.23: ADP-ribosylation in DarT-treated TARG1 KO cells is in the mono-ADP-ribose form. **(A)** UV detection of DNA oligonucleotide incubated with DarT (1 µM, 30 minutes) and the indicated PARPi (100 µM for all except 10 mM for benzamide). **(B)** U-2 OS TARG1 KO cells expressing DarT (24h) or treated with MMS (2 mM, 1h) were incubated with the indicated PARPi (10 µM, 24h) and immunoblotted with the indicated antibodies. **(C)** U-2 OS TARG1 KO were treated as in **B** and immunostained as indicated. Scale bar 10 µm.

We next wanted to elucidate if it was possible to detect DNA ADP-ribosylation by dot blot. To do so, we used a DarT ADP-ribosylated DNA oligonucleotide to compare a range of ADP-ribose recognising antibodies, all of which detect different forms of the modification. The PAN-ADP-ribose binding reagent is a macrodomain fused to a rabbit Fc tag that was developed by the Kraus Lab and is proposed to detect mono and poly-ADP-ribosylation [274]. Notably, this PAN-ADP-ribose binding reagent has been used to study the ADP-ribosylation of serine on histones [219, 275]. The Kraus Lab also developed another macrodomain fused to a rabbit Fc tag, which recognises mono-ADP-ribosylation (hereafter Millipore Mono ADPr) [274]. Cell Signalling Technologies (CST) have also recently released an antibody that is suggested to recognise poly and mono-ADP ribosylation (CST poly/mono ADP-ribose antibody). This antibody is described as being monoclonal and raised against an ADP-ribosylated lysine in a KLH peptide [276]. Before the recent development of these new antibodies, ADP-ribosylation recognising antibodies only detected long, poly forms of the modification. These antibodies often show different ADP-ribosylation patterns, suggesting different epitopes in the ADP-ribose polymer, such as branch points [200, 275, 277]. Of these antibodies, we used the the monoclonal PAR antibody from Trevigen and monoclonal 10H PAR antibody from Enzo.

Interestingly, we find that only PAN-ADP-ribose and CST poly/mono ADP-ribose binding antibodies are capable of detecting thymidine-linked ADP-ribosylation on DNA (Figure 2.24). The Millipore mono ADPr binding reagent shows no reactivity against the ADP-ribosylated DNA, suggesting that the preferred binding site is different than the thymidine-ADP-ribose linkage. The Enzo 10H and Trevigen PAR antibodies show no preferential binding to the ADP-ribosylated DNA oligonucleotide and seem to bind to DNA indiscriminately, perhaps due to the presence of adenine bases in the oligonucleotide that resemble ADP-ribose. The PAN-ADP-ribose binding reagent also seems to show some cross-reactivity with DNA. Remarkably, the CST poly/mono ADP-ribose antibody specifically binds ADP-ribose with no apparent cross-reactivity with DNA, even with extended exposures. This same CST ADP-ribose antibody was used to detect ADP-ribosylation

in the previous figures 2.17, 2.18 and 2.23B, C. Collectively, this result demonstrates that the CST poly/mono ADP-ribose antibody specifically detects thymidine-linked ADP-ribosylation of DNA and suggests that previous immunofluorescence data shown here is an *in vivo* detection of DNA ADP-ribosylation.

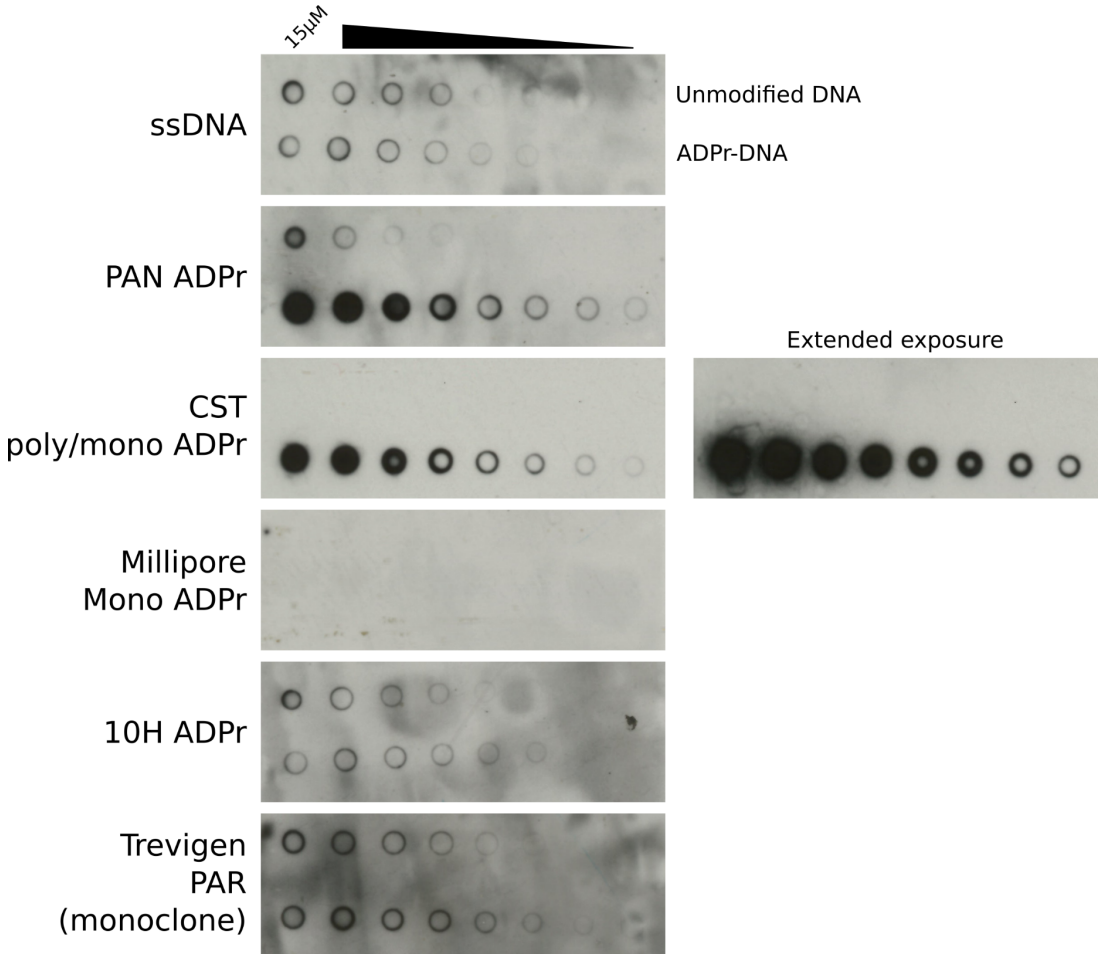


Figure 2.24: DarT modified oligonucleotide probed by a panel of ADP-ribose binding reagents by dot blot. 2-fold dilution of DNA from 15 μM. Anti-ssDNA blot serves as a loading control.

We next wanted to determine if it would be possible to detect ADP-ribosylated genomic DNA (gDNA) directly using the CST poly/mono ADP-ribose antibody. We find that ADP-ribosylated gDNA from bacteria expressing DarT is detectable by dot blot (Figure 2.25A, B). The ADP-ribosylation of gDNA is lost in bacteria expressing DarT in combination with DarG WT, but not when combined with the DarG K80A catalytic mutant, though

this K80A mutant does seem to retain some ADP-ribosylhydrolase activity. We next wanted to determine if gDNA ADP-ribosylation was detectable in human cells treated with the genotoxins HU, CPT, MMS or DarT. Indeed, we observe ADP-ribosylation of gDNA in DarT-treated TARG1 KO cells but not for any other genotoxin treatment (Figure 2.26). We also find that ADP-ribosylated gDNA from bacterial and human cells is reversible *in vitro* by the action of DarG or TARG1 (Figure 2.27A, B). For this, we also used the DarG K80A+N22A catalytic mutant that ablates any residual ADP-ribosylhydrolase activity (Figure 2.25A). Furthermore, detection of ADP-ribosylated gDNA is lost following benzonase treatment (Figure 2.27B). Taken together this shows the first detection of reversible DNA ADP-ribosylation *in vivo*. Moreover, this also suggests that the major source of immunofluorescence ADP-ribosylation signal observed in DarT-treated TARG1 KO cells is on DNA and that the catalytic activity of TARG1 protects against the accumulation of thymidine-linked ADP-ribose adducts.

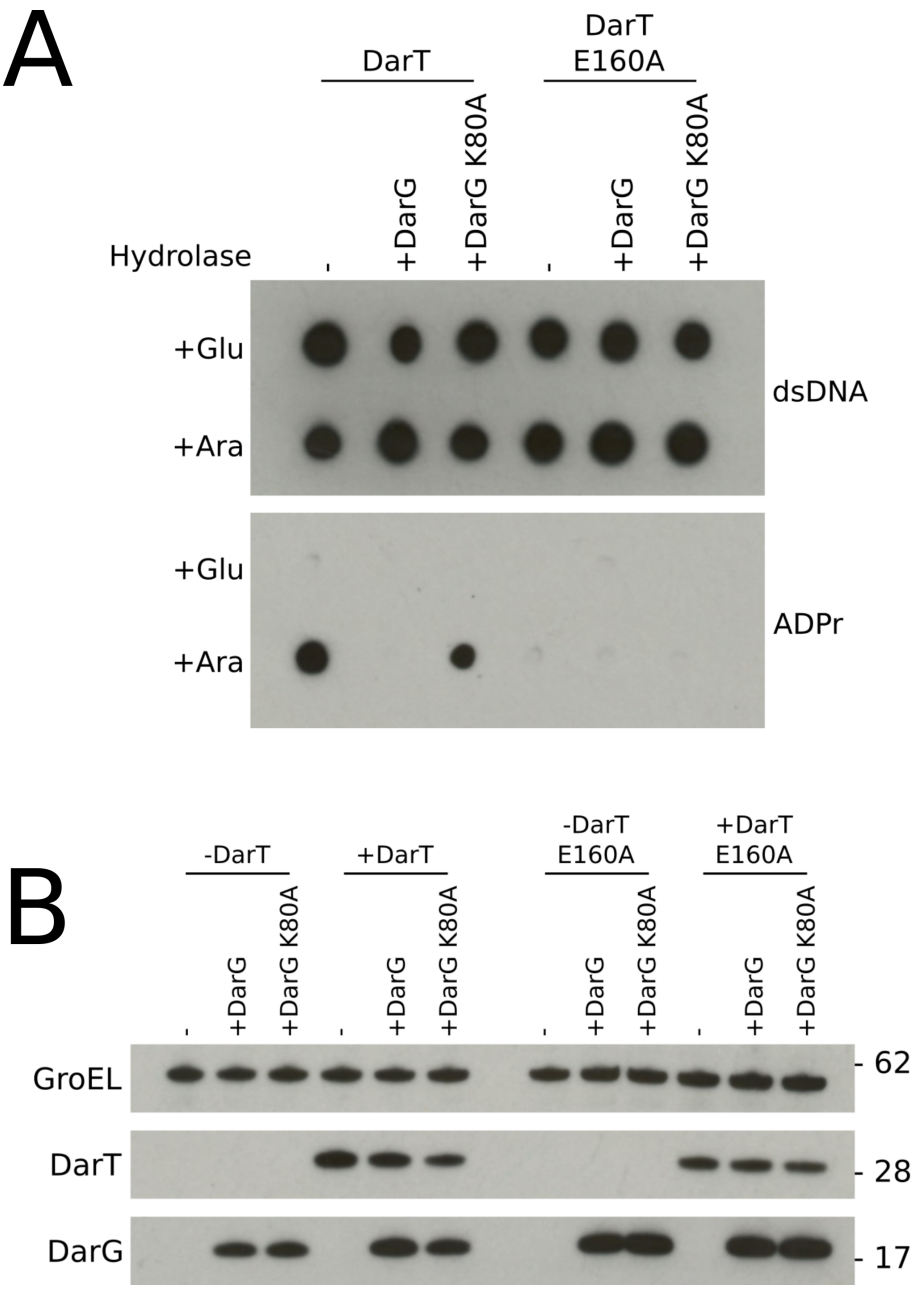


Figure 2.25: Detection of ADP-ribosylated genomic DNA in bacteria. **(A)** Dot blot of genomic DNA from BL21 DE3 expressing either DarT WT or DarT E160A. pBAD-DarT expression was repressed or induced by glucose or arabinose, respectively. pET expression of the hydrolases was controlled with IPTG. ADP-ribose levels were determined using the CST poly/mono ADP-ribose antibody (labelled ADPr) and anti-dsDNA serves as a loading control. **(B)** Cells from **A** were induced as indicated, lysed and immunoblotted for the indicated antibodies to detect DarT and hydrolase expression.

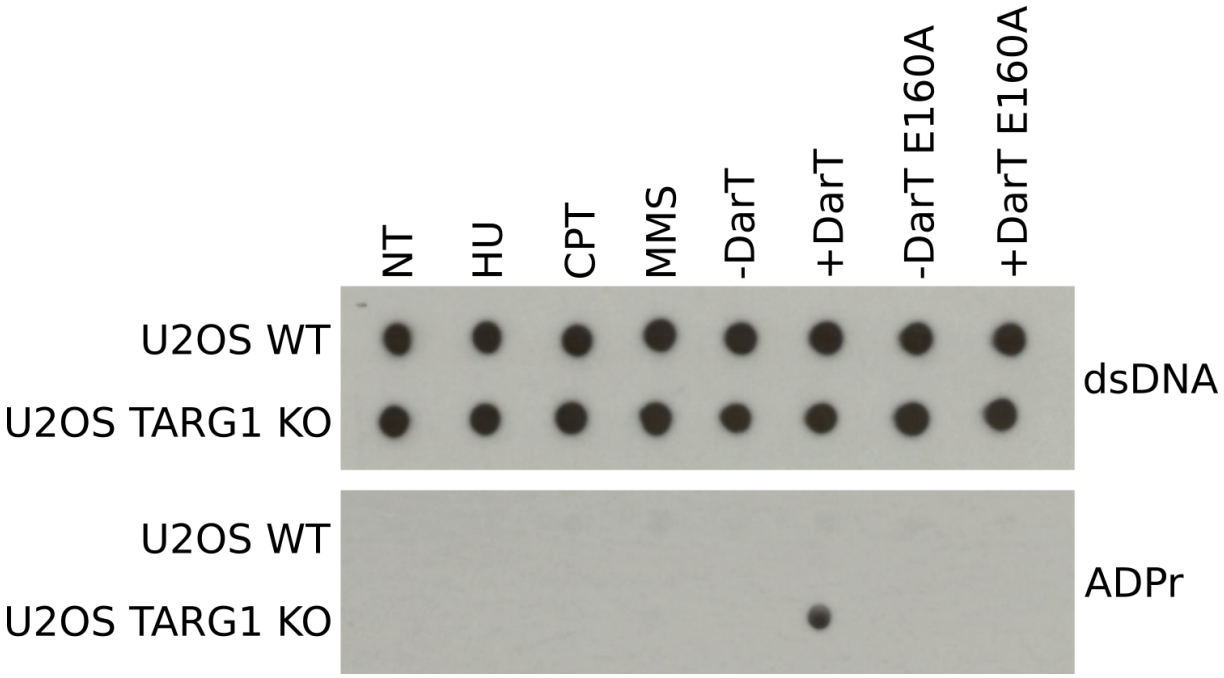


Figure 2.26: Detection of ADP-ribosylated genomic DNA in human cells. U-2 OS WT or TARG1 KO cells were treated with either HU (2 mM, 24h), CPT (1 µM, 1h), MMS (2 mM, 1h), DarT WT (24h) and DarT E160A (24h). Following treatment, genomic DNA was dot blotted and ADP-ribose levels were determined using the CST poly/mono ADP-ribose antibody (labelled ADPr) and anti-dsDNA serves as a loading control.

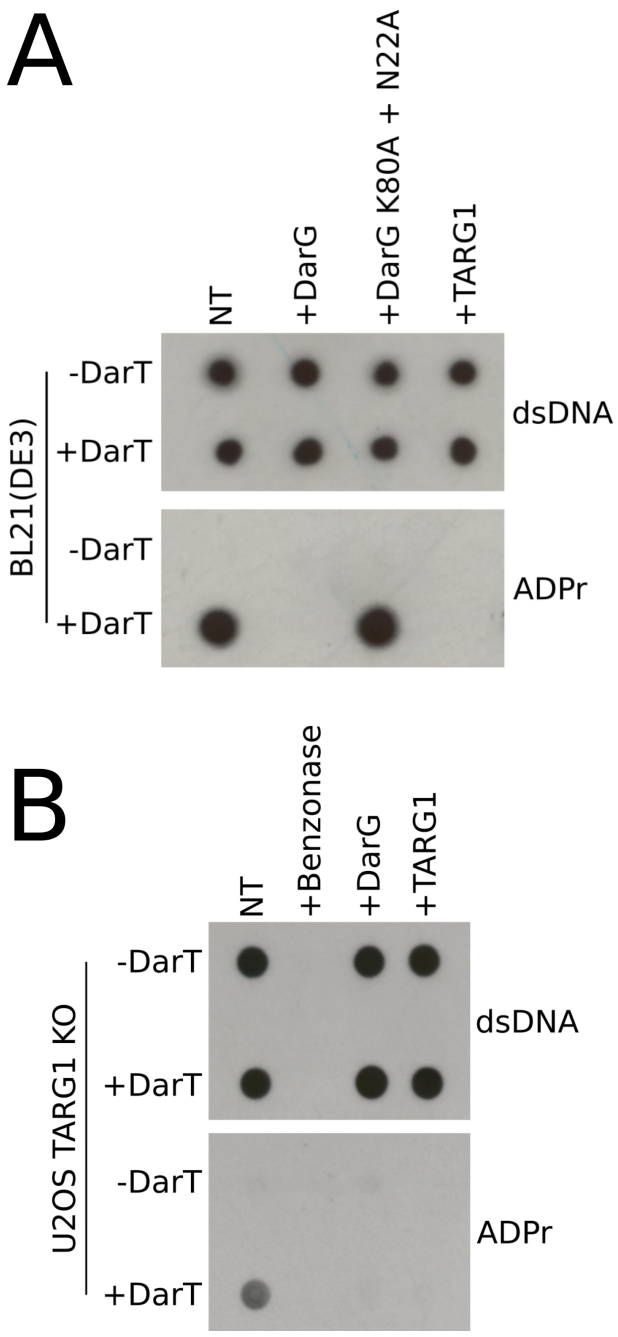


Figure 2.27: *In vitro* demodification of ADP-ribosylated genomic DNA. **(A)** Genomic DNA was extracted from BL21 DE3 expressing DarT WT. pBAD-DarT expression was repressed or induced by glucose or arabinose, respectively. Extracted genomic DNA was incubated with the indicated hydrolases (1 µM, 30 minutes) prior to dot blot. Levels of ADP-ribose were determined using the CST poly/mono ADP-ribose antibody (labelled ADPr) and anti-dsDNA serves as a loading control. **(B)** Genomic DNA was extracted from U-2 OS TARG1 KO cells expressing DarT and treated with the indicated hydrolases as in **A** or incubated with benzonase.

2.3 TARG1-deficient human cells are sensitive to PARG inhibition

Recently, a new PARG inhibitor (PARGi) was developed and it was revealed that a subset of ovarian cancers are sensitive to this inhibitor [235, 278]. This work demonstrated that the induction of replication stress via Chk1 inhibition or depletion of some DNA replication factors can sensitise cells to PARGi that are otherwise resistant to PARGi treatment. It was proposed that the mechanism for this sensitivity to PARG inhibition was due to stalled replication forks being unable to restart via RECQ1. Due to TARG1 also being a ADP-ribosylhydrolase, we aimed to examine if TARG1 KO cells were also sensitive to PARGi, perhaps due to PARG and TARG1 having a common substrate. We find that prolonged incubations with PARGi in TARG1 KO cells, but not WT cells, leads to the accumulation of excessive ADP-ribosylation and induction of the DDR (Figure 2.28). An independent repeat also revealed that prolonged PARGi incubations leads to an accumulation of cyclins B, A and E (Figure 2.29). Collectively, this suggests that TARG1 and PARG may have overlapping function in protecting against the accumulation of ADP-ribosylation.

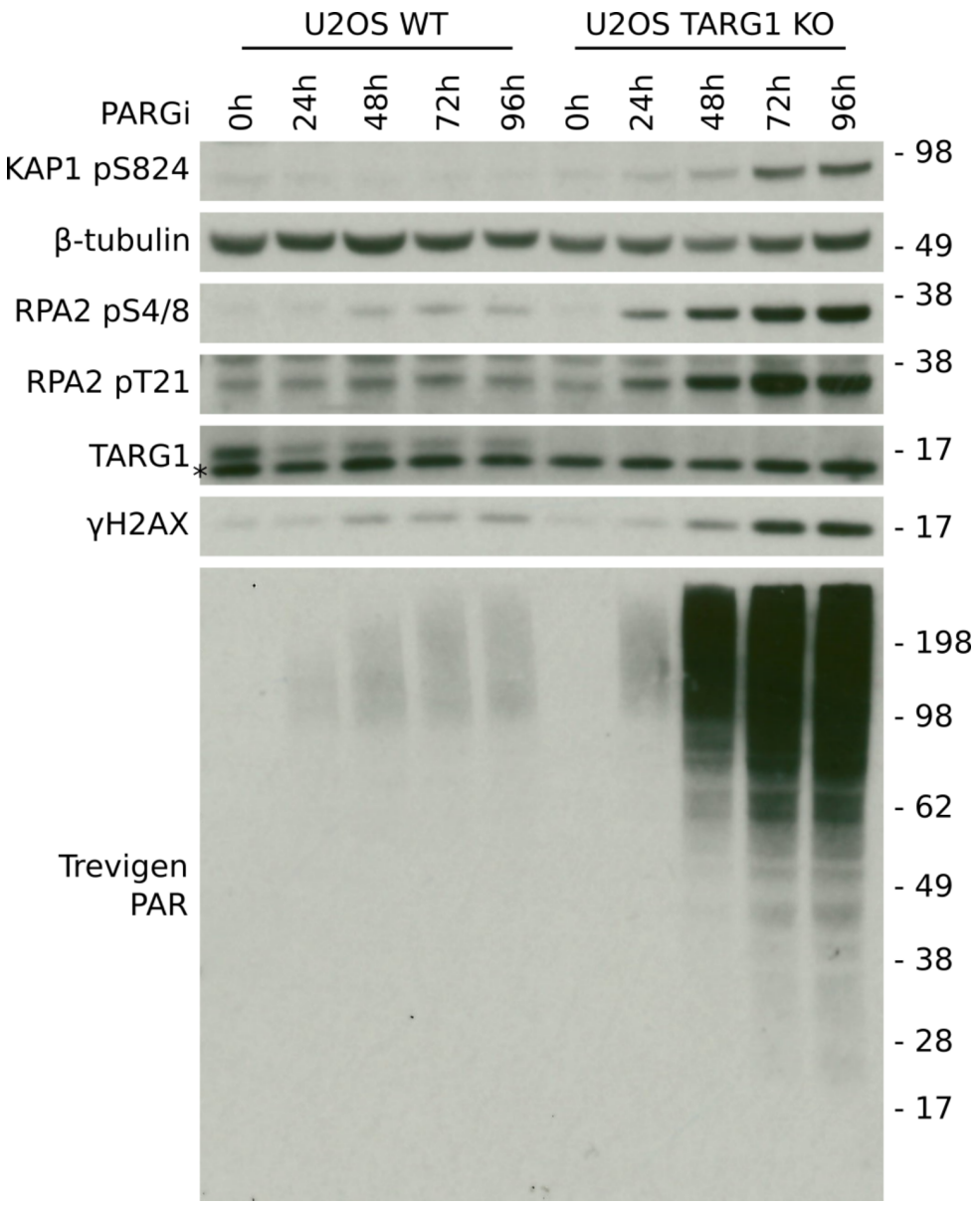


Figure 2.28: TARG1 KO cells treated with PARGi accumulate excessive ADP-ribosylation and replication stress. U-2 OS WT or TARG1 KO cells were treated with PARGi (PDD00017273, 10 µM) for the indicated durations. Levels of DDR proteins KAP1 pS824, RPA2 pS4/8, RPA2 pT21 and γH2AX, in addition to the levels of ADP-ribosylation using the Trevigen PAR antibody were examined.

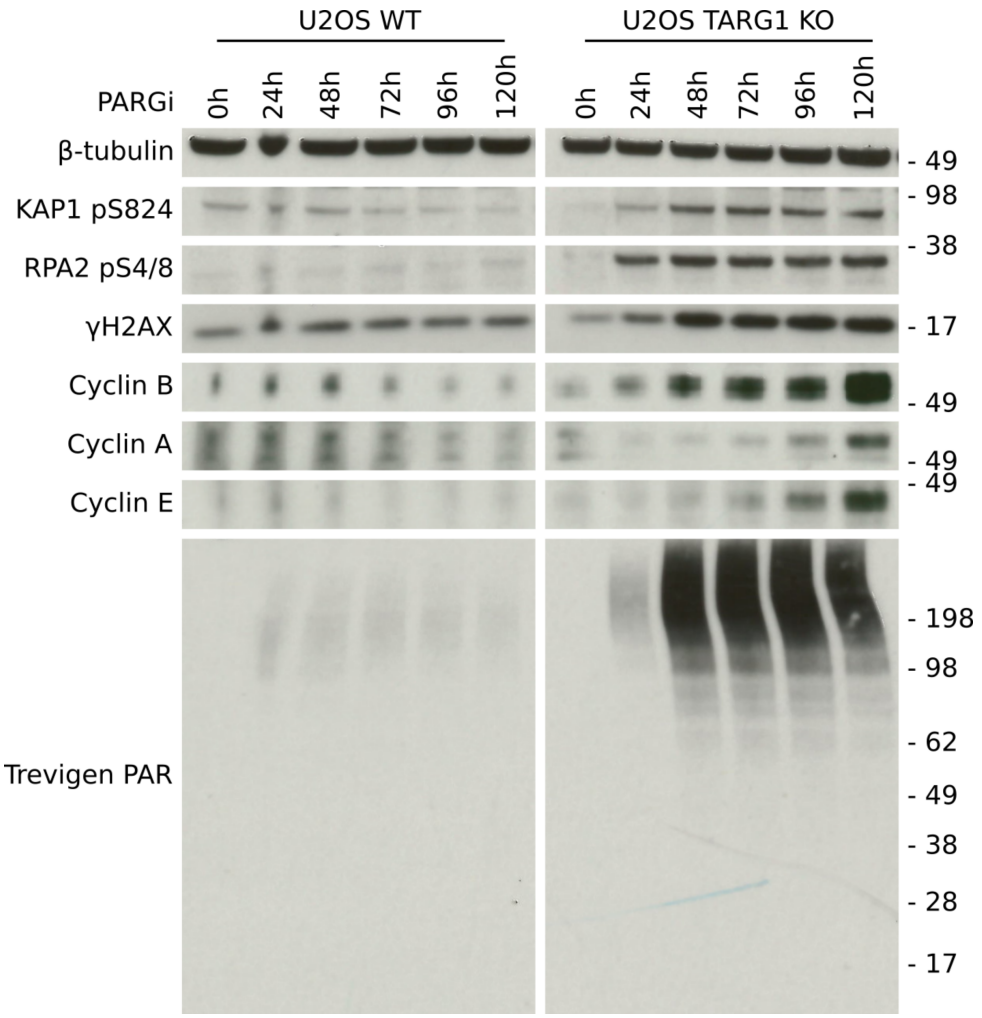


Figure 2.29: TARG1 KO cells treated with PARGi accumulate cell cycle markers. U-2 OS WT or TARG1 KO cells were treated with PARGi (PDD00017273, 10 µM) for the indicated durations. In this independent repeat, levels of DDR proteins KAP1 pS824, RPA2 pS4/8 and γH2AX were examined, in addition to that of cyclins B, A and E. Levels of ADP-ribosylation were determined using the Trevigen PAR antibody.

We next wanted to examine if knock-in of TARG1 WT or K84A could rescue the PARGi phenotype observed. We find that TARG1 WT is able to rescue the ADP-ribosylation signal but is unable to completely rescue the induction of DNA damage signalling (Figure 2.30). Moreover, we also find that in TARG1 KO cells, PARGi treatment leads to phosphorylation of p53 on S15, a modification that contributes to p53 stabilisation [279]. Curiously, for PARG and p53, incubation with PARGi lead to a shift in the electromobility at 24 and 96h (but only at 96h for WT cells). This change in mobility was observed over

independent repeats and occurred at the same time-points. These shifts, or lack thereof, could suggest the presence of additional modifications, such as ubiquitin, on protein that alters their mobility, though this has not been determined. We also find that PARGi treatment leads to reduced levels of TARG1 for both endogenous TARG1 in WT cells and exogenous, overexpressed TARG1.

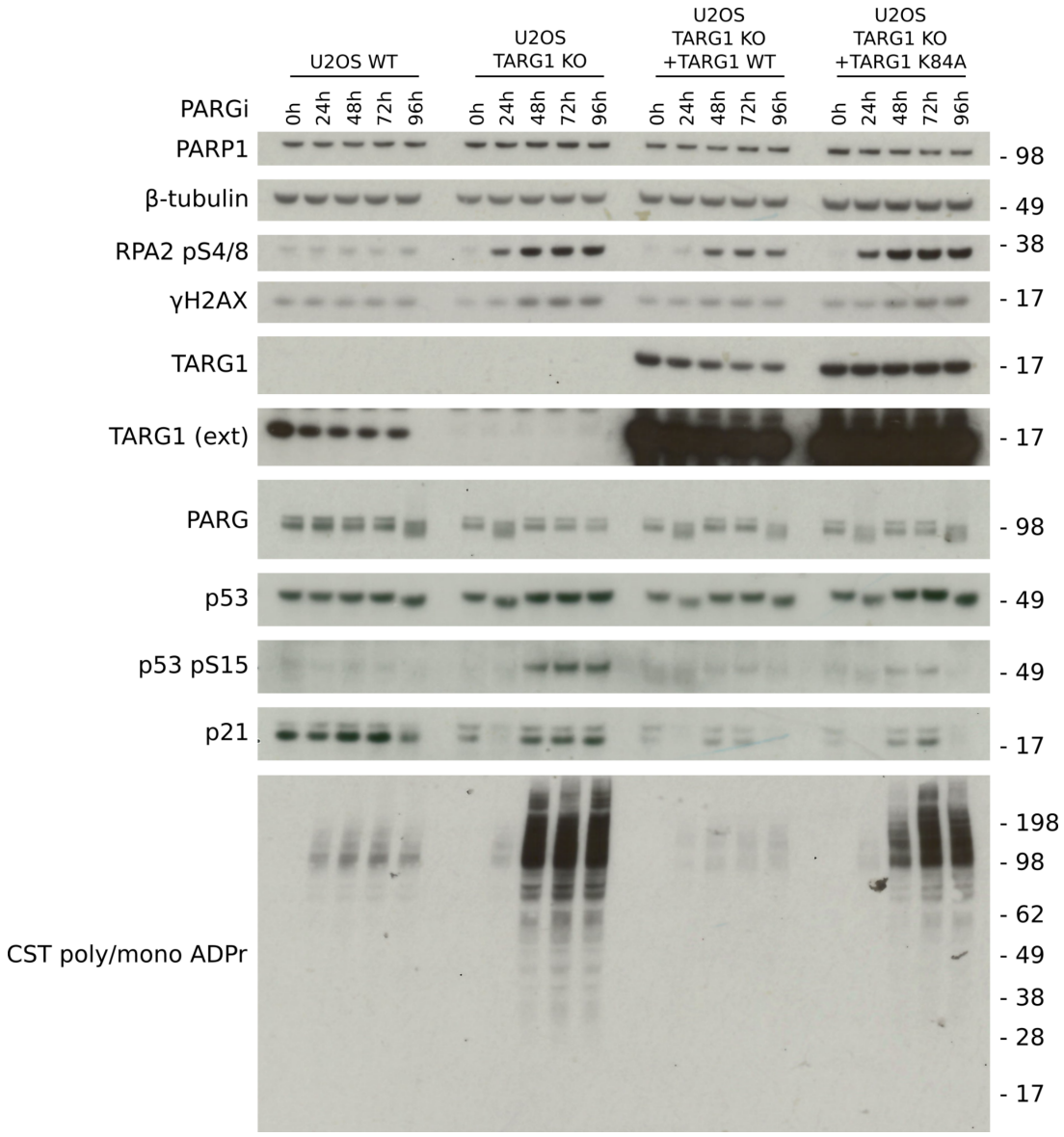


Figure 2.30: Overexpression of TARG1 WT, but not TARG1 K84A, partially rescues TARG1 KO sensitivity to PARGi. U-2 OS WT and TARG1 KO cells were treated with PARGi (PDD00017273, 10 µM) for the indicated durations. TARG1 KO cells constitutively expressing pLX304 TARG1 WT or TARG1 K84A were also similarly treated with PARGi. Levels of DDR proteins RPA2 pS4/8, γH2AX, p53 pS15 were checked, in addition to PARP1, PARG and p53. Levels of ADP-ribosylation were assessed using the CST poly/mono ADP-ribose antibody.

We next wanted to determine the ART responsible for the protein-linked ADP-ribosylation observed in PARGi-treated TARG1 KO cells. Since PARP1 is believed

to be responsible for 80-90% of PARP activity observed in human cells and PARP2 for part of the remainder, we began by examining the impact PARP inhibition (PARPi) using olaparib had in PARGi-treated cells [280]. We find that PARPi in combination with PARGi rescues the DNA damage and ADP-ribosylation phenotype observed in cells that are treated with PARGi alone (Figure 2.31). We also examined tankyrase inhibition (TANKi) and find that TANKi moderately reduces the ADP-ribosylation signal but does not rescue DNA damage. Taken together, these results suggest that PARP1-2 activity is responsible for ADP-ribosylation signal observed in PARGi-treated TARG1 KO cells.

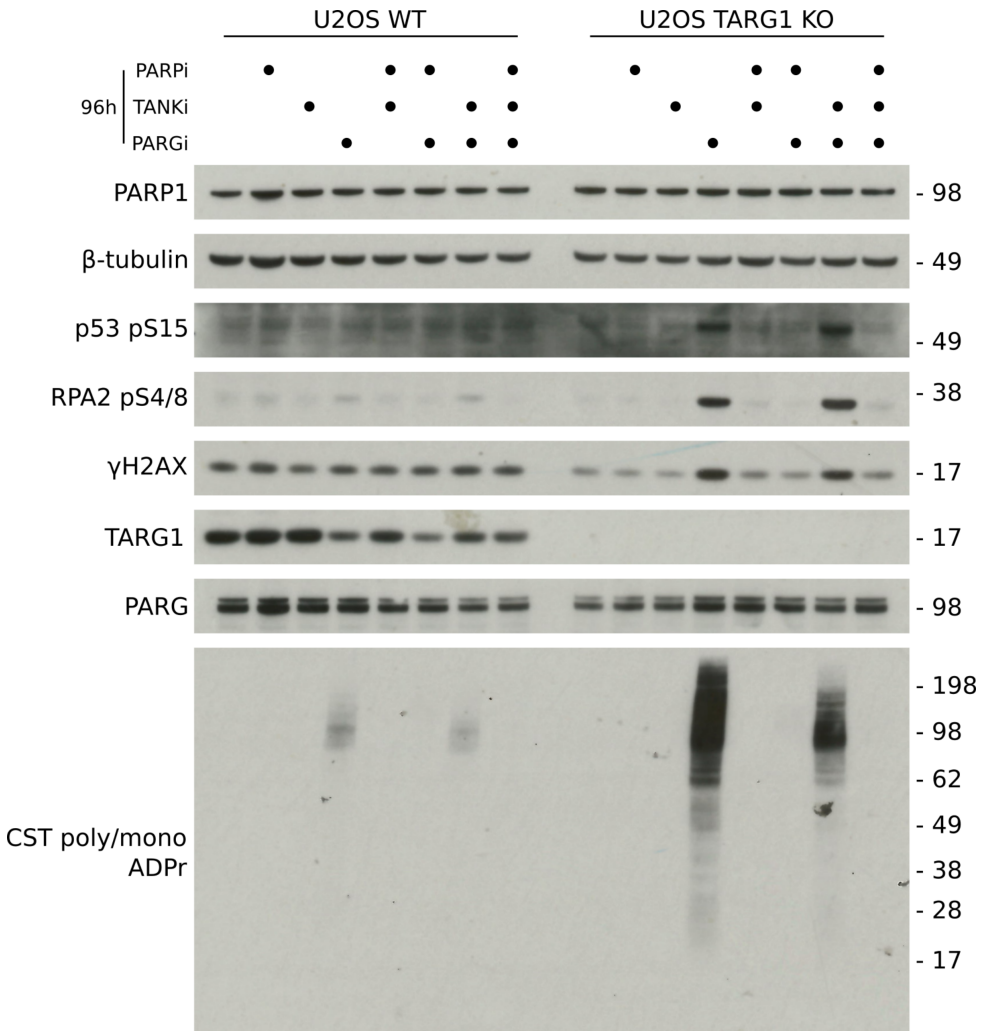


Figure 2.31: PARP inhibition rescues PARGi sensitivity in TARG1 KO cells. U-2 OS WT or TARG1 KO cells were incubated with the indicated combinations of PARPi (olaparib, 1 µM), TANKi (tankyrase1/2 inhibitor, XAV-939, 1 µM) or PARGi (PDD00017273, 10 µM) for 96h. Levels of DDR proteins p53 pS15, RPA2 pS4/8 and γH2AX were assessed. Levels of ADP-ribosylation were determined using the CST poly/mono ADP-ribose antibody.

Due to the induction of the DDR in TARG1 KO cells in response to PARGi treatment being similar to that observed in DarT-treated TARG1 KO cells, we wondered if DNA ADP-ribosylation was also occurring in PARGi-treated TARG1 KO cells. We hypothesised that in addition to protecting against the accumulation of protein-linked ADP-ribosylation that PARG and TARG1 may also have a common substrate in the form of ADP-ribosylated DNA since both of these ADP-ribosylhydrolases have been shown to reverse phosphate-

linked ADP-ribosylation of DNA [260]. To study this, we sought to extract gDNA from PARGi-treated TARG1 KO cells and detect gDNA ADP-ribosylation by dot blot as was shown for DarT modified gDNA (Figures 2.25, 2.26, 2.27). However, we find that free PAR chains, unlinked to DNA or protein, were detectable by dot blot. Thymidine-linked PAR treated with benzonase or protein-free PAR generated from auto-modified PARP1 were both able to UV crosslink to nitrocellulose membranes (Figure 2.32A, B). This contrasts benzonase treated MAR-DNA and bacterial gDNA, which are both mono-ADP-ribosylated by DarT, that do not crosslink to membranes. Collectively, this suggests that free PAR chains in lysates generated from PARGi-treated TARG1 KO cells could crosslink to membranes and potentially contaminate gDNA dot blots whereas mono-ADP-ribose cannot. Of note, we also find that benzonase itself has some activity towards PAR chains. We also observe the the DNA oligonucleotides used were not detectable by ssDNA antibody at the concentration used. Additionally, the MAR-DNA and 18-mer free PAR were loaded at an equal concentration of 0.1 µM per dot, as estimated by nanodrop, but due to the heterogenous nature of PAR-DNA it was loaded at the ratio used in figure 2.32A.

With the aforementioned data in mind, we next examined the ADP-ribosylation of gDNA extracted from U-2 OS WT or TARG1 KO cells treated with either DarT, MMS, PARGi or gDNA from DarT expressing bacteria. We find that both PARGi-treated WT and TARG1 KO cells have detectable ADP-ribosylation, however the yield for TARG1 KO cells was poor due to PARGi cytotoxicity (Figure 2.32C). While it is tempting to speculate that this could represent endogenous ADP-ribosylation of gDNA, the previous data indicate that this could be contamination by free PAR released from excessive protein ADP-ribosylation. Collectively, this data shows that poly-ADP-ribosylation, but not mono-ADP-ribosylation, can cross-link to nitrocellulose membranes and that there exists elevated levels of ADP-ribosylation detectable by both western blot and dot blot for all PARGi-treated cells.

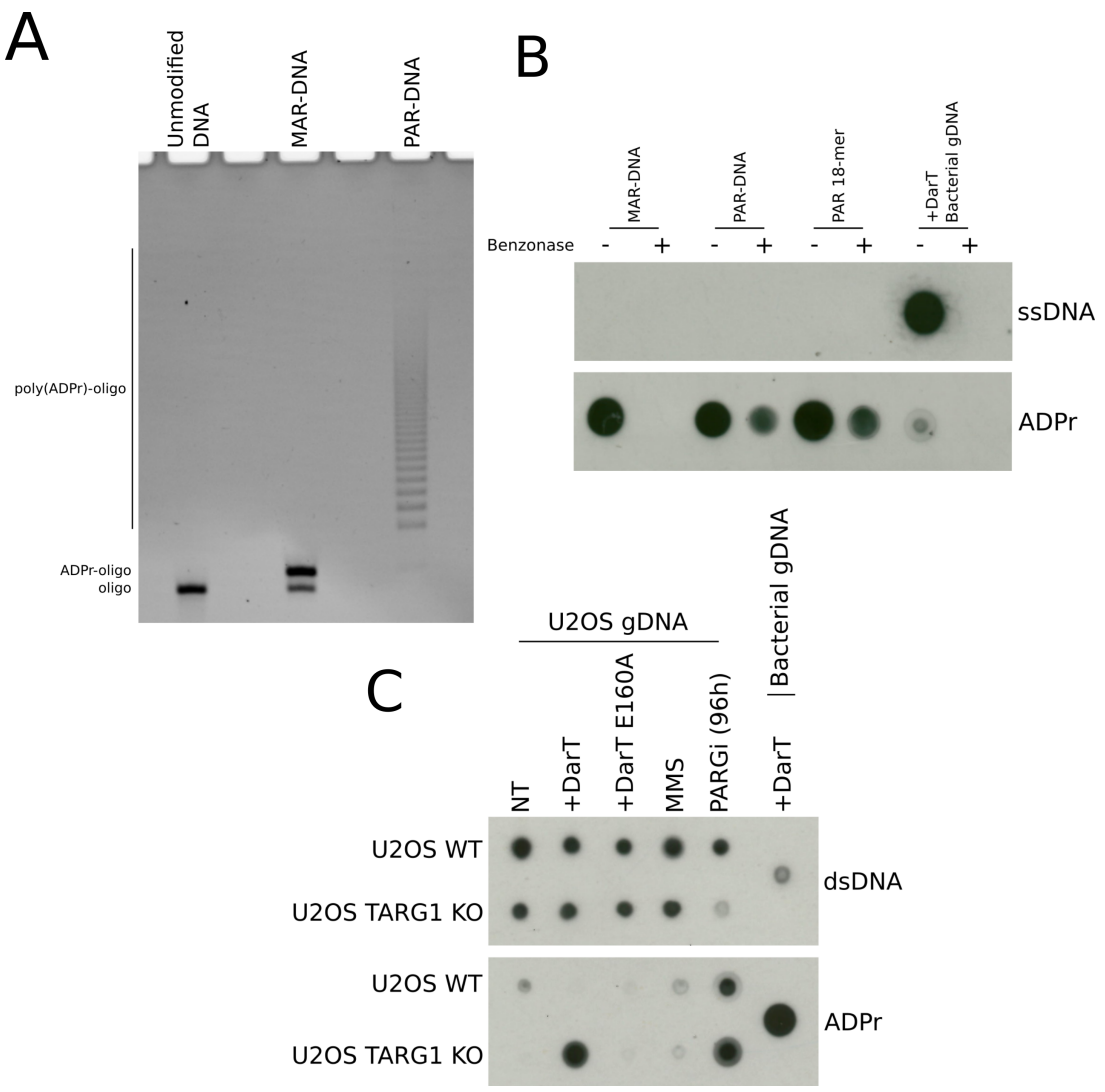


Figure 2.32: Free PAR is detectable by dot blot. **(A)** UV detection of DarT modified DNA oligonucleotide (thymidine-linked mono-ADP-ribosylated oligonucleotide, labelled MAR-DNA) and of PARP1 poly modification of thymidine-linked ADP-ribose oligonucleotide (thymidine-linked poly-ADP-ribosylated oligonucleotide, labelled PAR-DNA). **(B)** MAR-DNA or PAR-DNA from **A**, in combination with free PAR (18-mer) or bacterial genomic DNA expressing DarT WT were treated with benzonase (50U, 30 minutes) as indicated. Reactions were then dotted onto nitrocellulose membranes and immunoblotted for dsDNA and levels of ADP-ribose were determined using the CST poly/mono ADP-ribose antibody. **(C)** Genomic DNA from U-2 OS WT or TARG1 KO treated with DarT WT (24h), DarT E160A (24h), MMS (2 mM, 1h) or PARGi (10 µM, 96h) was extracted and immunoblotted for dsDNA and ADP-ribose using the CST poly/mono ADP-ribose antibody.

Chapter 3

Discussion

3.1 TARG1 protects against DNA ADP-ribosylation

ADP-ribosylation is a wide-spread and dynamic modification that can regulate a range of cellular processes such as DNA damage repair, chromatin remodelling and transcriptional regulation [200]. In these processes, ADP-ribosylation has been studied primarily as a post-translational modification of proteins. However, growing evidence is beginning to show that nucleic acids are also a target for ADP-ribosylation. For example, the roles for PARP1-3 in the DNA damage response have been intensely studied through both their auto-modification and ADP-ribosylation of target proteins. Recently, PARP1-3 have also been shown to ADP-ribosylate phosphate groups at DNA ends *in vitro* and each PARP recognises distinct DNA structures [259–262]. However, study into the consequences of DNA ADP-ribosylation *in vivo* have been scarcely studied [254, 255]. Here, our results reveal the damaging impact unchecked DNA ADP-ribosylation stress can impose on human cells that are deficient in the ADP-ribosylhydrolase TARG1. Moreover, we also demonstrate that DarT-mediated DNA ADP-ribosylation results in the robust activation of the DDR in replicating cells and limits DNA synthesis. We thereby conclude that TARG1 repairs and protects ssDNA exposed during DNA replication from the damaging impact of ADP-ribose base adducts.

We report that the enzymatic activity of TARG1 in the reversal of thymidine-linked ADP-ribosylation is similar to that of direct DNA damage reversal pathways, such as AGT [119, 281]. These pathways offer a simple and effective means of reversing DNA adducts

without requiring breakage of the DNA phosphodiester backbone, DNA synthesis, or a nucleotide template. This simple, error free DNA repair ensures preservation of genome integrity. We therefore propose TARG1 as a non-canonical direct DNA repair enzyme involved in the removal of ADP-ribose adducts from DNA.

The activity of TARG1 and other ADP-ribosylhydrolases PARG, MacroD2 and ARH3 have been shown *in vitro* to remove ADP-ribosylation from DNA phosphates. Here, we also find that MacroD1 and MacroD2, but not PARG or ARH3, have some activity in reversing thymidine-linked ADP-ribosylation *in vitro*. However, MacroD1 and MacroD2 were unable to rescue DarT toxicity in bacteria, perhaps due to steric hindrance blocking access of MacroD1 and MacroD2 to sites of DNA replication in order to reverse DNA ADP-ribosylation catalysed by DarT *in vivo*. Alternatively, it could be that these enzymes are less efficient at reversing thymidine-linked ADP-ribosylation when compared to TARG1 and are unable to degrade DarT-mediated DNA ADP-ribosylation efficiently enough to restore bacterial growth. Future work could perform activity assays between the aforementioned ADP-ribosylhydrolases to determine their efficiency in removing thymidine-linked and other forms of DNA ADP-ribosylation.

Here, we also find that TARG1-deficient humans cells are strikingly sensitive to DarT expression whereas WT cells show no apparent sensitivity. This suggests that TARG1 is remarkably effective in protecting WT cells against thymidine-linked ADP-ribosylation. A failure to protect against this form of DNA modification results in limited DNA synthesis, induction of the DDR in replicating cells and cytotoxicity. We also examined the potential of sensitising WT cells to DarT by inhibiting Chk1. Under normal conditions, Chk1 is involved in the constraint of origin firing during DNA replication [282, 283]. By inhibiting Chk1, origins fire uncontrollably and expose increasing levels of ssDNA that could be ADP-ribosylated by DarT. However, despite showing increased replication stress indicative of an increased ssDNA burden, no sensitivity to WT cells treated with both DarT and Chk1 inhibitor (Chk1i) was observed, further demonstrating the efficiency of TARG1 in

protecting against DNA ADP-ribosylation by DarT.

Interestingly, our data also suggests that endogenous ARTs, such as PARP1, can extend thymidine-linked ADP-ribosylation, indicating that this could be a potential form of ADP-ribosylation in DarT-treated TARG1 KO cells. However, inhibition of PARPs with olaparib or veliparib do not decrease in the levels of ADP-ribosylation or DarT toxicity. This suggests that endogenous ADP-ribosylhydrolases are able to prevent the stabilisation of thymidine-linked poly-ADP-ribosylation in DarT-treated TARG1 KO cells. This demonstrates the extensive activity of PARG and other ADP-ribosylhydrolases in degrading poly-ADP-ribosylation but also highlights their inability to degrade thymidine-linked ADP-ribose adducts and emphasises a unique role for TARG1.

The efficient reversal of thymidine-linked ADP-ribosylation by TARG1 shown here also led us to question if this was the physiological function of TARG1, which currently has not been defined. Previous work has demonstrated that a homozygous mutation of TARG1 in patients manifests in a neurodegenerative disease [239]. We therefore reasoned that thymidine-linked DNA ADP-ribose adducts may persist in TARG1-deficient neuronal cells as they are unable to be effectively repaired, which in turn contributes to neuropathological symptoms. While this could be the case, recent work has shown that low levels of thymidine-linked ADP-ribosylation catalysed by DarT can be repaired by the HR and NER pathways in bacteria [266]. Lawarée et al. proposed that the thymidine-linked ADP-ribose adduct on ssDNA is transferred to dsDNA by RecF-mediated HR, resulting in a DNA duplex distortion that then triggers the NER pathway. However, due to the post-replicative nature of neuronal cells, they would be unable to reply upon replication-associated HR and therefore unable to transfer ssDNA thymidine-linked ADP-ribose lesions into dsDNA to be repaired by NER [284]. This suggests that long-lived neuronal cells could be particularly sensitive to thymidine-linked ADP-ribosylation and explain why a TARG1 mutation in patients can manifest in a neurodegeneration phenotype. However, the data presented here suggests that DNA damage induced by DarT occurs in S-phase of replicating cells.

Owing to the typically quiescent nature of neurons, routine DNA replication would not occur and therefore the ssDNA substrate for DarT would not be exposed, suggesting that neuronal cells would not accumulate thymidine-linked ADP-ribosylation from DarT or a similar ART. However, what has not been addressed here is the possibility that ssDNA exposed through other pathways, such as transcription, could also be ADP-ribosylated. Alternatively, neuronal cells could have thymidine-linked ADP-ribosylation present from a preceding S-phase that could persist if cells lacked TARG1. Future work could aim to assess if serum depletion, which stalls cells in G0, leads to an accumulation of DarT mediated DNA ADP-ribosylation. Moreover, we cannot exclude that human cells may have alternative modes DNA repair other than HR and NER that could repair thymidine-linked ADP-ribosylation, albeit not as effectively as TARG1.

However, despite the promising thought that the physiological role of TARG1 is in the reversal of thymidine-linked ADP-ribosylation, there is currently no evidence that suggests this form ADP-ribosylation exists in human cells. Nonetheless, the ART superfamily is renowned for being tremendously diverged at the sequence level, making the prediction of new ARTs difficult [210]. Indeed, DarT was studied in bacteria due to its presence in an operon with another protein that contained a macrodomain, DarG [203]. Only later was DarT serendipitously characterised as an ART that specifically modifies DNA. This reveals the unexpected nature of ARTs and highlights the importance in characterising ARTs against a wide range of potential substrates. Furthermore, recent work has demonstrated that additional protein cofactors can alter the substrate specificity of ARTs. HPF1 has been shown to interact with PARP1-2 and shift the preferred ADP-ribosylation substrate to serine in a DNA damage context [218, 220]. This suggests that other cofactors that alter substrate specificity, perhaps to DNA, may also exist. Serine ADP-ribosylation was revealed as a highly modified site under genotoxic stress following the development of an unbiased mass spectrometry approach [208, 218]. As DNA ADP-ribosylation is further studied in an *in vivo* context, perhaps similar methodologies can be developed for the unbiased detection of DNA ADP-ribosylation and the conditions in which it is formed.

In order to elucidate if a PARP cofactor that shifts transferase activity towards DNA is present in human cells, future work could aim to incubate PARP KO cell extracts with an oligonucleotide and various recombinant PARPs *in vitro*. This may reveal that a cofactor present in the cell extract may enable the recombinant ART to modify DNA in a way that is not possible in an *in vitro* assay alone. Indeed, using cell extracts to ADP-ribosylate oligonucleotides *in vitro* has already shown success [261]. However, generating a human cell line with no ADP-ribosylation activity will present many challenges.

We also demonstrate the first detection of reversible ADP-ribosylated genomic DNA (gDNA) *in vivo*. This forms a proof-of-concept methodology for the future detection of DNA ADP-ribosylation. Moreover, the finding that nucleic acid ADP-ribosylation is detectable by immunofluorescence but not by western blot reveals the potentially hidden nature of this DNA modification. With this in mind, a possible explanation for the delay in the study of nucleic acid ADP-ribosylation when compared to its protein counterpart could be explained by the similarity of ADP-ribosylation to nucleic acids or the lability of the ADP-ribose to nucleic acid linkage. Both of these cases would make the modification difficult to detect. Moreover, traditional techniques for studying ADP-ribosylation, such as the western blot, treat DNA as a contaminant and thereby prevent the potential detection of DNA ADP-ribosylation through other blotting techniques. As further ADP-ribosyltransferases and ADP-ribosylhydrolases are characterised against an array of potential substrates and additional methods are developed for the detection of DNA ADP-ribosylation, we envisage future work will begin to extend current *in vitro* ADP-ribosylation data to an *in vivo* context.

Our discovery of the striking sensitivity of TARG1-deficient cells to DarT with no apparent impact in WT cells also yields potential avenues of cancer therapy. The cBioPortal curation of cancer genomic databases reveals that TARG1 is altered in approximately 1% of cancers [285]. Although a rare mutation, the subset of cancers deficient in TARG1 catalytic activity could be targeted for precise therapy by the specifically cytotoxic genotoxin DarT.

Bacterial toxins conjugated with proteins that bind an overexpressed cell receptor have previously been developed and approved for use in cancer therapy. For example, diptheria toxin, which ADP-ribosylates eEF2 and blocks protein translation, was conjugated to interleukin-2 (ONTAK) and approved by the FDA for the treatment of T-cell lymphomas [286, 287]. Recent work has also shown that the ART TccC3 from the insect pathogen *Photorhabdus luminescence*, which ADP-ribosylates actin, can be conjugated to a modified form of the protective antigen (PA) from *Bacillus anthracis* and specifically guided to cancer cells overexpressing HER2 or EGFR receptors [288]. In this context, PA forms an oligomeric pore following receptor binding and can facilitates the transport of a wide range of heterologous proteins into the cytosol of target cells [289–292]. Similar strategies could also be used in the targeted killing of TARG1-deficient cells by DarT with minimal off-target effects.

Here, we have shown that TARG1 is a non-canonical DNA repair enzyme that directly removes ADP-ribose adducts from DNA. We also reveal that TARG1-deficient cells are uniquely sensitive to DNA ADP-ribosylation, resulting in a strong induction of the DDR in replicating cells. Moreover, by using DarT as a tool to induce DNA ADP-ribosylation stress, we reveal the techniques and considerations required to detect this modification *in vivo*. With growing *in vitro* evidence demonstrating that nucleic acids can be ADP-ribosylated by PARPs we hope that the techniques demonstrated here will be further developed to reveal the endogenous ADP-ribosylation of nucleic acids.

3.2 PARG inhibitor sensitivity in TARG1-deficient cells

The recent development of the PARG inhibitor (PARGi) used here has instigated a flurry of research into the impact a lack of ADP-ribosylation degradation can have [235]. Some of this work has demonstrated that a subset ovarian cancer cells are sensitive to PARGi therapy and that these cells accumulate ADP-ribosylation and induction of the DDR

[278]. This study hypothesised that PARGi sensitivity in ovarian cancer cells was due to ADP-ribosylation stabilisation at stalled replication forks that prevents their dissolution by the helicase RECQ1 [272, 293]. However, the underlying mechanism that led to an increase in stalled forks in ovarian cancer cells was not determined. A synthetic lethality screen in PARGi-resistant cells revealed that knockdown of some DNA replication factors or inhibition of Chk1 lead to replication stress that sensitised cells to PARGi. It was therefore suggested that underlying replication stress could also be the cause of PARGi sensitivity in some ovarian cancers.

Here, we reveal that TARG1-deficient cells are also sensitive to PARG inhibition. Prolonged PARGi treatment in TARG1 KO cells leads to the accumulation of ADP-ribosylation and induction of DDR signalling, similar to that of the aforementioned ovarian cancers treated with PARGi [278]. This suggests that TARG1 and PARG may have overlapping functions in limiting the accumulation of ADP-ribosylation and protecting against the DNA damage phenotype observed. However, it is difficult to precisely dissect from the data shown here if the presence of excessive ADP-ribosylation is a cause or consequence of the DDR signalling observed. On one hand, a failure to degrade normal ADP-ribosylation signalling could result in an aberrant accumulation of ADP-ribosylation that disrupts important metabolic processes in the cell and subsequently leads to DNA damage. On the other hand, it could be that stochastic DNA damage, such as SSBs, or stalled replication forks at natural impediments may trigger PARP activation first, leading to ADP-ribosylation that is unable to be reversed and prevents effective repair of the original damage [294]. These two scenarios are not mutually exclusive.

We find that PARP inhibition with olaparib rescues both the ADP-ribosylation and DDR induction phenotype we observe in TARG1 KO cells treated with PARGi. This suggests that the initial formation of ADP-ribosylation leads to DNA damage in PARGi treated TARG1 KO cells. Thus, it is the activity of PARP1 and PARP2, which are both inhibited by olaparib, that is responsible for PARGi sensitivity in TARG1 KO

cells. By inhibiting PARP and PARG activity simultaneously, we restore the balance of ADP-ribosylation synthesis and degradation. However, this does not address the source of initial PARP activation observed in TARG1 KO cells treated with PARGi alone.

Previous work has shown that depletion of PARG under conditions of prolonged replication stress results in the accumulation of excessive PAR which also limits effective repair of DSBs at collapsed forks [234]. This suggests that the accumulation of excessive PAR in TARG1 KO cells treated with PARGi could also have impaired DNA repair, which therefore leads to the accumulation of DNA damage. However, this still fails to address the source of initial PARP activation in PARGi-treated TARG1 KO cells. PARP activity may be initially triggered by forks stalling at natural impediments, such as transcription machinery [294]. These forks may then attract PARP activity and accumulate ADP-ribosylation which in turn blocks RECQ1-mediated fork restart [272, 293]. These stalled forks may then undergo aberrant fork restart or fork collapse that then becomes the source of DNA damage in PARGi-treated TARG1 KO cells. In the case of aberrant fork restart, a lack of RECQ1-mediated restart may push the cells to utilise an alternative but futile method of restart, such as HR, that is impaired by excessive PAR [295]. Future work should aim to elucidate the status of replication forks in PARGi treated TARG1 KO cells directly through methods such as a DNA fiber assay.

We find that TARG1 KO cells treated with PARGi that overexpress TARG1 WT are able to rescue the ADP-ribosylation phenotype but are unable to completely rescue DDR activation. We also find that the TARG1 K84A mutant is unable to rescue DDR activation but seems to have some residual activity towards ADP-ribosylation. Previously, the activity of TARG1 was suggested to release full PAR chains from ADP-ribosylated protein [239]. Therefore, in PARGi treated TARG1 KO cells that also overexpress TARG1 WT, the accumulation of protein-linked ADP-ribosylation could be released, resulting in free PAR that blocks repair of DNA damage. Or, the release free PAR may itself trigger a cellular stress response such as parthanatos [239, 296]. However, WT cells do not show

DDR activation in the presence of PARGi with endogenous TARG1 expression which would presumably also release free PAR. This could be due to exogenous TARG1 being overexpressed to a greater magnitude than endogenous TARG1 that then removes a greater proportion of PAR chains than the endogenous TARG1. An alternative hypothesis could be that when the balance of ADP-ribosylation is skewed heavily towards degradation by an overexpressed TARG1, severe NAD^+ depletion is likely to occur as PARPs fruitlessly convert NAD^+ into nicotinamide and ADP-ribose which could also lead to a cell stress response and result in DNA damage. We also find that PARGi treatment reduces TARG1 protein levels, discussed later, which may also reduce the ability for exogenous TARG1 to fully rescue PARGi toxicity.

Future work should aim to assess if other TARG1-deficient cell lines are also sensitive to PARGi as previous studies have shown that loss of some DNA replication factors can sensitise cells to PARGi [278]. Thus, there may be as yet unknown mutations present in the TARG1 KO cells used here that lead to PARGi sensitivity. Additionally, assessing NAD^+ levels in PARGi-treated WT, TARG1 KO and rescue cell lines may reveal conditions of severe NAD^+ depletion that could be artificially restored in an attempt to rescue the DDR phenotype fully in TARG1 overexpressing cells. Here, we also use a constitutively overexpressed TARG1 system that prevents delicate control of TARG1 expression. This could be improved by implementing an inducible system to control TARG1 expression. With such a system, it would be interesting to examine the influence of PARGi treatment in TARG1 KO cells with titrated levels of TARG1 expression. Perhaps as TARG1 expression decreases, PARGi sensitivity may increase as the capacity for ADP-ribosylation degradation is reduced. This could lead to the finding that cancer cells with reduced, but not ablated, TARG1 expression may be sensitive to PARGi therapy. Furthermore, it would also be of interest to examine if TARG1 overexpression in WT cells could also result in RPA2 phosphorylation when combined with PARGi.

Strangely, we also find that TARG1 KO cells treated with PARGi show elevated levels of cyclin B, A, and E, which are responsible for regulating mitotic entry, S-phase or the G1

to S-phase transition, respectively, with elevated levels of cyclin B observed the earliest. Normally, cyclin B interacts with the regulator kinase CDK1 and it is this complex that drives entry into mitosis [297]. Phosphorylation of CDK1 at Y15 by the kinase Wee1 is critical in order to inhibit the CDK1-cyclin B complex, therefore preventing mitotic entry [298]. CDK1 Y15 dephosphorylation can be carried out by the phosphatase Cdc25, which activates the CDK1-cyclin B complex and permits mitotic entry. Our observation of γH2AX and RPA2 phosphorylation following PARG inhibition indicates activation of the DNA damage kinases, which could phosphorylate and activate Chk2. An active Chk2 can phosphorylate Cdc25 and inhibit its phosphatase activity. This would stabilise CDK1 Y15 phosphorylation and therefore block mitotic entry [299].

However, phosphorylation of CDK1 is an equilibrium and increasing expression of cyclin B over the PARGi time-course may enable some cells to eventually slip past the mitotic entry checkpoint. Following mitosis, cells may then enter a new phase of the cell cycle, thus explaining the increase in cyclin E and A levels in combination with cyclin B. Indeed, elevated cyclin B expression has previously been shown to force cells to enter mitosis despite the presence of DNA damage which would otherwise arrest cells in G2 phase [300]. Furthermore, the gradual accumulation of cyclin B observed here is indicative that PARGi treated TARG1 KO cells are stalling in G2 phase and mitosis. Future work should aim to determine if CDK1 Y15 and Chk2 phosphorylation is observed in TARG1 KO cells treated with PARGi. Additionally, QIBC analysis could reveal distinct sub-populations of TARG1 KO cells treated with PARGi that are stuck in different stages of the cell cycle. This could also explain the combined elevated levels of cyclin B, A, and E as observed by western blot since this technique is unable to resolve distinct sub-populations of cells in an asynchronous cell population. Such analyses could also determine the cell cycle stage in which DNA damage is observed and how this damage is transmitted through the cell cycle.

Here, we also observe that following PARGi treatment, TARG1 protein levels decrease. Strangely, overexpressed exogenous TARG1 WT in TARG1 KO cells also shows a similar reduction in TARG1 protein levels in response to PARGi treatment. However, the

TARG1 K84A mutant does not show a decrease following PARGi treatment, suggesting the reduction in TARG1 WT levels is due to the catalytic activity of lysine 84. Due to TARG1 being suggested to release free PAR chains from protein, this free PAR could form aggregates with TARG1 WT, but not for the K84A mutant, that then leads to a reduction of TARG1 levels resolved by western blot. This would therefore explain why we observe reduction in TARG1 levels for PARGi-treated cells as PARG is required to degrade PAR chains into mono-ADP-ribose units and therefore prevent the formation of PAR aggregates. We also hypothesised that free PAR in PARGi treated WT cells could be bound by TARG1 and other ADP-ribose reading proteins. For example, the WWE domain containing protein RNF146 is an E3 ubiquitin ligase that could bind to sites of ADP-ribosylation alongside TARG1 [248]. When in close proximity on PAR chains, RNF146 could ubiquitylate TARG1 and target it for degradation. Future work should aim to address if there is indeed an accumulation of free PAR in PARGi-treated cells and if PAR chain release is dependent upon TARG1. Furthermore, it would be interesting to examine if proteasome inhibitors in PARGi-treated cells could rescue the decrease in TARG1 expression. Moreover, future work should further characterise the binding affinity of TARG1 to free PAR chains and how different TARG1 mutants respond to PARG inhibition.

The sensitivity of TARG1-deficient cancer cells to PARG inhibition could also lead to the development of TARG1-related therapies. The aforementioned study by Pillay and Tighe et al. demonstrated that some ovarian cancers are sensitive to PARGi treatment [278]. This was deemed to be a consequence of DNA replication vulnerabilities and PARGi treatment led to the accumulation of DNA damage, protein-linked ADP-ribosylation and cell death. Here, we observed the same induction of DNA damage and protein-linked ADP-ribosylation in TARG1-deficient cells, suggesting that TARG1 loss is synthetically lethal with PARGi. This finding that TARG1-deficient cells are sensitive to PARGi also leads to potential therapeutic treatment of TARG1-deficient cancers with PARGi. However, this raises the question about the status of TARG1 in the PARGi sensitive ovarian cancer cells used in the aforementioned study [278]. Future work should aim to determine the

status of TARG1 expression in these ovarian cancers cells in order to determine if TARG1 loss is responsible for PARGi sensitivity observed, or if multiple mechanisms can contribute to PARGi synthetic lethality.

PARG inhibition and DNA ADP-ribosylation

The work shown in this thesis has demonstrated that TARG1 is involved in the direct repair of thymidine-linked ADP-ribose adducts. We also show that TARG1 KO cells are uniquely sensitive to this form of DNA ADP-ribosylation and DarT-treated TARG1 KO cells show a pattern of DDR induction similar to that found in PARGi-treated TARG1 KO cells. We therefore hypothesised that perhaps DNA ADP-ribosylation on an unknown site may also occur in PARGi treated cells. We find that when analysed by dot blot, PARGi treated WT and TARG1 KO cells show elevated levels of detectable ADP-ribosylation in gDNA extracts. It it tempting to suggest that the TARG1 KO cells show more ADP-ribosylation in response to PARGi, but due to uneven yield of gDNA this can not be concretely concluded. Additionally, we also reveal that free PAR can crosslink to membranes in the dot blot assay. This suggests that free PAR in the cell can contaminate gDNA extracts and give a false-positive result in subsequent dot blot analysis. PARG has been shown to possess endoglycosidase activity and ARH3 has been proposed to also have this activity, suggesting that both of these ADP-ribosylhydrolases could lead to release of free PAR chains from ADP-ribosylated substrates [232, 301]. This therefore indicates that the accumulation of protein-linked ADP-ribosylation observed in PARGi treated TARG1 KO cells could result in free PAR release that may contaminate downstream detection.

Interestingly, we find that mono-ADP-ribose (as shown by benzonase treated MAR-DNA) is unable to crosslink to the membrane used in a dot blot assay. This suggests that an ADP-ribosylhydrolase that can trim PAR chains into their mono-ADP-ribose form and not degrade the DNA-ADP-ribose linkage could be used to clean free PAR contamination from gDNA. For example, we show that thymidine-linked ADP-ribosylation is unable to be cleaved by PARG or ARH3, which could be used to trim PAR chains into

mono-ADP-ribose units. However, there is currently no evidence that thymidine-linked ADP-ribosylation exists in human cells. The best evidence for DNA ADP-ribosylation in human cells comes from *in vitro* work which has shown that PARP1-3 can ADP-ribosylate phosphates at DNA ends, suggesting that phosphate-linked ADP-ribosylation could be the predominant form of DNA ADP-ribosylation in human cells. Unfortunately, it was revealed that TARG1, MacroD2, ARH3 and PARG can all remove ADP-ribosylation from DNA end phosphates *in vitro* [260]. Crucially however, Nudix Hydrolase 16 (NUDT16) did not cleave the phosphate-linked ADP-ribose transferred by PARP1 or PARP3. Instead, NUDT16 cleaves the pyrophosphate bond in ADP-ribose and, assuming this activity is maintained at the DNA proximal ADP-ribose, the persisting signal will be that of the radioactive alpha phosphate of ADP-ribose. However, the precise form of ADP-ribose on DNA that remains following NUDT16 treatment is unknown. Previous work has shown that NUDT16 treatment on poly-ADP-ribosylated proteins leaves behind a ribose-5'-phosphate on the modified residue [302]. This suggests that the residual ADP-ribosylation mark remaining on NUDT16-treated ADP-ribosylated DNA could be a phosphate-linked ribose-5'-phosphate. The ADP-ribose recognising antibody used here to detect thymidine-linked ADP-ribosylation was serendipitously shown to specifically detect this form of DNA ADP-ribosylation. However, it is unknown if this antibody would also be able to recognise a phosphate-linked ribose-5'-phosphate adduct. It is therefore imperative that a range of ADP-ribosylhydrolases and antibodies are tested as further serendipity may reveal a better methods for detection of phosphate-linked ADP-ribosylation.

Here, we have shown that TARG1 KO cells are sensitive to PARGi treatment and accumulate ADP-ribosylation and DNA damage. However, we were unable to resolve the initial source of PARP activation or damage. Interestingly, recent work has revealed that short incubations with PARGi lead to S-phase specific ADP-ribosylation in WT cells [236]. This S-phase ADP-ribosylation was shown to be essential for Okazaki fragment maturation and could be examined as a potential source of initial PARP activation in TARG1 KO cells treated with PARGi. In this context, S-phase ADP-ribosylation could fail to be degraded

and lead to impaired Okazaki fragment maturation that is subsequently perceived by the cell as DNA damage. Moreover, both Okazaki fragments and regressed arms at stalled forks may contain DNA phosphates in a context that is similar to substrates that have been shown to be ADP-ribosylated *in vitro* and could therefore be as yet unidentified *in vivo* ADP-ribosylation substrates [259–262]. We also show here the efficient nature of TARG1 in the reversal of thymidine-linked DNA ADP-ribosylation at sites of DNA replication and both TARG1 and PARG have been shown to reverse phosphate-linked DNA ADP-ribosylation. Thus, a shared substrate for TARG1 and PARG could be a nucleic acid.

It's tempting to speculate the wide variety of endogenous processes DNA ADP-ribosylation may be involved in. It seems clear from *in vitro* work that the context of target nucleic acid phosphates to be ADP-ribosylated are important and additional factors may facilitate end processing to yield such structures prior to modification. Thus, to study these processes it is crucial that robust methods are developed to detect nucleic acid ADP-ribosylation that could potentially reveal a new and widespread facet of ADP-ribosylation.

Chapter 4

Materials and Methods

Structural and sequence alignments

For structural alignments, *Taq*DarG-macro (PDB: 5M3E) was aligned with TARG1 (PDB: 4J5S, chain D, over 136 α-carbons), MacroD1 (PDB: 2X47, over 144 α-carbons) or MacroD2 (PDB: 4IQY, chain A, over 144 α-carbons) and RMSD values were calculated using the CE algorithm in PyMOL [203, 237, 239, 303]. Sequence alignments for the neighbour-joining phylogenetic trees were generated using the MAFFT server (https://mafft.cbrc.jp/alignment/server/) and the tree was visualised with iTOL (https://itol.embl.de/) [304]. Protein sequence UniProt reference numbers used in the tree are as follows: DarG-macrodomain (B7A854), TARG1 (Q9Y530), MacroD1 (Q9BQ69), MacroD2 (A1Z1Q3), mH2A1.1 (O75367), PARG (Q86W56), Alc1 (Q86WJ1), Sco6735 (Q9X7P1), GDAP2 (Q9NXN4).

Oligonucleotides

GJ1: *GAGCTGTACAAGTCAGATCTCGAGCTC*
27mer: *CACGACACGAGCAGGCATGTCCACGTG*

Thymidine-linked ADP-ribosylated DNA purification

Unmodified GJ1 or 27mer DNA oligonucleotides at a concentration of 0.5 mM were incubated with 1 µM DarT, 5 mM EDTA, ADP-ribosylation buffer (50 mM Tris-Cl pH8, 150 mM NaCl) and 0.5 mM NAD^+ up to a volume of 50 µL with H_2O. Reactions were incubated overnight at 37°C. DarT ADP-ribosylated DNA oligonucleotides were purified by denaturing urea PAGE, stained using ethidium bromide (Sigma) and gel pieces containing ADP-ribosylated DNA were extracted using UV shadow. Gel pieces

were incubated at 50°C in ∼500 µL TE buffer for 10 minutes, three times. TE buffer containing ADP-ribosylated DNA was pooled, passed through a 0.2 µM filter and desalted with G-25 spin columns (GE Healthcare). The concentration of ADP-ribosylated DNA was determined by nanodrop using A260 and Beer-Lambert law with a 13,500 $\mu M^{-1}cm^{-1}$ extinction coefficient for ADP-ribose and an extinction coefficient of 262000 $\mu M^{-1}cm^{-1}$ for the ssDNA oligonucleotides GJ1 or 27mer. If required, DNA was further concentrated using a speedvac.

De-ADP-ribosylation assay

DarT ADP-ribosylated DNA oligonucleotides were purified as described in the thymidine-linked ADP-ribose DNA purification method. ADP-ribosylated oligonucleotides were used as a substrate at 2 µM. The indicated hydrolases were added at a concentration of 1 µM for 30 minutes at 37°C. In assays involving the demodification of thymidine-linked poly-ADP-ribosylated DNA, PARP1 reactions were stopped by heating to 95°C for 3 minutes followed by the addition of 1 µM olaparib. As before, 1 µM of the indicated hydrolase was added and incubated for 30 minutes at 37°C. In both cases, samples were heated to 95°C for 3 minutes in 2x TBE urea samples buffer (8 M urea, 1 mM EDTA pH8, 20 mM Tris pH8 and 0.05% bromophenol blue). Samples were loaded onto a prerun (30 minutes at 6W) denaturing urea PAGE gel containing 8M urea, 1x TBE and 20% polyacrylamide. The gel was run at 6W per gel in 1x TBE. The gel was then stained with ethidium bromide and DNA visualised by UV using a gel documentation system.

Plasmids

Plasmids	Source
pBAD33-V5-*Taq*DarT	Jankevicius and Ariza et al. [203]
pET28a-6xHis-*Taq*DarG-WT-1-155aa	Jankevicius and Ariza et al. [203]
pET28a-6xHis-*Taq*DarG-K80A-1-155aa	Jankevicius and Ariza et al. [203]
pET28a-6xHis-TARG1-WT	For this thesis
pET28a-6xHis-TARG1-K84A	For this thesis
pET-28a-6xHis-ARH3-WT	For this thesis
pET-28a-PARG-WT-448-976aa	For this thesis
pET-28a-MacroD1-WT-58-325aa	For this thesis
pET-28a-MacroD2-WT-7-243aa	For this thesis
pLIX_403-GFP-*Taq*DarT-WT	For this thesis
pLIX_403-GFP-*Taq*DarT-E160A	For this thesis
pLX304-TARG1-WT	For this thesis
pLX304-TARG1-K84A	For this thesis
pCMV-dR8.2 dvpr	Addgene plasmid #8455
pCMV-VSV-G	Addgene plasmid #8454

Bacterial toxicity rescue assay

BL21 DE3 cells were transformed with the indicated plasmids and grown in liquid culture supplemented with 0.8% glucose with the appropriate antibiotics overnight in order to inhibit pBAD33-DarT expression. Cultures were spread onto LB agar containing the appropriate antibiotics and either 0.8% glucose or 0.8% arabinose with or without 50 µM IPTG. Plates were incubated overnight at 37°C. For western blot analysis of DarT and hydrolase expression, cultures were induced with 0.8% arabinose and 50 µM IPTG for 1h at 37°C. Bacteria were pelleted at 800xg for 3 minutes, washed in PBS, pelleted again before being resuspended in boiling lysis buffer (1% SDS, 10 mM Tris pH8, 1 mM EDTA) and heated to 95°C for 3 minutes. Lysates were prepared for western blot analysis as

indicated by the western blot method.

Cell culture

Cell lines	Source
U-2 OS WT	ATCC HTB-96
U-2 OS TARG1 KO	Giuliana K. Moeller and Gyula Timinszky [305]
HEK 293T	ATCC CRL-3216

All cells were grown in a sterile environment and routinely checked for the presence of mycoplasma. U-2 OS or HEK 293T (hereafter 293T, used for lentivirus generation) cells were grown under standard cell culture conditions (humidified atmosphere and 5% CO_2) in Dulbecco's modified Eagle's medium (DMEM. Sigma, D6429) supplemented with 10% fetal bovine serum (Sigma) and penicillin-streptomycin antibiotics (Thermo Fisher). Unless stated otherwise, the following drugs were used at the indicated final concentrations: hydroxyurea (2 mM, Sigma), camptothecin (1 µM, Selleckchem), MMS (2 mM, Sigma), olaparib (1 µM, Selleckchem), veliparib (1 µM, Selleckchem), talazoparib (100 µM, Selleckchem), PJ-34 (100 µM, Enzo Life Sciences), benzamide (10 mM, Sigma), Chk1i (UCN-01, 300 nM, Sigma), doxycycline (concentration varied to match GFP expression between cell lines, Sigma), PARGi (PDD00017273, 10 µM, Torcis).

Antibodies

Primary antibodies used here include: β-tubulin (ab6046, Abcam), TARG1 (25249-1-AP, Proteintech), γH2AX (05-636, Merck), RPA2 (ab2175, Abcam), RPA2 pS4/8 (A300-245A, Bethyl), RPA2 pT21 (ab61065, Abcam), PARP1 (ab32138, Abcam), Cyclin A (sc-271682, Santa Cruz), Cyclin B (4138, CST), Cyclin E (4129, CST), GFP (ab5450, Abcam), PCNA (sc-56, Santa Cruz), KAP1 pS824 (A700-013, Bethyl), PARG (MABS61, Merck), 6xHis (631212, Takara), V5 (A190-120A, Bethyl), ssDNA (autoanti-ssDNA, DSHB), dsDNA (autoanti-dsDNA, DSHB), PAN-ADP-ribose (MABE1016, Merck), CST poly/Mono ADP-ribose (83732, CST), Trevigen PAR monoclone (4335-MC-100, Trevigen), Millipore mono ADP-ribose (MABE1076, Millipore), 10H ADP-ribose (ALX-804-220-R100, Enzo Life

Sciences). Secondary antibodies used here include: Alexa Fluor 488 donkey anti-goat, Alexa Fluor 555 donkey anti-rabbit, Alexa Fluor 555 donkey anti-mouse, Alexa Fluor 647 donkey anti-rabbit, Alexa Fluor 647 donkey anti-mouse (Thermo Fisher), goat anti-mouse HRP (P0447, Dako), goat anti-rabbit HRP (P0448, Dako).

autoanti-ssDNA and autoanti-dsDNA were deposited to the DSHB by Voss, E.W. (DSHB Hybridoma Product autoanti-ssDNA or autoanti-dsDNA).

Lentiviral transduction

Lentivirus production was carried out by transfecting 293T cells with pCMV-VSV-G (1 µg), pCMV-dR8.2 dvpr (5 µg) in combination with DarT-pLIX_403 or TARG1-pLX304 (5 µg) using polyfect transfection reagent (QIAgen). 293T cells were transfected for 12h and media was replaced and incubated for a further 48h. This lentivirus containing media was collected and filtered through a 0.45 µM filter and a 2-fold dilution was added to target U-2 OS cells for 48h. U-2 OS media was then replaced without selection antibiotic and incubated for a further 24h. Media was then changed for selection antibiotic-containing media (puromycin 0.1 µg/mL or blasticidin 1 µg/mL) and incubated until control cells died. Surviving cells from the lowest viral dilution were expanded and monoclones were selected using cloning discs (Sigma). Monoclones were then tested for expression (doxycycline for pLIX_403, no induction necessary for pLX304) and clones with similar levels of expression were taken forward for subsequent experiments.

Clonogenic survival assay

U-2 OS cells were seeded at a density of 500 cells per well of a 6-well plate and incubated for 24h. Cells were then incubated with the desired condition for 14 days. After this time, cells were washed in PBS and fixed using methanol with crystal violet (25% methanol, 0.5% crystal violet with distilled water) for 30 minutes. Following staining, cells were washed with water and imaged with a Nikon DSLR using identical exposure settings.

Western blot

Whole cell extracts were obtained by lysing cells in boiling SDS lysis buffer (1% SDS, 10 mM Tris pH8, 1 mM EDTA) and heating the lysate to 95°C for 3 minutes. Lysates were cooled to RT and supplemented with 2 mM $MgCl_2$ and 0.5 U/µL of benzonase and incubated at RT for 1-2h before being heated again to 95°C for 3 minutes and cooled to RT. Protein concentrations were quantified using the standard Bradford assay (Bio-Rad, 5000006). Protein concentrations were equalised and mixed with sample buffer (Thermo, NP0008). Proteins were resolved by SDS-polyacrylamide gel electrophoresis (SDS-PAGE) and transferred onto nitrocellulose membranes (Bio-Rad). Membranes were blocked using 5% milk powder in PBS-Tween 20 (0.01%, hereafter PBST) for 1h at RT. Membranes were briefly washed and probed for the indicated primary antibodies in 5% BSA in PBST at a dilution of 1:2500 at 4°C overnight. Membranes were washed for 3x5 minutes in PBST and subsequently incubated with the appropriate HRP-conjugated secondary antibodies (Dako) in 5% milk powder in PBST for 1h. ECL-based chemiluminescence was then detected using Pierce ECL (Thermo, 32106) with Hyperfilms (GE).

Immunostaining

Cells were seeded onto 12 mm glass coverslips and grown to a density of approximately 70-90% prior to treatment. Following the indicated treatments, cells were fixed in 3% formaldehyde for 15 minutes. For conditions where chromatin-bound RPA2 and PCNA were examined, cells were pre-extracted with ice-cold 0.2% Triton X-100 in PBS for 1 minute on ice prior to fixation. Following fixation, cells were washed 3x in PBS and permeabilised using 0.2% Triton X-100 in PBS for 5 minutes. For experiments requiring PCNA labelling, permeabilisation was instead carried out using an ice cold methanol:acetone solution (1:1) for 5 minutes following fixation. In both scenarios, cells were washed 3x in PBS following permeabilisation. When EdU was visualised, this was performed following the manufacturer's instructions before primary antibody incubation. Primary antibodies were incubated at a 1:500 dilution in DMEM supplemented with 10% FBS and penicillin-

streptomycin antibiotics. Individual coverslips were incubated with 100 µL of the desired antibodies for 1-2h at room temperature. Following primary antibody incubation, cells were washed 3x in PBS and secondary antibody incubations were performed as described for primary antibodies. Following antibody incubations, cells were washed 3x in PBS prior to incubation with 0.1 µg/ml DAPI in PBS for 10 minutes. Cells were again washed in 3x PBS before being washed in distilled water and air-dried on filter paper at RT. Dried coverslips were mounted onto glass slides using 5 µL of Mowiol-based mounting media (Mowiol 4-88 [Sigma, 81381] in Glycerol/TRIS).

Microscopy

Cells were imaged using standard wide-field microscopy on a BX61 Olympus microscope equipped with 20x/0.5 and 40x/0.75 dry objectives, a CoolSNAP HQ2 14-bit detector (Roper Scientific), motorised stage (Prior), and MetaMorph 7.5 imaging software (Molecular Devices).

Quantitative image based cytometry

Multichannel images for quantitative image based cytometry (QIBC) were acquired using the microscope as described in the microscopy method. Typically, 25-50 non-overlapping images were randomly acquired with the 20x objective to yield at least 1,000 cells per condition. All images were acquired under non-saturating conditions at a single software autofocus directed z-position. For all conditions in one experiment identical settings were used.

Nuclei segmentation was performed using Otsu thresholding and watershed with CellProfiler [306]. Identified nuclei objects were used as a mask across all image channels and the pixel intensities for each channel were recorded and are depicted here as arbitrary units (A.U.). For subsequent analysis, nuclei were filtered to contain only interphase cells containing a 2C-4C DNA content, as defined by total DAPI intensity. Coloured scatter plots and dot-bar plots were created using R. Within one experiment, similar

numbers of identified nuclei were compared across different conditions. For dot-bar plot visualisations, random x-axis jittering was applied to displace overlapping data points. All QIBC visualisations for each condition that contain at least 1,000 cells are shown. CellProfiler pipelines and R scripts used to generate QIBC plots are available at: github.com/callum-jpg/qibcPlot.

Genomic DNA extraction

For bacterial genomic DNA (gDNA) extraction, cells were grown to OD 0.2 before DarT expression was induced with 0.8% arabinose for 1 hour. Cells were pelleted at 800xg for 3 minutes, washed with PBS, pelleted again, before being resuspended in boiling lysis buffer (1% SDS, 10 mM Tris pH8, 1 mM EDTA) and heated to 95°C for 3 minutes.

For U-2 OS gDNA extraction, cells were incubated with the indicated genotoxins and grown to 70-90% confluency. Cells were trypsinised, pelleted at 800xg for 3 minutes at 4°C, pellet gently washed with ice-cold PBS, pelleted again, before being resuspended in boiling lysis (as above, but also supplemented with 1 µM olaparib and 1 µM PARGi) buffer and heated to 95°C for 3 minutes.

Lysates were cooled to RT and treated with 20 µg/mL of RNase at 37°C for 1h in a shaking incubator. Next, lysates were incubated with 100 µg/mL of proteinase K at 50°C for 1h in a shaking incubator. Lysates were cooled to RT and incubated with an equal volume of phenol:chloroform:isoamyl alcohol pH8 (Sigma, P3803) and inverted until an emulsion formed. This emulsion was centrifuged for 3 minutes at 15,000xg and the upper aqueous layer was removed, added to a fresh tube and re-extracted with fresh phenol:chloroform:isoamyl alcohol as before. This process was repeated until there was no white protein precipitate present at the interphase between the phenol and aqueous phases. Genomic DNA from the collected aqueous phase was precipitated using 0.2 volumes of 10 M ammonium acetate and 2 volumes of 100% ethanol and inverted at RT until DNA precipitated. Genomic DNA was pelleted at 5000xg for 3 minutes and the DNA pellet was

washed twice with 70% ethanol before being resuspended in TE buffer. Genomic DNA concentrations were estimated using a DeNovix DS-11 FX nanodrop and concentrated by speecvac if required.

ADP-ribosylated DNA detection by dot blot

Approximately 1 µg of gDNA was dotted onto a nitrocellulose membrane (Amersham Protran 0.45 NC nitrocellulose) using a multichannel pipette, dried and and crosslinked with 1200 J using a Stratalinker UV crosslinker. The crosslinked DNA was immunoblotted for gDNA (autoanti-dsDNA, DSHB, 1:200) or ADPr-gDNA (Poly/Mono-ADP ribose, E6F6A, Cell Signalling Technology, 1:1000) for 1h at RT in 5% powdered milk in PBST. Secondary peroxidase-couple antibodies (Dako) were incubated at RT for 1h. ECL-based chemiluminescence was detected using Pierce ECL (Thermo, 32106) with Hyperfilms (GE).

PARP1 thymidine-linked DNA ADP-ribosylation assay

DarT ADP-ribosylated DNA oligonucleotides were purified as described in the thymidine-linked ADP-ribose DNA purification method. Purified ADP-ribosylated oligonucleotides were used as a substrate at approximately 2 µM and with PARP1 (0.2 µM), NAD^+ (100 µM) and 1x PARP buffer (20 mM HEPES-KOH pH 7.6, 50 mM KCl, 5 mM $MgCl_2$, 1 mM DTT, and 100 µG/mL BSA). Reactions were incubated at 37°C for 30 minutes. Samples were prepared for a denaturing urea PAGE gel as described in the de-ADP-ribosylation assay method and stained using ethidium bromide.

Counting motifs in gDNA

Non-overlapping motifs in genomic DNA were counted using the Python package MotifSearch (Available at: https://github.com/callum-jpg/motifSearch). The following bacterial species genomes were analysed: *Thermus aquaticus* (NZ_CP010822.1) and *Escherichia coli* (NC_000913.3). For human autosomes, the GRCh38.p13 genome assembly was used.

References

1. Lord, C. J. & Ashworth, A. The DNA damage response and cancer therapy. *Nature* **481,** 287–294 (2012).
2. Lindahl, T. Instability and decay of the primary structure of DNA. *Nature* **362,** 709–715 (Apr. 1993).
3. Hoeijmakers, J. H. DNA Damage, Aging, and Cancer. *New England Journal of Medicine* **361,** 1475–1485 (2009).
4. Jackson, S. P. & Bartek, J. The DNA-damage response in human biology and disease. *Nature* **461,** 1071–1078 (2009).
5. Ciccia, A. & Elledge, S. J. The DNA damage response: making it safe to play with knives. *Molecular cell* **40,** 179–204 (2010).
6. Blackford, A. N. & Jackson, S. P. ATM, ATR, and DNA-PK: the trinity at the heart of the DNA damage response. *Molecular cell* **66,** 801–817 (2017).
7. Friedberg, E. C., Walker, G. C., Siede, W. & Wood, R. D. *DNA repair and mutagenesis* (American Society for Microbiology Press, 2005).
8. Lindahl, T. & Nyberg, B. Rate of depurination of native deoxyribonucleic acid. *Biochemistry* **11,** 3610–3618 (1972).
9. Lindahl, T. & Karlstrom, O. Heat-induced depyrimidination of deoxyribonucleic acid in neutral solution. *Biochemistry* **12,** 5151–5154 (1973).
10. Lindahl, T. in (ed Cohn, W. E.) 135–192 (Academic Press, 1979).
11. Lindahl, T. & Nyberg, B. Heat-induced deamination of cytosine residues in deoxyribonucleic acid. *Biochemistry* **13,** 3405–3410 (1974).

12. Ehrlich, M., Zhang, X.-Y. & Inamdar, N. M. Spontaneous deamination of cytosine and 5-methylcytosine residues in DNA and replacement of 5-methylcytosine residues with cytosine residues. *Mutation Research/Reviews in Genetic Toxicology* **238,** 277–286 (1990).

13. Karran, P. & Lindahl, T. Hypoxanthine in deoxyribonucleic acid: generation by heat-induced hydrolysis of adenine residues and release in free form by a deoxyribonucleic acid glycosylase from calf thymus. *Biochemistry* **19,** 6005–6011 (1980).

14. Chaudhuri, J. *et al.* Transcription-targeted DNA deamination by the AID antibody diversification enzyme. *Nature* **422,** 726–730 (Apr. 2003).

15. Muramatsu, M. *et al.* Specific expression of activation-induced cytidine deaminase (AID), a novel member of the RNA-editing deaminase family in germinal center B cells. *Journal of Biological Chemistry* **274,** 18470–18476 (1999).

16. COOKE, M. S., EVANS, M. D., DIZDAROGLU, M. & LUNEC, J. Oxidative DNA damage: mechanisms, mutation, and disease. *The FASEB Journal* **17.** PMID: 12832285, 1195–1214 (2003).

17. Shibutani, S., Takeshita, M. & Grollman, A. P. Insertion of specific bases during DNA synthesis past the oxidation-damaged base 8-oxodG. *Nature* **349,** 431–434 (Jan. 1991).

18. Wood, M. L., Dizdaroglu, M., Gajewski, E. & Essigmann, J. M. Mechanistic studies of ionizing radiation and oxidative mutagenesis: genetic effects of a single 8-hydroxyguanine (7-hydro-8-oxoguanine) residue inserted at a unique site in a viral genome. *Biochemistry* **29.** PMID: 2223758, 7024–7032 (1990).

19. Kasai, H. Analysis of a form of oxidative DNA damage, 8-hydroxy-2'-deoxyguanosine, as a marker of cellular oxidative stress during carcinogenesis. *Mutation Research/Reviews in Mutation Research* **387,** 147–163 (1997).

20. Xie, Y. *et al.* Deficiencies in Mouse Myh and Ogg1 Result in Tumor Predisposition and G to T Mutations in Codon 12 of the K-Ras Oncogene in Lung Tumors. *Cancer Research* **64,** 3096–3102 (2004).

21. Boiteux, S. & Radicella, J. The Human OGG1 Gene: Structure, Functions, and Its Implication in the Process of Carcinogenesis. *Archives of Biochemistry and Biophysics* **377,** 1–8 (2000).

22. Slupska, M. M., Luther, W. M., Chiang, J.-H., Yang, H. & Miller, J. H. Functional Expression of hMYH, a Human Homolog of the Escherichia coli MutY Protein. *Journal of Bacteriology* **181,** 6210–6213 (1999).

23. Fu, D., Calvo, J. A. & Samson, L. D. Balancing repair and tolerance of DNA damage caused by alkylating agents. *Nature Reviews Cancer* **12,** 104–120 (Feb. 2012).

24. Shuker, D. E., Bailey, E., Parry, A., Lamb, J. & Farmer, B. The determination of urinary 3-methyladenine in humans as a potential monitor of exposure to methylating agents. *Carcinogenesis* **8,** 959–962 (July 1987).

25. Hemminki, K., Peltonen, K. & Vodicka, P. Depurination from DNA of 7-methylguanine, 7-(2-aminoethyl)-guanine and ring-opened 7-methylguanines. *Chemico-Biological Interactions* **70,** 289–303 (1989).

26. Engelward, B. P. *et al.* A Chemical and Genetic Approach Together Define the Biological Consequences of 3-Methyladenine Lesions in the Mammalian Genome. *Journal of Biological Chemistry* **273,** 5412–5418 (1998).

27. Johnson, R. E., Yu, S.-L., Prakash, S. & Prakash, L. A Role for Yeast and Human Translesion Synthesis DNA Polymerases in Promoting Replication through 3-Methyl Adenine. *Molecular and Cellular Biology* **27,** 7198–7205 (2007).

28. Kielman, M. F., Smits, R. & Bernini, L. F. Structure of the mouse 3-Methyladenine DNA Glycosylase gene and exact localization upstream of the α-globin gene cluster on Chromosome 11. *Mammalian Genome* **6,** 499–504 (Aug. 1995).

29. Moore, L. D., Le, T. & Fan, G. DNA Methylation and Its Basic Function. *Neuropsychopharmacology* **38,** 23–38 (Jan. 2013).

30. Pfeifer, G. P. *et al.* Tobacco smoke carcinogens, DNA damage and p53 mutations in smoking-associated cancers. *Oncogene* **21,** 7435–7451 (2002).

31. Swann, P. & Magee, P. Nitrosamine-induced carcinogenesis. The alkylation of nucleic acids of the rat by N-methyl-N-nitrosourea, dimethylnitrosamine, dimethyl sulphate and methyl methanesulphonate. *Biochemical Journal* **110,** 39–47 (1968).

32. Mirvish, S. S. Role of N-nitroso compounds (NOC) and N-nitrosation in etiology of gastric, esophageal, nasopharyngeal and bladder cancer and contribution to cancer of known exposures to NOC. *Cancer letters* **93,** 17–48 (1995).

33. Wang, L. *et al.* Pyridyloxobutyl adduct O 6-[4-oxo-4-(3-pyridyl) butyl] guanine is present in 4-(acetoxymethylnitrosamino)-1-(3-pyridyl)-1-butanone-treated DNA and is a substrate for O 6-alkylguanine-DNA alkyltransferase. *Chemical research in toxicology* **10,** 562–567 (1997).

34. Shimada, T. & Fujii-Kuriyama, Y. Metabolic activation of polycyclic aromatic hydrocarbons to carcinogens by cytochromes P450 1A1 and1B1. *Cancer science* **95,** 1–6 (2004).

35. Hanrahan, C. J. *et al.* Sequence Specific Mutagenesis of the Major (+)-anti-Benzo[a]pyrene Diol Epoxide-DNA Adduct at a Mutational Hot Spot in Vitro and in Escherichia coli Cells. *Chemical Research in Toxicology* **10.** PMID: 9114972, 369–377 (1997).

36. Alekseyev, Y. O. & Romano, L. J. In Vitro Replication of Primer-Templates Containing Benzo[a]pyrene Adducts by Exonuclease-Deficient Escherichia coli DNA Polymerase I (Klenow Fragment): Effect of Sequence Context on Lesion Bypass. *Biochemistry* **39.** PMID: 10956033, 10431–10438 (2000).

37. Denissenko, M. F., Pao, A., Tang, M.-s. & Pfeifer, G. P. Preferential formation of benzo [a] pyrene adducts at lung cancer mutational hotspots in P53. *Science* **274,** 430–432 (1996).

38. Tornaletti, S. & Pfeifer, G. P. Complete and tissue-independent methylation of CpG sites in the p53 gene: implications for mutations in human cancers. *Oncogene* **10,** 1493–1499 (1995).

39. Matter, B., Wang, G., Jones, R. & Tretyakova, N. Formation of diastereomeric benzo [a] pyrene diol epoxide-guanine adducts in p53 gene-derived DNA sequences. *Chemical research in toxicology* **17,** 731–741 (2004).

40. Muniandy, P. A., Liu, J., Majumdar, A., Liu, S.-t. & Seidman, M. M. DNA interstrand crosslink repair in mammalian cells: step by step. *Critical reviews in biochemistry and molecular biology* **45,** 23–49 (2010).

41. Deans, A. J. & West, S. C. DNA interstrand crosslink repair and cancer. *Nature reviews cancer* **11,** 467–480 (2011).

42. Von Sonntag, C. *et al. The chemical basis of radiation biology* (Taylor & Francis London, 1987).

43. Box, H. C. *et al.* Radiation-induced formation of a crosslink between base moieties of deoxyguanosine and thymidine in deoxygenated solutions of d (CpGpTpA). *Radiation research* **145,** 641–643 (1996).

44. Box, H. C., Budzinski, E. E., Dawidzik, J. B., Gobey, J. S. & Freund, H. G. Free radical-induced tandem base damage in DNA oligomers. *Free Radical Biology and Medicine* **23,** 1021–1030 (1997).

45. Box, H. C., Budzinski, E. E., Dawidzik, J. B., Wallace, J. C. & Iijima, H. Tandem lesions and other products in X-irradiated DNA oligomers. *Radiation research* **149,** 433–439 (1998).

46. Bellon, S., Ravanat, J.-L., Gasparutto, D. & Cadet, J. Cross-linked thymine-purine base tandem lesions: Synthesis, characterization, and measurement in γ-irradiated isolated DNA. *Chemical research in toxicology* **15,** 598–606 (2002).

47. Mouret, S. *et al.* Cyclobutane pyrimidine dimers are predominant DNA lesions in whole human skin exposed to UVA radiation. *Proceedings of the National Academy of Sciences* **103,** 13765–13770 (2006).

48. Gu, C. *et al.* Recognition and incision of oxidative intrastrand cross-link lesions by UvrABC nuclease. *Biochemistry* **45,** 10739–10746 (2006).

49. Gu, C. & Wang, Y. LC-MS/MS identification and yeast polymerase η bypass of a novel γ-irradiation-induced intrastrand cross-link lesion G [8- 5] C. *Biochemistry* **43,** 6745–6750 (2004).

50. Gu, C. & Wang, Y. Thermodynamic and in vitro replication studies of an intrastrand G [8-5] C cross-link lesion. *Biochemistry* **44,** 8883–8889 (2005).

51. Jiang, Y., Hong, H., Cao, H. & Wang, Y. In Vivo Formation and in Vitro Replication of a Guanine- Thymine Intrastrand Cross-Link Lesion. *Biochemistry* **46,** 12757–12763 (2007).

52. Douki, T., Laporte, G. & Cadet, J. Inter-strand photoproducts are produced in high yield within A-DNA exposed to UVC radiation. *Nucleic acids research* **31,** 3134–3142 (2003).

53. Dutta, S., Chowdhury, G. & Gates, K. S. Interstrand cross-links generated by abasic sites in duplex DNA. *Journal of the American Chemical Society* **129,** 1852–1853 (2007).

54. Stingele, J., Bellelli, R. & Boulton, S. J. Mechanisms of DNA–protein crosslink repair. *Nature Reviews Molecular Cell Biology* **18,** 563–573 (2017).

55. Nakano, T. *et al.* T7 RNA polymerases backed up by covalently trapped proteins catalyze highly error prone transcription. *Journal of Biological Chemistry* **287,** 6562–6572 (2012).

56. Nakano, T. *et al.* Translocation and stability of replicative DNA helicases upon encountering DNA-protein cross-links. *Journal of Biological Chemistry* **288,** 4649–4658 (2013).

57. Fu, Y. V. *et al.* Selective bypass of a lagging strand roadblock by the eukaryotic replicative DNA helicase. *Cell* **146,** 931–941 (2011).

58. Hsiang, Y.-H., Hertzberg, R., Hecht, S. & Liu, L.-F. Camptothecin induces protein-linked DNA breaks via mammalian DNA topoisomerase I. *Journal of Biological Chemistry* **260,** 14873–14878 (1985).

59. Staker, B. L. *et al.* The mechanism of topoisomerase I poisoning by a camptothecin analog. *Proceedings of the National Academy of Sciences* **99,** 15387–15392 (2002).

60. DeMott, M. S. *et al.* Covalent trapping of human DNA polymerase β by the oxidative DNA lesion 2-deoxyribonolactone. *Journal of Biological Chemistry* **277,** 7637–7640 (2002).

61. Murai, J. *et al.* Trapping of PARP1 and PARP2 by clinical PARP inhibitors. *Cancer research* **72,** 5588–5599 (2012).

62. Chválová, K., Brabec, V. & Kašpárková, J. Mechanism of the formation of DNA–protein cross-links by antitumor cisplatin. *Nucleic acids research* **35,** 1812–1821 (2007).

63. Sczepanski, J. T., Wong, R. S., McKnight, J. N., Bowman, G. D. & Greenberg, M. M. Rapid DNA–protein cross-linking and strand scission by an abasic site in a nucleosome core particle. *Proceedings of the National Academy of Sciences* **107,** 22475–22480 (2010).

64. Traut, T. W. Physiological concentrations of purines and pyrimidines. *Molecular and cellular biochemistry* **140,** 1–22 (1994).

65. McElhinny, S. A. N. *et al.* Abundant ribonucleotide incorporation into DNA by yeast replicative polymerases. *Proceedings of the National Academy of Sciences* **107,** 4949–4954 (2010).

66. Joyce, C. M. Choosing the right sugar: how polymerases select a nucleotide substrate. *Proceedings of the National Academy of Sciences* **94,** 1619–1622 (1997).

67. McElhinny, S. A. N. *et al.* Genome instability due to ribonucleotide incorporation into DNA. *Nature chemical biology* **6,** 774–781 (2010).

68. Reijns, M. A. *et al.* Enzymatic removal of ribonucleotides from DNA is essential for mammalian genome integrity and development. *Cell* **149,** 1008–1022 (2012).

69. Hiller, B. *et al.* Mammalian RNase H2 removes ribonucleotides from DNA to maintain genome integrity. *Journal of Experimental Medicine* **209,** 1419–1426 (2012).

70. Lim, Y. W., Sanz, L. A., Xu, X., Hartono, S. R. & Chédin, F. Genome-wide DNA hypomethylation and RNA: DNA hybrid accumulation in Aicardi–Goutières syndrome. *Elife* **4,** e08007 (2015).

71. Rossi, M. L., Purohit, V., Brandt, P. D. & Bambara, R. A. Lagging strand replication proteins in genome stability and DNA repair. *Chemical reviews* **106,** 453–473 (2006).

72. Caldecott, K. W. Single-strand break repair and genetic disease. *Nature Reviews Genetics* **9,** 619 (2008).

73. Breen, A. P. & Murphy, J. A. Reactions of oxyl radicals with DNA. *Free radical biology and medicine* **18,** 1033–1077 (1995).

74. Dedon, P. C. The chemical toxicology of 2-deoxyribose oxidation in DNA. *Chemical research in toxicology* **21,** 206–219 (2008).

75. Zharkov, D. Base excision DNA repair. *Cellular and molecular life sciences* **65,** 1544–1565 (2008).

76. Champoux, J. J. DNA topoisomerases: structure, function, and mechanism. *Annual review of biochemistry* **70,** 369–413 (2001).

77. Pommier, Y. *et al.* Repair of and checkpoint response to topoisomerase I-mediated DNA damage. *Mutation Research/Fundamental and Molecular Mechanisms of Mutagenesis* **532,** 173–203 (2003).

78. El-Khamisy, S. F. *et al.* Defective DNA single-strand break repair in spinocerebellar ataxia with axonal neuropathy-1. *Nature* **434,** 108–113 (2005).

79. Starcevic, D., Dalal, S. & Sweasy, J. B. Is there a link between DNA polymerase beta and cancer? *Cell cycle* **3,** 996–999 (2004).

80. Khanna, K. K. & Jackson, S. P. DNA double-strand breaks: signaling, repair and the cancer connection. *Nature genetics* **27,** 247–254 (2001).

81. Shrivastav, M., De Haro, L. P. & Nickoloff, J. A. Regulation of DNA double-strand break repair pathway choice. *Cell research* **18,** 134–147 (2008).

82. Hanada, K. *et al.* The structure-specific endonuclease Mus81 contributes to replication restart by generating double-strand DNA breaks. *Nature structural & molecular biology* **14,** 1096–1104 (2007).

83. Obe, G., Johannes, C. & Schulte-Frohlinde, D. DNA double-strand breaks induced by sparsely ionizing radiation and endonucleases as critical lesions foe cell death, chromosomal aberrations, mutations and oncogenic transformation. *Mutagenesis* **7,** 3–12 (1992).

84. Pfeiffer, P., Goedecke, W. & Obe, G. Mechanisms of DNA double-strand break repair and their potential to induce chromosomal aberrations. *Mutagenesis* **15,** 289–302 (2000).

85. Lee, J.-H. & Paull, T. T. Direct activation of the ATM protein kinase by the Mre11/Rad50/Nbs1 complex. *Science* **304,** 93–96 (2004).

86. Rogakou, E. P., Pilch, D. R., Orr, A. H., Ivanova, V. S. & Bonner, W. M. DNA double-stranded breaks induce histone H2AX phosphorylation on serine 139. *Journal of biological chemistry* **273,** 5858–5868 (1998).

87. Savic, V. *et al.* Formation of dynamic γ-H2AX domains along broken DNA strands is distinctly regulated by ATM and MDC1 and dependent upon H2AX densities in chromatin. *Molecular cell* **34,** 298–310 (2009).

88. Mailand, N. *et al.* Rapid destruction of human Cdc25A in response to DNA damage. *Science* **288,** 1425–1429 (2000).

89. Falck, J., Mailand, N., Syljuåsen, R. G., Bartek, J. & Lukas, J. The ATM–Chk2–Cdc25A checkpoint pathway guards against radioresistant DNA synthesis. *Nature* **410,** 842–847 (2001).

90. Banin, S. *et al.* Enhanced phosphorylation of p53 by ATM in response to DNA damage. *Science* **281,** 1674–1677 (1998).

91. Shieh, S.-Y., Ikeda, M., Taya, Y. & Prives, C. DNA damage-induced phosphorylation of p53 alleviates inhibition by MDM2. *Cell* **91,** 325–334 (1997).

92. Cheng, Q. & Chen, J. Mechanism of p53 stabilization by ATM after DNA damage. *Cell cycle* **9,** 472–478 (2010).

93. Maya, R. *et al.* ATM-dependent phosphorylation of Mdm2 on serine 395: role in p53 activation by DNA damage. *Genes & development* **15,** 1067–1077 (2001).

94. Chen, J. The cell-cycle arrest and apoptotic functions of p53 in tumor initiation and progression. *Cold Spring Harbor perspectives in medicine* **6,** a026104 (2016).

95. Fridman, J. S. & Lowe, S. W. Control of apoptosis by p53. *Oncogene* **22,** 9030–9040 (2003).

96. Béroud, C. & Soussi, T. The UMD-p53 database: new mutations and analysis tools. *Human mutation* **21,** 176–181 (2003).

97. Zou, L. & Elledge, S. J. Sensing DNA damage through ATRIP recognition of RPA-ssDNA complexes. *Science* **300,** 1542–1548 (2003).

98. Byun, T. S., Pacek, M., Yee, M.-c., Walter, J. C. & Cimprich, K. A. Functional uncoupling of MCM helicase and DNA polymerase activities activates the ATR-dependent checkpoint. *Genes & development* **19,** 1040–1052 (2005).

99. Toledo, L. I. *et al.* ATR prohibits replication catastrophe by preventing global exhaustion of RPA. *Cell* **155,** 1088–1103 (2013).

100. Brown, E. J. & Baltimore, D. ATR disruption leads to chromosomal fragmentation and early embryonic lethality. *Genes & development* **14,** 397–402 (2000).

101. Casper, A. M., Nghiem, P., Arlt, M. F. & Glover, T. W. ATR regulates fragile site stability. *Cell* **111,** 779–789 (2002).

102. Sørensen, C. S. *et al.* Chk1 regulates the S phase checkpoint by coupling the physiological turnover and ionizing radiation-induced accelerated proteolysis of Cdc25A. *Cancer cell* **3,** 247–258 (2003).

103. Bartek, J., Lukas, C. & Lukas, J. Checking on DNA damage in S phase. *Nature reviews Molecular cell biology* **5,** 792–804 (2004).

104. Ward, I. M. & Chen, J. Histone H2AX is phosphorylated in an ATR-dependent manner in response to replicational stress. *Journal of Biological Chemistry* **276,** 47759–47762 (2001).

105. Walker, J. R., Corpina, R. A. & Goldberg, J. Structure of the Ku heterodimer bound to DNA and its implications for double-strand break repair. *Nature* **412,** 607–614 (2001).

106. Boehme, K. A., Kulikov, R. & Blattner, C. p53 stabilization in response to DNA damage requires Akt/PKB and DNA-PK. *Proceedings of the National Academy of Sciences* **105,** 7785–7790 (2008).

107. Bozulic, L., Surucu, B., Hynx, D. & Hemmings, B. A. PKBα/Akt1 acts downstream of DNA-PK in the DNA double-strand break response and promotes survival. *Molecular cell* **30,** 203–213 (2008).

108. Stiff, T. *et al.* ATM and DNA-PK function redundantly to phosphorylate H2AX after exposure to ionizing radiation. *Cancer research* **64,** 2390–2396 (2004).

109. Chen, B. P. *et al.* Ataxia telangiectasia mutated (ATM) is essential for DNA-PKcs phosphorylations at the Thr-2609 cluster upon DNA double strand break. *Journal of Biological Chemistry* **282,** 6582–6587 (2007).

110. Yajima, H., Lee, K.-J. & Chen, B. P. ATR-dependent phosphorylation of DNA-dependent protein kinase catalytic subunit in response to UV-induced replication stress. *Molecular and cellular biology* **26,** 7520–7528 (2006).

111. Ma, Y., Pannicke, U., Schwarz, K. & Lieber, M. R. Hairpin opening and overhang processing by an Artemis/DNA-dependent protein kinase complex in nonhomologous end joining and V (D) J recombination. *Cell* **108,** 781–794 (2002).

112. Goodarzi, A. A. *et al.* DNA-PK autophosphorylation facilitates Artemis endonuclease activity. *The EMBO journal* **25,** 3880–3889 (2006).

113. Povirk, L. F., Zhou, T., Zhou, R., Cowan, M. J. & Yannone, S. M. Processing of 3′-phosphoglycolate-terminated DNA double strand breaks by Artemis nuclease. *Journal of Biological Chemistry* **282,** 3547–3558 (2007).

114. Cary, R. B. *et al.* DNA looping by Ku and the DNA-dependent protein kinase. *Proceedings of the National Academy of Sciences* **94,** 4267–4272 (1997).

115. Graham, T. G., Walter, J. C. & Loparo, J. J. Two-stage synapsis of DNA ends during non-homologous end joining. *Molecular cell* **61,** 850–858 (2016).

116. Gurley, K. E. & Kemp, C. J. Synthetic lethality between mutation in Atm and DNA-PKcs during murine embryogenesis. *Current Biology* **11,** 191–194 (2001).

117. Reaper, P. M. *et al.* Selective killing of ATM-or p53-deficient cancer cells through inhibition of ATR. *Nature chemical biology* **7,** 428 (2011).

118. Middleton, F. K. *et al.* Common cancer-associated imbalances in the DNA damage response confer sensitivity to single agent ATR inhibition. *Oncotarget* **6,** 32396 (2015).

119. Yi, C. & He, C. DNA repair by reversal of DNA damage. *Cold Spring Harbor perspectives in biology* **5,** a012575 (2013).

120. Pegg, A. E. Multifaceted roles of alkyltransferase and related proteins in DNA repair, DNA damage, resistance to chemotherapy, and research tools. *Chemical research in toxicology* **24,** 618–639 (2011).

121. Xu-Welliver, M. & Pegg, A. E. Degradation of the alkylated form of the DNA repair protein, O 6-alkylguanine-DNA alkyltransferase. *Carcinogenesis* **23,** 823–830 (2002).

122. Trewick, S. C., Henshaw, T. F., Hausinger, R. P., Lindahl, T. & Sedgwick, B. Oxidative demethylation by Escherichia coli AlkB directly reverts DNA base damage. *Nature* **419,** 174–178 (2002).

123. Falnes, P. Ø., Johansen, R. F. & Seeberg, E. AlkB-mediated oxidative demethylation reverses DNA damage in Escherichia coli. *Nature* **419,** 178–182 (2002).

124. Sancar, A. Structure and function of photolyase and in vivo enzymology: 50th anniversary. *Journal of Biological Chemistry* **283,** 32153–32157 (2008).

125. Krokan, H. E. & Bjørås, M. Base excision repair. *Cold Spring Harbor perspectives in biology* **5,** a012583 (2013).

126. Wilson, S. H. & Kunkel, T. A. Passing the baton in base excision repair. *Nature structural biology* **7,** 176–178 (2000).

127. David, S. S. & Williams, S. D. Chemistry of glycosylases and endonucleases involved in base-excision repair. *Chemical reviews* **98,** 1221–1262 (1998).

128. Sobol, R. W. *et al.* Requirement of mammalian DNA polymerase-β in base-excision repair. *Nature* **379,** 183–186 (1996).

129. Sleeth, K. M., Robson, R. L. & Dianov, G. L. Exchangeability of mammalian DNA ligases between base excision repair pathways. *Biochemistry* **43,** 12924–12930 (2004).

130. Friedberg, E. C. How nucleotide excision repair protects against cancer. *Nature Reviews Cancer* **1,** 22–33 (2001).

131. Schärer, O. D. Nucleotide excision repair in eukaryotes. *Cold Spring Harbor perspectives in biology* **5,** a012609 (2013).

132. Marteijn, J. A., Lans, H., Vermeulen, W. & Hoeijmakers, J. H. Understanding nucleotide excision repair and its roles in cancer and ageing. *Nature reviews Molecular cell biology* **15,** 465–481 (2014).

133. Batty, D., Levine, A. S., Wood, R. D., *et al.* Stable binding of human XPC complex to irradiated DNA confers strong discrimination for damaged sites. *Journal of molecular biology* **300,** 275–290 (2000).

134. Sugasawa, K. *et al.* A multistep damage recognition mechanism for global genomic nucleotide excision repair. *Genes & development* **15,** 507–521 (2001).

135. Scrima, A. *et al.* Structural basis of UV DNA-damage recognition by the DDB1–DDB2 complex. *Cell* **135,** 1213–1223 (2008).

136. Fischer, E. S. *et al.* The molecular basis of CRL4DDB2/CSA ubiquitin ligase architecture, targeting, and activation. *Cell* **147,** 1024–1039 (2011).

137. Evans, E., Moggs, J. G., Hwang, J. R., Egly, J.-M. & Wood, R. D. Mechanism of open complex and dual incision formation by human nucleotide excision repair factors. *The EMBO journal* **16,** 6559–6573 (1997).

138. Van Gool, A. J. *et al.* The Cockayne syndrome B protein, involved in transcription-coupled DNA repair, resides in an RNA polymerase II-containing complex. *The EMBO Journal* **16,** 5955–5965 (1997).

139. Van der Weegen, Y. *et al.* The cooperative action of CSB, CSA, and UVSSA target TFIIH to DNA damage-stalled RNA polymerase II. *Nature Communications* **11,** 1–16 (2020).

140. Lehmann, A. R. DNA polymerases and repair synthesis in NER in human cells. *DNA repair* **10,** 730–733 (2011).

141. Li, G.-M. Mechanisms and functions of DNA mismatch repair. *Cell research* **18,** 85–98 (2008).

142. Acharya, S., Foster, P. L., Brooks, P. & Fishel, R. The coordinated functions of the E. coli MutS and MutL proteins in mismatch repair. *Molecular cell* **12,** 233–246 (2003).

143. Goellner, E. M., Putnam, C. D. & Kolodner, R. D. Exonuclease 1-dependent and independent mismatch repair. *DNA repair* **32,** 24–32 (2015).

144. Kolodner, R. D. & Marsischky, G. T. Eukaryotic DNA mismatch repair. *Current opinion in genetics & development* **9,** 89–96 (1999).

145. Fishel, R. & Lee, J.-B. in *DNA Replication, Recombination, and Repair* 305–339 (Springer, 2016).

146. Mu, D. *et al.* DNA interstrand cross-links induce futile repair synthesis in mammalian cell extracts. *Molecular and cellular biology* **20,** 2446–2454 (2000).

147. Räschle, M. *et al.* Mechanism of replication-coupled DNA interstrand crosslink repair. *Cell* **134,** 969–980 (2008).

148. Knipscheer, P. *et al.* The Fanconi anemia pathway promotes replication-dependent DNA interstrand cross-link repair. *Science* **326,** 1698–1701 (2009).

149. Semlow, D. R., Zhang, J., Budzowska, M., Drohat, A. C. & Walter, J. C. Replication-dependent unhooking of DNA interstrand cross-links by the NEIL3 glycosylase. *Cell* **167,** 498–511 (2016).

150. Neale, M. J., Pan, J. & Keeney, S. Endonucleolytic processing of covalent protein-linked DNA double-strand breaks. *Nature* **436,** 1053–1057 (2005).

151. Lee, K. C. *et al.* MRE11 facilitates the removal of human topoisomerase II complexes from genomic DNA. *Biology open* **1,** 863–873 (2012).

152. Hoa, N. N. *et al.* Mre11 is essential for the removal of lethal topoisomerase 2 covalent cleavage complexes. *Molecular cell* **64,** 580–592 (2016).

153. Deshpande, R. A., Lee, J.-H., Arora, S. & Paull, T. T. Nbs1 converts the human Mre11/Rad50 nuclease complex into an endo/exonuclease machine specific for protein-DNA adducts. *Molecular cell* **64,** 593–606 (2016).

154. Pommier, Y. *et al.* Tyrosyl-DNA-phosphodiesterases (tdp1 and tdp2). *DNA repair* **19,** 114–129 (2014).

155. Debéthune, L., Kohlhagen, G., Grandas, A. & Pommier, Y. Processing of nucleopeptides mimicking the topoisomerase I–DNA covalent complex by tyrosyl-DNA phosphodiesterase. *Nucleic acids research* **30,** 1198–1204 (2002).

156. Lin, C.-P., Ban, Y., Lyu, Y. L., Desai, S. D. & Liu, L. F. A ubiquitin-proteasome pathway for the repair of topoisomerase I-DNA covalent complexes. *Journal of Biological Chemistry* **283,** 21074–21083 (2008).

157. El-Khamisy, S. F. To live or to die: a matter of processing damaged DNA termini in neurons. *EMBO molecular medicine* **3,** 78–88 (2011).

158. Duxin, J. P., Dewar, J. M., Yardimci, H. & Walter, J. C. Repair of a DNA-protein crosslink by replication-coupled proteolysis. *Cell* **159,** 346–357 (2014).

159. Vaz, B. *et al.* Metalloprotease SPRTN/DVC1 orchestrates replication-coupled DNA-protein crosslink repair. *Molecular cell* **64,** 704–719 (2016).

160. Stingele, J. *et al.* Mechanism and regulation of DNA-protein crosslink repair by the DNA-dependent metalloprotease SPRTN. *Molecular cell* **64,** 688–703 (2016).

161. Lopez-Mosqueda, J. *et al.* SPRTN is a mammalian DNA-binding metalloprotease that resolves DNA-protein crosslinks. *Elife* **5,** e21491 (2016).

162. Morocz, M. *et al.* DNA-dependent protease activity of human Spartan facilitates replication of DNA–protein crosslink-containing DNA. *Nucleic acids research* **45,** 3172–3188 (2017).

163. Maskey, R. S. *et al.* Spartan deficiency causes accumulation of Topoisomerase 1 cleavage complexes and tumorigenesis. *Nucleic acids research* **45,** 4564–4576 (2017).

164. Sparks, J. L. *et al.* RNase H2-initiated ribonucleotide excision repair. *Molecular cell* **47,** 980–986 (2012).

165. Eder, P. & Walder, J. Ribonuclease H from K562 human erythroleukemia cells. Purification, characterization, and substrate specificity. *Journal of Biological Chemistry* **266,** 6472–6479 (1991).

166. Chaudhuri, A. R. & Nussenzweig, A. The multifaceted roles of PARP1 in DNA repair and chromatin remodelling. *Nature reviews Molecular cell biology* **18,** 610 (2017).

167. Hanzlikova, H., Gittens, W., Krejcikova, K., Zeng, Z. & Caldecott, K. W. Overlapping roles for PARP1 and PARP2 in the recruitment of endogenous XRCC1 and PNKP into oxidized chromatin. *Nucleic acids research* **45,** 2546–2557 (2017).

168. Whitehouse, C. J. *et al.* XRCC1 stimulates human polynucleotide kinase activity at damaged DNA termini and accelerates DNA single-strand break repair. *Cell* **104,** 107–117 (2001).

169. Jilani, A. *et al.* Molecular cloning of the human gene, PNKP, encoding a polynucleotide kinase 3′-phosphatase and evidence for its role in repair of DNA strand breaks caused by oxidative damage. *Journal of Biological Chemistry* **274,** 24176–24186 (1999).

170. Parsons, J. L., Dianova, I. I. & Dianov, G. L. APE1 is the major 3′-phosphoglycolate activity in human cell extracts. *Nucleic acids research* **32,** 3531–3536 (2004).

171. Pouliot, J. J., Yao, K. C., Robertson, C. A. & Nash, H. A. Yeast gene for a Tyr-DNA phosphodiesterase that repairs topoisomerase I complexes. *Science* **286,** 552–555 (1999).

172. Ahel, I. *et al.* The neurodegenerative disease protein aprataxin resolves abortive DNA ligation intermediates. *Nature* **443,** 713–716 (2006).

173. Fortini, P., Pascucci, B., Belisario, F. & Dogliotti, E. DNA polymerase β is required for efficient DNA strand break repair induced by methyl methanesulfonate but not by hydrogen peroxide. *Nucleic acids research* **28,** 3040–3046 (2000).

174. Caldecott, K. W., McKeown, C. K., Tucker, J. D., Ljungquist, S. & Thompson, L. H. An interaction between the mammalian DNA repair protein XRCC1 and DNA ligase III. *Molecular and cellular biology* **14,** 68–76 (1994).

175. Simsek, D. *et al.* Crucial role for DNA ligase III in mitochondria but not in Xrcc1-dependent repair. *Nature* **471,** 245–248 (2011).

176. Mortusewicz, O., Rothbauer, U., Cardoso, M. C. & Leonhardt, H. Differential recruitment of DNA Ligase I and III to DNA repair sites. *Nucleic acids research* **34,** 3523–3532 (2006).

177. Takata, M. *et al.* Homologous recombination and non-homologous end-joining pathways of DNA double-strand break repair have overlapping roles in the maintenance of chromosomal integrity in vertebrate cells. *The EMBO journal* **17,** 5497–5508 (1998).

178. Grawunder, U. *et al.* Activity of DNA ligase IV stimulated by complex formation with XRCC4 protein in mammalian cells. *Nature* **388,** 492–495 (1997).

179. Stinson, B. M., Moreno, A. T., Walter, J. C. & Loparo, J. J. A mechanism to minimize errors during non-homologous end joining. *Molecular Cell* **77,** 1080–1091 (2020).

180. Hsu, P. D., Lander, E. S. & Zhang, F. Development and applications of CRISPR-Cas9 for genome engineering. *Cell* **157,** 1262–1278 (2014).

181. Bétermier, M., Bertrand, P. & Lopez, B. S. Is non-homologous end-joining really an inherently error-prone process? *PLoS genetics* **10** (2014).

182. Beucher, A. *et al.* ATM and Artemis promote homologous recombination of radiation-induced DNA double-strand breaks in G2. *The EMBO journal* **28,** 3413–3427 (2009).

183. Decottignies, A. Alternative end-joining mechanisms: a historical perspective. *Frontiers in genetics* **4,** 48 (2013).

184. Truong, L. N. *et al.* Microhomology-mediated End Joining and Homologous Recombination share the initial end resection step to repair DNA double-strand breaks in mammalian cells. *Proceedings of the National Academy of Sciences* **110,** 7720–7725 (2013).

185. Koole, W. *et al.* A Polymerase Theta-dependent repair pathway suppresses extensive genomic instability at endogenous G4 DNA sites. *Nature communications* **5,** 1–10 (2014).

186. Kent, T., Chandramouly, G., McDevitt, S. M., Ozdemir, A. Y. & Pomerantz, R. T. Mechanism of microhomology-mediated end-joining promoted by human DNA polymerase θ. *Nature structural & molecular biology* **22,** 230 (2015).

187. Grabarz, A. *et al.* A role for BLM in double-strand break repair pathway choice: prevention of CtIP/Mre11-mediated alternative nonhomologous end-joining. *Cell reports* **5,** 21–28 (2013).

188. Bhargava, R., Onyango, D. O. & Stark, J. M. Regulation of single-strand annealing and its role in genome maintenance. *Trends in Genetics* **32,** 566–575 (2016).

189. Zhu, Z., Chung, W.-H., Shim, E. Y., Lee, S. E. & Ira, G. Sgs1 helicase and two nucleases Dna2 and Exo1 resect DNA double-strand break ends. *Cell* **134,** 981–994 (2008).

190. Motycka, T. A., Bessho, T., Post, S. M., Sung, P. & Tomkinson, A. E. Physical and functional interaction between the XPF/ERCC1 endonuclease and hRad52. *Journal of Biological Chemistry* **279,** 13634–13639 (2004).

191. Prakash, R., Zhang, Y., Feng, W. & Jasin, M. Homologous recombination and human health: the roles of BRCA1, BRCA2, and associated proteins. *Cold Spring Harbor perspectives in biology* **7,** a016600 (2015).

192. Van der Heijden, T. *et al.* Homologous recombination in real time: DNA strand exchange by RecA. *Molecular cell* **30,** 530–538 (2008).

193. McVey, M., Khodaverdian, V. Y., Meyer, D., Cerqueira, P. G. & Heyer, W.-D. Eukaryotic DNA polymerases in homologous recombination. *Annual review of genetics* **50,** 393–421 (2016).

194. Jasin, M. & Rothstein, R. Repair of strand breaks by homologous recombination. *Cold Spring Harbor perspectives in biology* **5,** a012740 (2013).

195. Bizard, A. H. & Hickson, I. D. The dissolution of double Holliday junctions. *Cold Spring Harbor perspectives in biology* **6,** a016477 (2014).

196. Karanam, K., Kafri, R., Loewer, A. & Lahav, G. Quantitative live cell imaging reveals a gradual shift between DNA repair mechanisms and a maximal use of HR in mid S phase. *Molecular cell* **47,** 320–329 (2012).

197. Helleday, T., Lo, J., van Gent, D. C. & Engelward, B. P. DNA double-strand break repair: from mechanistic understanding to cancer treatment. *DNA repair* **6,** 923–935 (2007).

198. Budzowska, M. & Kanaar, R. Mechanisms of dealing with DNA damage-induced replication problems. *Cell biochemistry and biophysics* **53,** 17–31 (2009).

199. Scully, R., Panday, A., Elango, R. & Willis, N. A. DNA double-strand break repair-pathway choice in somatic mammalian cells. *Nature Reviews Molecular Cell Biology* **20,** 698–714 (2019).

200. Barkauskaite, E., Jankevicius, G. & Ahel, I. Structures and mechanisms of enzymes employed in the synthesis and degradation of PARP-dependent protein ADP-ribosylation. *Molecular cell* **58,** 935–946 (2015).

201. Gibson, B. A. & Kraus, W. L. New insights into the molecular and cellular functions of poly (ADP-ribose) and PARPs. *Nature reviews Molecular cell biology* **13,** 411–424 (2012).

202. d'AMOURS, D., DESNOYERS, S., d'SILVA, I. & Poirier, G. G. Poly (ADP-ribosyl) ation reactions in the regulation of nuclear functions. *Biochemical Journal* **342,** 249–268 (1999).

203. Jankevicius, G., Ariza, A., Ahel, M. & Ahel, I. The toxin-antitoxin system DarTG catalyzes reversible ADP-ribosylation of DNA. *Molecular cell* **64,** 1109–1116 (2016).

204. Culver, G. M. *et al.* An NAD derivative produced during transfer RNA splicing: ADP-ribose 1"-2" cyclic phosphate. *Science* **261,** 206–208 (1993).

205. Spinelli, S. L., Kierzek, R., Turner, D. H. & Phizicky, E. M. Transient ADP-ribosylation of a 2′-phosphate implicated in its removal from ligated tRNA during splicing in yeast. *Journal of Biological Chemistry* **274,** 2637–2644 (1999).

206. Dabbs, E. R. *et al.* Ribosylation by mycobacterial strains as a new mechanism of rifampin inactivation. *Antimicrobial agents and chemotherapy* **39,** 1007–1009 (1995).

207. Daniels, C. M., Ong, S.-E. & Leung, A. K. Phosphoproteomic approach to characterize protein mono-and poly (ADP-ribosyl) ation sites from cells. *Journal of proteome research* **13,** 3510–3522 (2014).

208. Leidecker, O. *et al.* Serine is a new target residue for endogenous ADP-ribosylation on histones. *Nature chemical biology* **12,** 998 (2016).

209. Pedrioli, D. M. L. *et al.* Comprehensive ADP-ribosylome analysis identifies tyrosine as an ADP-ribose acceptor site. *EMBO reports* **19** (2018).

210. Aravind, L., Zhang, D., de Souza, R. F., Anand, S. & Iyer, L. M. in *Endogenous ADP-Ribosylation* 3–32 (Springer, 2014).

211. Cohen, M. S. & Chang, P. Insights into the biogenesis, function, and regulation of ADP-ribosylation. *Nature chemical biology* **14,** 236 (2018).

212. Kleine, H. *et al.* Substrate-assisted catalysis by PARP10 limits its activity to mono-ADP-ribosylation. *Molecular cell* **32,** 57–69 (2008).

213. Gupte, R., Liu, Z. & Kraus, W. L. PARPs and ADP-ribosylation: recent advances linking molecular functions to biological outcomes. *Genes & Development* **31,** 101–126 (2017).

214. Pascal, J. M. The comings and goings of PARP-1 in response to DNA damage. *DNA repair* **71,** 177–182 (2018).

215. Langelier, M.-F., Planck, J. L., Roy, S. & Pascal, J. M. Crystal structures of poly (ADP-ribose) polymerase-1 (PARP-1) zinc fingers bound to DNA structural and functional insights into DNA-dependent PARP-1 activity. *Journal of biological chemistry* **286,** 10690–10701 (2011).

216. Ali, A. A. *et al.* The zinc-finger domains of PARP1 cooperate to recognize DNA strand breaks. *Nature structural & molecular biology* **19,** 685 (2012).

217. Gibbs-Seymour, I., Fontana, P., Rack, J. G. M. & Ahel, I. HPF1/C4orf27 is a PARP-1-interacting protein that regulates PARP-1 ADP-ribosylation activity. *Molecular cell* **62,** 432–442 (2016).

218. Bonfiglio, J. J. *et al.* Serine ADP-ribosylation depends on HPF1. *Molecular cell* **65,** 932–940 (2017).

219. Palazzo, L. *et al.* Serine is the major residue for ADP-ribosylation upon DNA damage. *Elife* **7,** e34334 (2018).

220. Suskiewicz, M. J. *et al.* HPF1 completes the PARP active site for DNA damage-induced ADP-ribosylation. *Nature* **579,** 598–602 (2020).

221. Langelier, M.-F., Planck, J. L., Roy, S. & Pascal, J. M. Structural basis for DNA damage–dependent poly (ADP-ribosyl) ation by human PARP-1. *Science* **336,** 728–732 (2012).

222. Dawicki-McKenna, J. M. *et al.* PARP-1 activation requires local unfolding of an autoinhibitory domain. *Molecular cell* **60,** 755–768 (2015).

223. El-Khamisy, S. F., Masutani, M., Suzuki, H. & Caldecott, K. W. A requirement for PARP-1 for the assembly or stability of XRCC1 nuclear foci at sites of oxidative DNA damage. *Nucleic acids research* **31,** 5526–5533 (2003).

224. Polo, L. M. *et al.* Efficient single-strand break repair requires binding to both Poly (ADP-ribose) and DNA by the central BRCT domain of XRCC1. *Cell reports* **26,** 573–581 (2019).

225. Haince, J.-F. *et al.* PARP1-dependent kinetics of recruitment of MRE11 and NBS1 proteins to multiple DNA damage sites. *Journal of Biological Chemistry* **283,** 1197–1208 (2008).

226. Luijsterburg, M. S. *et al.* PARP1 links CHD2-mediated chromatin expansion and H3. 3 deposition to DNA repair by non-homologous end-joining. *Molecular cell* **61,** 547–562 (2016).

227. Collier, R. Understanding the mode of action of diphtheria toxin: a perspective on progress during the 20th century. *Toxicon* **39,** 1793–1803 (2001).

228. Cassel, D. & Pfeuffer, T. Mechanism of cholera toxin action: covalent modification of the guanyl nucleotide-binding protein of the adenylate cyclase system. *Proceedings of the National Academy of Sciences* **75,** 2669–2673 (1978).

229. Holbourn, K. P., Shone, C. C. & Acharya, K. A family of killer toxins. *The FEBS journal* **273,** 4579–4593 (2006).

230. Miwa, M. & Sugimura, T. Splitting of the ribose-ribose linkage of poly (adenosine diphosphate-ribose) by a calf thymus extract. *Journal of Biological Chemistry* **246,** 6362–6364 (1971).

231. Slade, D. *et al.* The structure and catalytic mechanism of a poly (ADP-ribose) glycohydrolase. *Nature* **477,** 616–620 (2011).

232. Barkauskaite, E. *et al.* Visualization of poly (ADP-ribose) bound to PARG reveals inherent balance between exo-and endo-glycohydrolase activities. *Nature communications* **4,** 2164 (2013).

233. Pourfarjam, Y. *et al.* PARG has a robust endo-glycohydrolase activity that releases protein-free poly (ADP-ribose) chains. *Biochemical and Biophysical Research Communications* (2020).

234. Illuzzi, G. *et al.* PARG is dispensable for recovery from transient replicative stress but required to prevent detrimental accumulation of poly (ADP-ribose) upon prolonged replicative stress. *Nucleic acids research* **42,** 7776–7792 (2014).

235. James, D. I. *et al.* First-in-class chemical probes against poly (ADP-ribose) glycohydrolase (PARG) inhibit DNA repair with differential pharmacology to olaparib. *ACS chemical biology* **11,** 3179–3190 (2016).

236. Hanzlikova, H. *et al.* The importance of poly (ADP-ribose) polymerase as a sensor of unligated Okazaki fragments during DNA replication. *Molecular cell* **71,** 319–331 (2018).

237. Jankevicius, G. *et al.* A family of macrodomain proteins reverses cellular mono-ADP-ribosylation. *Nature structural & molecular biology* **20,** 508 (2013).

238. Peterson, F. C. *et al.* Orphan macrodomain protein (human C6orf130) is an O-acyl-ADP-ribose deacylase SOLUTION STRUCTURE AND CATALYTIC PROPERTIES. *Journal of Biological Chemistry* **286,** 35955–35965 (2011).

239. Sharifi, R. *et al.* Deficiency of terminal ADP-ribose protein glycohydrolase TARG1/C6orf130 in neurodegenerative disease. *The EMBO journal* **32,** 1225–1237 (2013).

240. Bütepage, M. *et al.* Nucleolar-nucleoplasmic shuttling of TARG1 and its control by DNA damage-induced poly-ADP-ribosylation and by nucleolar transcription. *Scientific reports* **8,** 1–17 (2018).

241. Žaja, R. *et al.* Comparative analysis of MACROD1, MACROD2 and TARG1 expression, localisation and interactome. *Scientific Reports* **10,** 1–16 (2020).

242. Mashimo, M., Kato, J. & Moss, J. Structure and function of the ARH family of ADP-ribosyl-acceptor hydrolases. *DNA repair* **23,** 88–94 (2014).

243. Kato, J., Zhu, J., Liu, C. & Moss, J. Enhanced sensitivity to cholera toxin in ADP-ribosylarginine hydrolase-deficient mice. *Molecular and cellular biology* **27,** 5534–5543 (2007).

244. Oka, S., Kato, J. & Moss, J. Identification and characterization of a mammalian 39-kDa poly (ADP-ribose) glycohydrolase. *Journal of Biological Chemistry* **281,** 705–713 (2006).

245. Fontana, P. *et al.* Serine ADP-ribosylation reversal by the hydrolase ARH3. *Elife* **6,** e28533 (2017).

246. Mashimo, M., Kato, J. & Moss, J. ADP-ribosyl-acceptor hydrolase 3 regulates poly (ADP-ribose) degradation and cell death during oxidative stress. *Proceedings of the National Academy of Sciences* **110,** 18964–18969 (2013).

247. Ahel, I. *et al.* Poly (ADP-ribose)-binding zinc finger motifs in DNA repair/checkpoint proteins. *Nature* **451,** 81–85 (2008).

248. Zhang, Y. *et al.* RNF146 is a poly (ADP-ribose)-directed E3 ligase that regulates axin degradation and Wnt signalling. *Nature cell biology* **13,** 623–629 (2011).

249. Wang, Z. *et al.* Recognition of the iso-ADP-ribose moiety in poly (ADP-ribose) by WWE domains suggests a general mechanism for poly (ADP-ribosyl) ation-dependent ubiquitination. *Genes & development* **26,** 235–240 (2012).

250. Weixler, L. *et al.* ADP-ribosylation of RNA and DNA: from in vitro characterization to in vivo function. *Nucleic Acids Research* **49,** 3634–3650 (2021).

251. Takamura-Enya, T. *et al.* Mono (ADP-ribosyl) ation of 2′-deoxyguanosine residue in DNA by an apoptosis-inducing protein, pierisin-1, from cabbage butterfly. *Proceedings of the National Academy of Sciences* **98,** 12414–12419 (2001).

252. Takahashi-Nakaguchi, A. *et al.* Demonstration of cytotoxicity against wasps by pierisin-1: a possible defense factor in the cabbage white butterfly. *PloS one* **8** (2013).

253. Watanabe, M. *et al.* Developmental stage-specific expression and tissue distribution of pierisin-1, a guanine-specific ADP-ribosylating toxin, in Pieris rapae. *Comparative Biochemistry and Physiology Part A: Molecular & Integrative Physiology* **139,** 125–131 (2004).

254. Kanazawa, T. *et al.* Distinct roles for the N-and C-terminal regions in the cytotoxicity of pierisin-1, a putative ADP-ribosylating toxin from cabbage butterfly, against mammalian cells. *Proceedings of the National Academy of Sciences* **98,** 2226–2231 (2001).

255. Kanazawa, T. *et al.* Bcl-2 blocks apoptosis caused by pierisin-1, a guanine-specific ADP-ribosylating toxin from the cabbage butterfly. *Biochemical and biophysical research communications* **296,** 20–25 (2002).

256. Nakano, T. *et al.* Purification and molecular cloning of a DNA ADP-ribosylating protein, CARP-1, from the edible clam Meretrix lamarckii. *Proceedings of the National Academy of Sciences* **103,** 13652–13657 (2006).

257. Nakano, T. *et al.* ADP-ribosylation of guanosine by SCO5461 protein secreted from Streptomyces coelicolor. *Toxicon* **63,** 55–63 (2013).

258. Lyons, B. *et al.* Scabin, a novel DNA-acting ADP-ribosyltransferase from Streptomyces scabies. *Journal of Biological Chemistry* **291,** 11198–11215 (2016).

259. Talhaoui, I. *et al.* Poly (ADP-ribose) polymerases covalently modify strand break termini in DNA fragments in vitro. *Nucleic acids research* **44,** 9279–9295 (2016).

260. Munnur, D. & Ahel, I. Reversible mono-ADP-ribosylation of DNA breaks. *The FEBS journal* **284,** 4002–4016 (2017).

261. Zarkovic, G. *et al.* Characterization of DNA ADP-ribosyltransferase activities of PARP2 and PARP3: new insights into DNA ADP-ribosylation. *Nucleic acids research* **46,** 2417–2431 (2018).

262. Belousova, E., Ishchenko, A. & Lavrik, O. Dna is a new target of Parp3. *Scientific reports* **8,** 1–12 (2018).

263. Matta, E., Kiribayeva, A., Khassenov, B., Matkarimov, B. T. & Ishchenko, A. A. Insight into DNA substrate specificity of PARP1-catalysed DNA poly (ADP-ribosyl) ation. *Scientific reports* **10,** 1–11 (2020).

264. Munir, A., Banerjee, A. & Shuman, S. NAD+-dependent synthesis of a 5′-phospho-ADP-ribosylated RNA/DNA cap by RNA 2′-phosphotransferase Tpt1. *Nucleic acids research* **46,** 9617–9624 (2018).

265. Munnur, D. *et al.* Reversible ADP-ribosylation of RNA. *Nucleic acids research* **47,** 5658–5669 (2019).

266. Lawarée, E. *et al.* DNA ADP-Ribosylation Stalls Replication and Is Reversed by RecF-Mediated Homologous Recombination and Nucleotide Excision Repair. *Cell reports* **30,** 1373–1384 (2020).

267. Kuzminov, A. Recombinational Repair of DNA Damage inEscherichia coli and Bacteriophage λ. *Microbiology and molecular biology reviews* **63,** 751–813 (1999).

268. Zellweger, R. *et al.* Rad51-mediated replication fork reversal is a global response to genotoxic treatments in human cells. *Journal of Cell Biology* **208,** 563–579 (2015).

269. Wyatt, M. D. & Pittman, D. L. Methylating agents and DNA repair responses: Methylated bases and sources of strand breaks. *Chemical research in toxicology* **19,** 1580–1594 (2006).

270. Yang, Y.-G., Cortes, U., Patnaik, S., Jasin, M. & Wang, Z.-Q. Ablation of PARP-1 does not interfere with the repair of DNA double-strand breaks, but compromises the reactivation of stalled replication forks. *Oncogene* **23,** 3872–3882 (2004).

271. Sugimura, K., Takebayashi, S.-i., Taguchi, H., Takeda, S. & Okumura, K. PARP-1 ensures regulation of replication fork progression by homologous recombination on damaged DNA. *Journal of Cell Biology* **183,** 1203–1212 (2008).

272. Bryant, H. E. *et al.* PARP is activated at stalled forks to mediate Mre11-dependent replication restart and recombination. *The EMBO journal* **28,** 2601–2615 (2009).

273. Maya-Mendoza, A. *et al.* High speed of fork progression induces DNA replication stress and genomic instability. *Nature* **559,** 279–284 (2018).

274. Gibson, B. A., Conrad, L. B., Huang, D. & Kraus, W. L. Generation and characterization of recombinant antibody-like ADP-ribose binding proteins. *Biochemistry* **56,** 6305–6316 (2017).

275. Hanzlikova, H. *et al.* Pathogenic ARH3 mutations result in ADP-ribose chromatin scars during DNA strand break repair. *Nature communications* **11,** 1–13 (2020).

276. *Poly/Mono-ADP Ribose (E6F6A) Rabbit mAb*

277. Lu, A. Z. *et al.* Enabling drug discovery for the PARP protein family through the detection of mono-ADP-ribosylation. *Biochemical pharmacology* **167,** 97–106 (2019).

278. Pillay, N. *et al.* DNA replication vulnerabilities render ovarian cancer cells sensitive to poly (ADP-ribose) glycohydrolase inhibitors. *Cancer Cell* **35,** 519–533 (2019).

279. Meek, D. W. Tumour suppression by p53: a role for the DNA damage response? *Nature Reviews Cancer* **9,** 714–723 (2009).

280. Amé, J.-C. *et al.* PARP-2, A novel mammalian DNA damage-dependent poly (ADP-ribose) polymerase. *Journal of Biological Chemistry* **274,** 17860–17868 (1999).

281. Pegg, A. E. Repair of O6-alkylguanine by alkyltransferases. *Mutation Research/Reviews in Mutation Research* **462,** 83–100 (2000).

282. Maya-Mendoza, A., Petermann, E., Gillespie, D. A., Caldecott, K. W. & Jackson, D. A. Chk1 regulates the density of active replication origins during the vertebrate S phase. *The EMBO journal* **26,** 2719–2731 (2007).

283. Petermann, E., Woodcock, M. & Helleday, T. Chk1 promotes replication fork progression by controlling replication initiation. *Proceedings of the National Academy of Sciences* **107,** 16090–16095 (2010).

284. Rulten, S. L. & Caldecott, K. W. DNA strand break repair and neurodegeneration. *DNA repair* **12,** 558–567 (2013).

285. Gao, J. *et al.* Integrative analysis of complex cancer genomics and clinical profiles using the cBioPortal. *Science signaling* **6,** pl1–pl1 (2013).

286. Olsen, E. *et al.* Pivotal phase III trial of two dose levels of denileukin diftitox for the treatment of cutaneous T-cell lymphoma. *Journal of Clinical Oncology* **19,** 376–388 (2001).

287. Prince, H. M. *et al.* Phase III placebo-controlled trial of denileukin diftitox for patients with cutaneous T-cell lymphoma. *Journal of clinical oncology* **28,** 1870–1877 (2010).

288. Zahaf, N.-I. *et al.* Targeted delivery of an ADP-ribosylating bacterial toxin into cancer cells. *Scientific reports* **7,** 1–10 (2017).

289. Arora, N., Klimpel, K., Singh, Y. & Leppla, S. Fusions of anthrax toxin lethal factor to the ADP-ribosylation domain of Pseudomonas exotoxin A are potent cytotoxins which are translocated to the cytosol of mammalian cells. *Journal of Biological Chemistry* **267,** 15542–15548 (1992).

290. Milne, J. C., Blanket, S. R., Hanna, P. C. & Collier, R. J. Protective antigen-binding domain of anthrax lethal factor mediates translocation of a heterologous protein fused to its amino-or carboxy-terminus. *Molecular microbiology* **15,** 661–666 (1995).

291. Pentelute, B. L., Sharma, O. & Collier, R. J. Chemical dissection of protein translocation through the anthrax toxin pore. *Angewandte Chemie* **123,** 2342–2344 (2011).

292. Mechaly, A., McCluskey, A. J. & Collier, R. J. Changing the receptor specificity of anthrax toxin. *MBio* **3** (2012).

293. Berti, M. *et al.* Human RECQ1 promotes restart of replication forks reversed by DNA topoisomerase I inhibition. *Nature structural & molecular biology* **20,** 347 (2013).

294. Mirkin, E. V. & Mirkin, S. M. Replication fork stalling at natural impediments. *Microbiology and molecular biology reviews* **71,** 13–35 (2007).

295. Petermann, E., Orta, M. L., Issaeva, N., Schultz, N. & Helleday, T. Hydroxyurea-stalled replication forks become progressively inactivated and require two different RAD51-mediated pathways for restart and repair. *Molecular cell* **37,** 492–502 (2010).

296. Yu, S.-W. *et al.* Apoptosis-inducing factor mediates poly (ADP-ribose)(PAR) polymer-induced cell death. *Proceedings of the National Academy of Sciences* **103,** 18314–18319 (2006).

297. Nurse, P. & Thuriaux, P. Regulatory genes controlling mitosis in the fission yeast Schizosaccharomyces pombe. *Genetics* **96,** 627–637 (1980).

298. Morgan, D. O. Principles of CDK regulation. *Nature* **374,** 131–134 (1995).

299. Matsuoka, S., Huang, M. & Elledge, S. J. Linkage of ATM to cell cycle regulation by the Chk2 protein kinase. *Science* **282,** 1893–1897 (1998).

300. Jin, P., Hardy, S. & Morgan, D. O. Nuclear localization of cyclin B1 controls mitotic entry after DNA damage. *The Journal of cell biology* **141,** 875–885 (1998).

301. Rack, J. G. M. *et al.* (ADP-ribosyl) hydrolases: structural basis for differential substrate recognition and inhibition. *Cell chemical biology* **25,** 1533–1546 (2018).

302. Palazzo, L. *et al.* Processing of protein ADP-ribosylation by Nudix hydrolases. *Biochemical Journal* **468,** 293–301 (2015).

303. Chen, D. *et al.* Identification of macrodomain proteins as novel O-acetyl-ADP-ribose deacetylases. *Journal of Biological Chemistry* **286,** 13261–13271 (2011).

304. Saitou, N. & Nei, M. The neighbor-joining method: a new method for reconstructing phylogenetic trees. *Molecular biology and evolution* **4,** 406–425 (1987).

305. Möller, G. K. *Identifying the molecular function of MacroD2 and TARG1* PhD thesis (lmu, 2020).

306. McQuin, C. *et al.* CellProfiler 3.0: Next-generation image processing for biology. *PLoS biology* **16,** e2005970 (2018).

Supplementary Figures

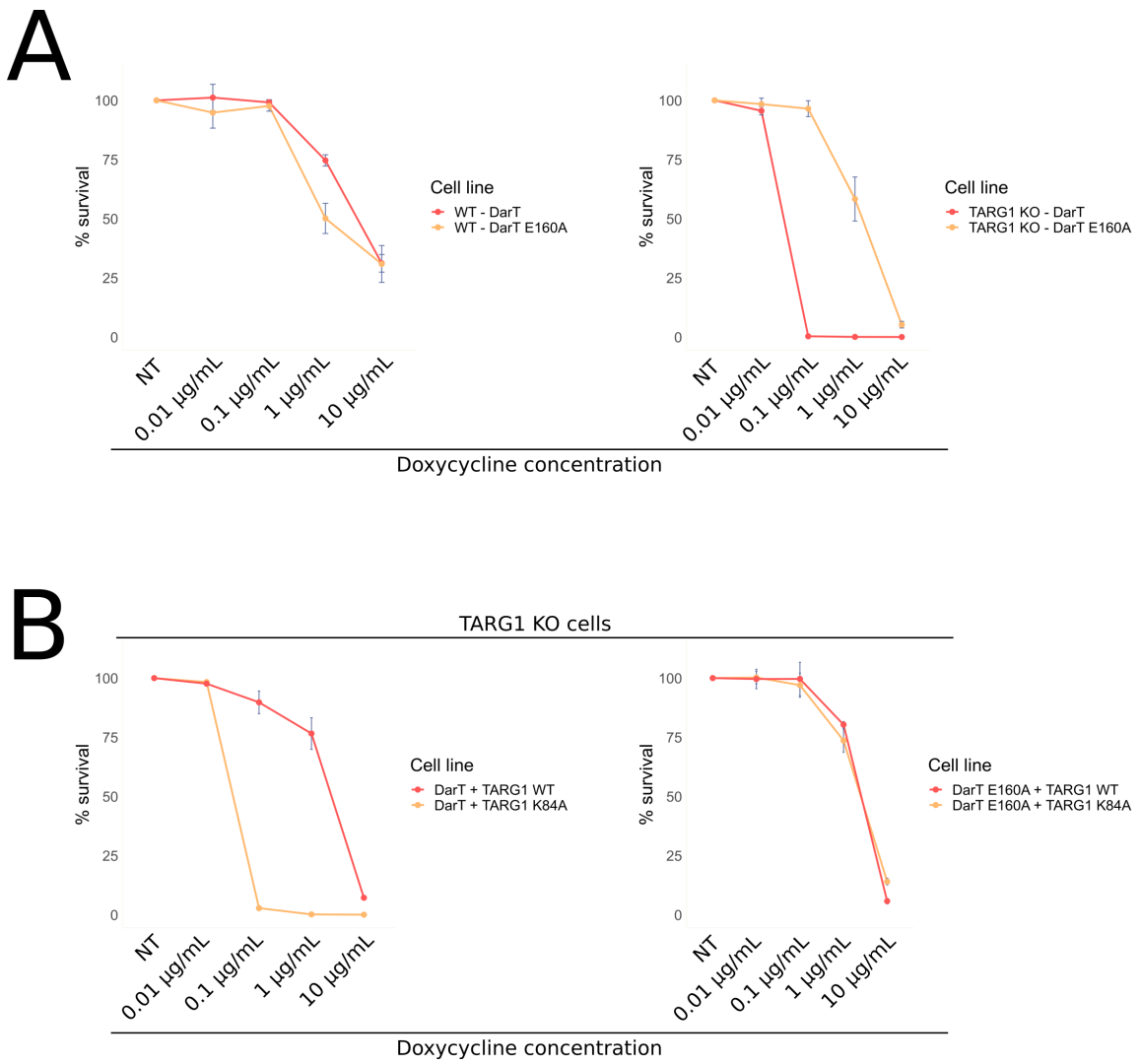
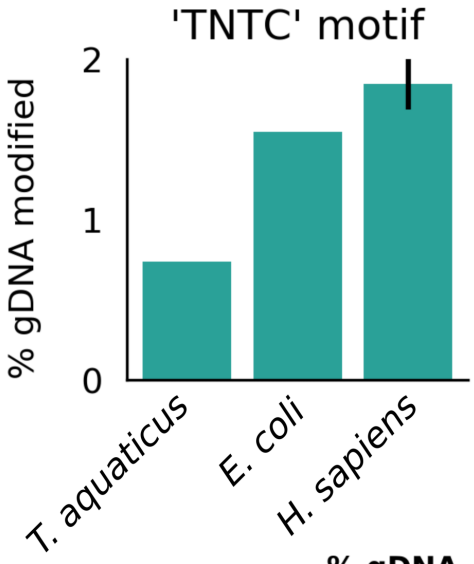


Figure S1: Quantification of WT or TARG1 KO cells treated with DarT. **(A)** Clonogenic survival for U-2 OS WT or TARG1 KO cells expressing pLIX_403 GFP-DarT WT or GFP-DarT E160A. Error bars represent the SEM. Representative images at a doxycycline concentration of 0.1 µg/mL found in Figure 2.6A. **(B)** Clonogenic survival in U-2 OS TARG1 KO cells expressing DarT WT or E160A in the presence of constitutively expressed pLX304 TARG1 WT or TARG1 K84A. Error bars represent the SEM. Representative images at a doxycycline concentration of 0.1 µg/mL found in Figure 2.6B.



Species	% gDNA modified
Thermus aquaticus	0.74
Escherichia coli	1.55
Homo sapiens	1.85±0.16

Figure S2: Estimation of the maximum number of DarT modification sites. Bioinformatic search for the theoretical maximum number of non-overlapping TNTC DNA motifs on ssDNA that could be modified by DarT for the indicated genome. Values represent the percentage of DNA that contained a TNTC motif. For *H. sapiens* only the autosomes were analysed with SD displayed.

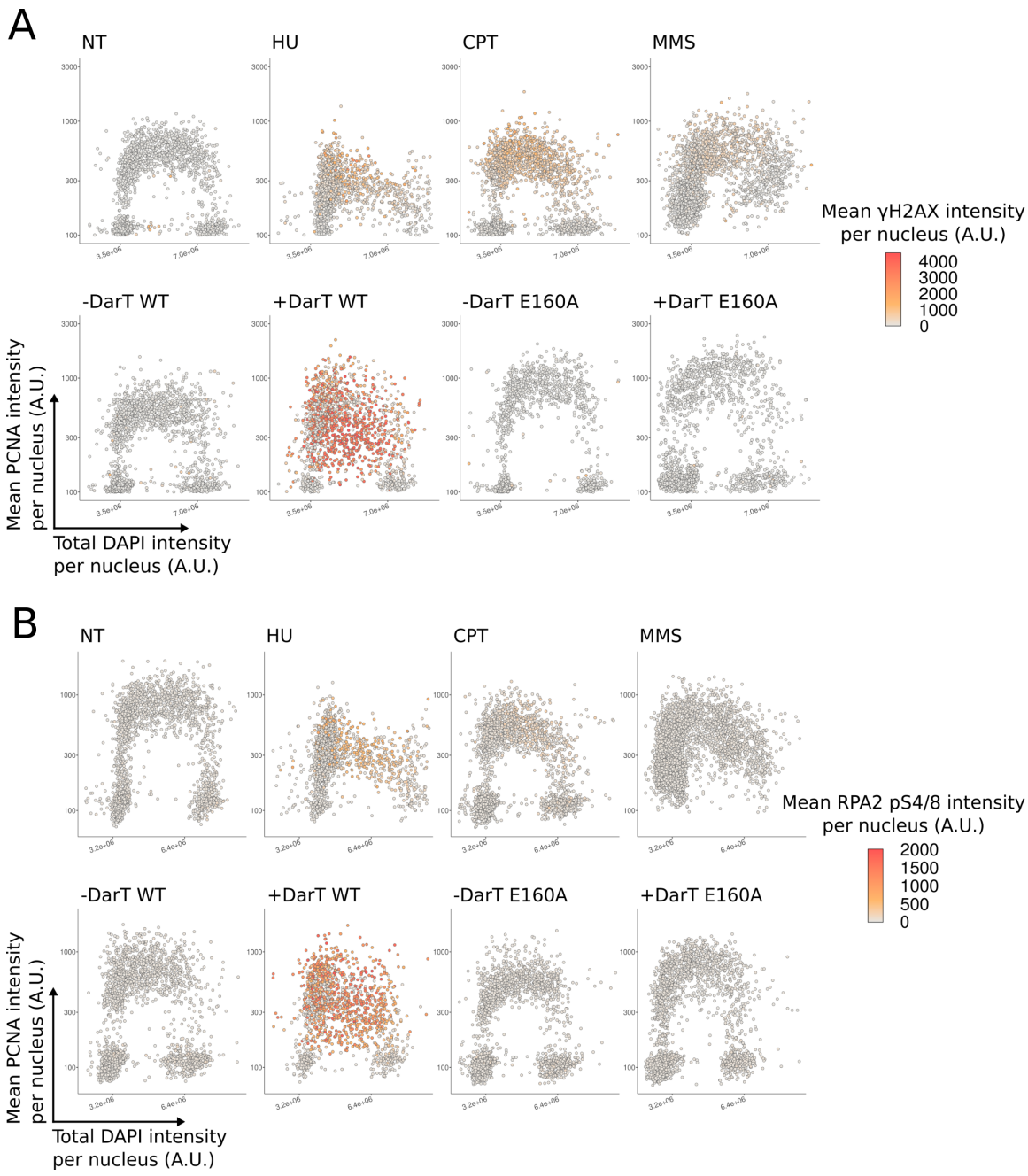


Figure S3: DarT induces γH2AX and RPA2 pS4/8 in S-phase cells. **(A)** QIBC analysis of asynchronous U-2 OS TARG1 KO cells treated with genotoxins as in Figure 2.9. Cells were pre-extracted, fixed and immunostained as in Figure 2.15A. QIBC was used to record total DAPI intensity, mean PCNA, and mean γH2AX intensities per nucleus for >1,000 cells. Total DAPI and mean PCNA intensities for individual cells were used to generate the scatter plot and mean γH2AX intensity was used to colour points. **(B)** U-2 OS TARG1 KO were treated and analysed as in **A** followed by immunostaining as in Figure 2.15B.

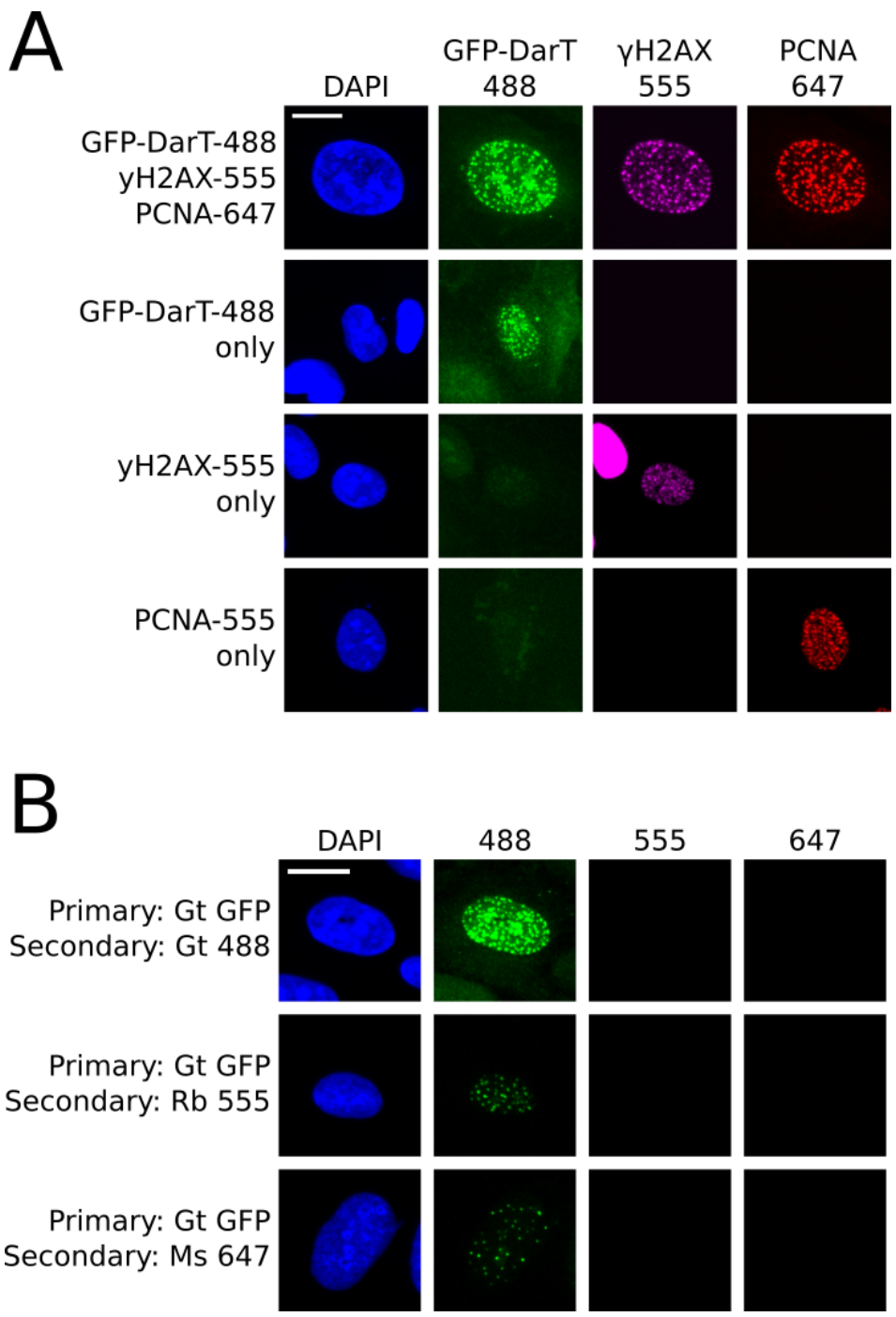


Figure S4: Immunofluorescence cross-reactivity and secondary antibody bleed-through test. **(A)** U-2 OS TARG1 KO cells expressing DarT (24h) were immunostained for GFP-DarT, γH2AX and PCNA together or individually in order to test for bleed-through. Scale bar 10 µm. **(B)** U-2 OS TARG1 KO cells expressing DarT (24h) were immunostained for GFP-DarT and the indicated secondary antibody to examine if the GFP primary antibody showed cross-reactivity with other secondary antibodies.

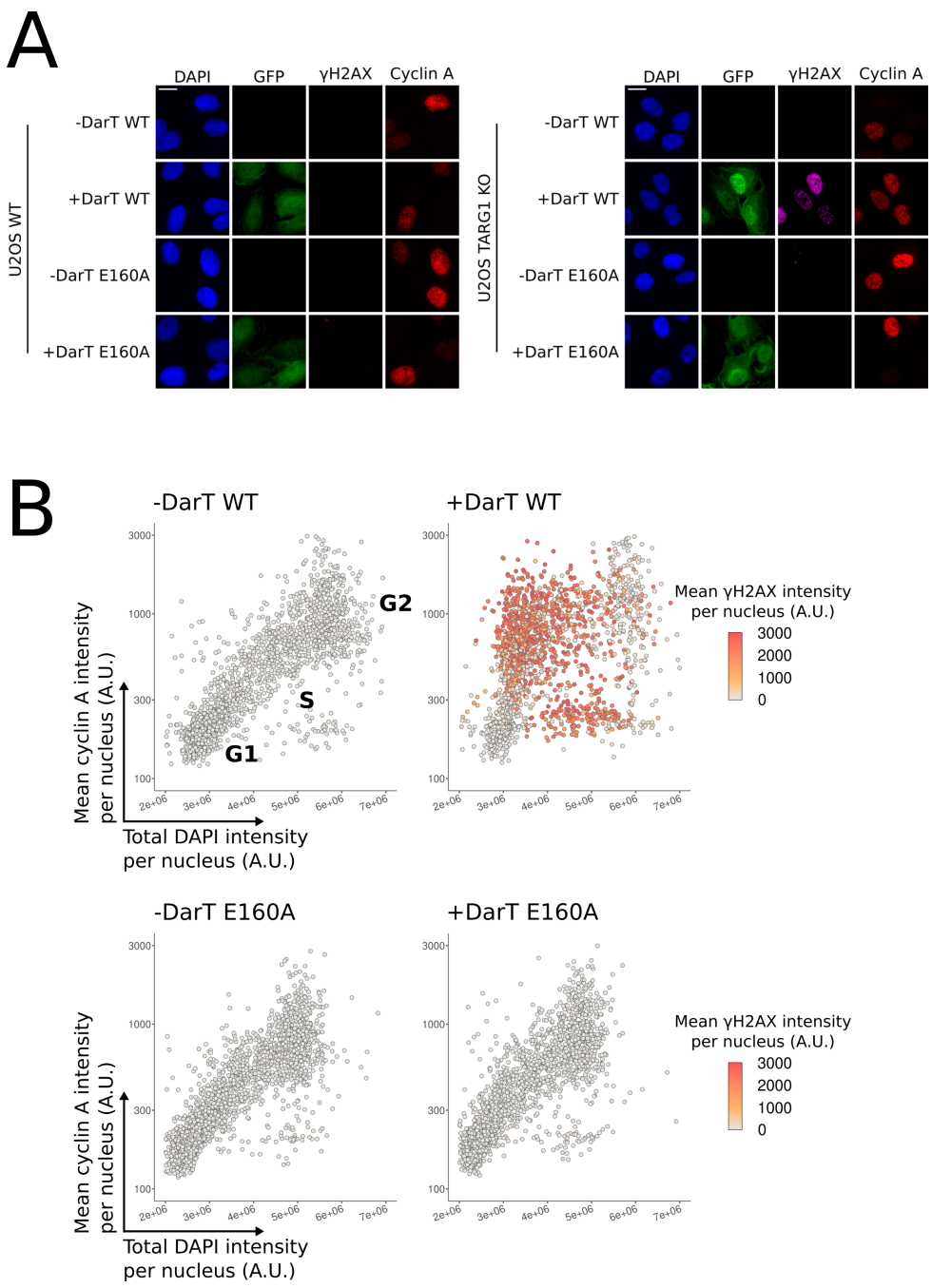


Figure S5: Alternative QIBC cell cycle staging using cyclin A reveals γH2AX is found in S-phase cells. **(A)** U-2 OS WT or TARG1 KO representative cells expressing either DarT WT or E160A (24h) were immunostained as indicated. **(B)** Cells were immunostained as in **A** and were analysed by QIBC. Approximate cell cycle stages are indicated on the -DarT WT plot. Total DAPI and mean cyclin A intensities for individual cells were used to generate the scatter plot and mean γH2AX intensity was used to colour points.

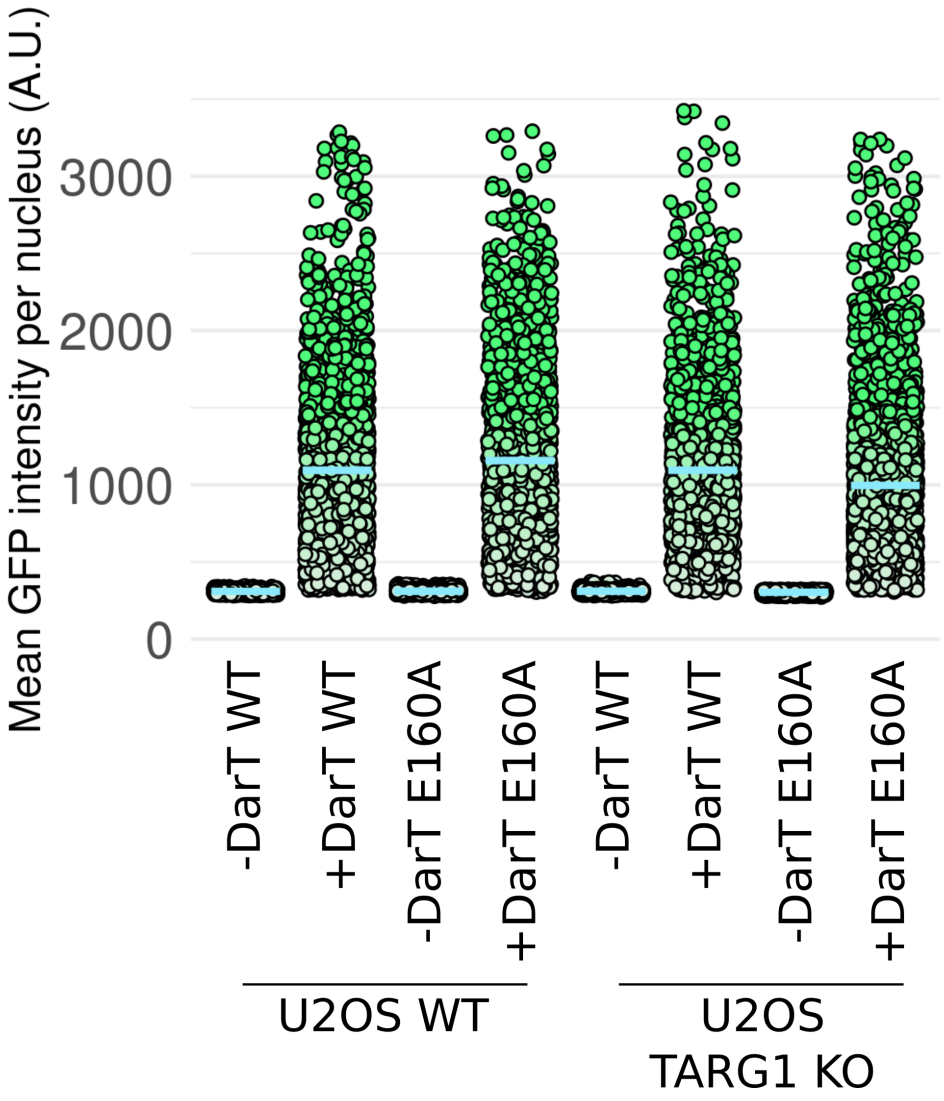


Figure S6: Quantification of GFP-DarT expression across cell lines. Individual GFP intensities per nucleus from cells in Supplementary Figure S5 visualised as a bar plot. Blue bars represent the population mean GFP intensity for each condition.

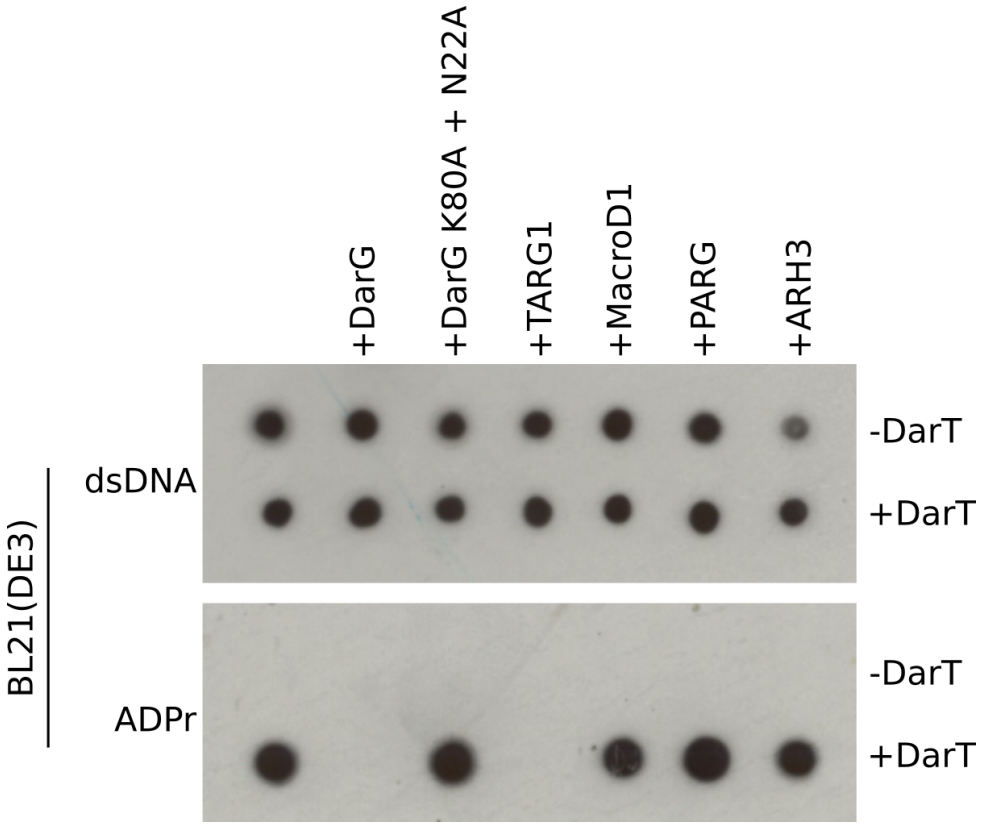


Figure S7: Bacterial gDNA de-ADP-ribosylation assay with DarG, TARG1, MacroD1, PARG, ARH3. Extension of Figure 2.27A.